US010637605B2

(12) **United States Patent**
Chang et al.

(10) **Patent No.: US 10,637,605 B2**
(45) **Date of Patent: Apr. 28, 2020**

(54) **COMPOSITE DATA TRANSPORT AND STORAGE VIA WAVEFRONT MULTIPLEXING**

(71) Applicant: **SPATIAL DIGITAL SYSTEMS, INC.**, Agoura Hills, CA (US)

(72) Inventors: **Donald C. D. Chang**, Thousand Oaks, CA (US); **Juo-Yu Lee**, Westlake Village, CA (US); **Tzer-Hso Lin**, Chatsworth, CA (US)

(73) Assignee: **SPATIAL DIGITAL SYSTEMS, INC.**, Agoura Hills, CA (US)

(*) Notice: Subject to any disclaimer, the term of this patent is extended or adjusted under 35 U.S.C. 154(b) by 0 days.

(21) Appl. No.: **16/695,125**

(22) Filed: **Nov. 25, 2019**

(65) **Prior Publication Data**

US 2020/0099464 A1 Mar. 26, 2020

Related U.S. Application Data

(63) Continuation of application No. 15/933,322, filed on Mar. 22, 2018, now Pat. No. 10,491,325.

(60) Provisional application No. 62/475,026, filed on Mar. 22, 2017.

(51) **Int. Cl.**

H04K 1/10	(2006.01)
G06F 3/06	(2006.01)
H04J 99/00	(2009.01)
H04B 7/06	(2006.01)
H04L 29/08	(2006.01)

(52) **U.S. Cl.**
CPC ***H04K 1/10*** (2013.01); ***G06F 3/067*** (2013.01); ***G06F 3/0623*** (2013.01); ***G06F 3/0659*** (2013.01); ***H04B 7/0617*** (2013.01); ***H04J 15/00*** (2013.01); *H04L 67/1097* (2013.01)

(58) **Field of Classification Search**
CPC . H04K 1/10; H04J 15/00; G06F 3/067; G06F 3/0659; G06F 3/0623; H04B 7/0617; H04L 67/1097
See application file for complete search history.

(56) **References Cited**

U.S. PATENT DOCUMENTS

2010/0117903 A1*	5/2010	Zheng	....	H01Q 3/2605 342/373
2017/0085315 A1*	3/2017	Atkinson	....	G01S 5/0294

* cited by examiner

Primary Examiner — Vineeta S Panwalkar
(74) *Attorney, Agent, or Firm* — Phuong-Quan Hoang

(57) **ABSTRACT**

An apparatus comprises an antenna array having N elements to receive N input streams from a plurality of transmitters and a post-processing device to perform a wavefront demultiplexing transform on the N input streams corresponding to M orthogonal beams to generate M output streams using a weight matrix having M beam weight vectors (BWVs) associated with the M orthogonal beams, where M and N are positive integers and 1<M≤N. The M BWVs are calculated using an optimization procedure based on performance constraints. The performance constraints for one of the M orthogonal beams with an orthogonal beam radiation pattern include designated peak and null positions.

20 Claims, 38 Drawing Sheets

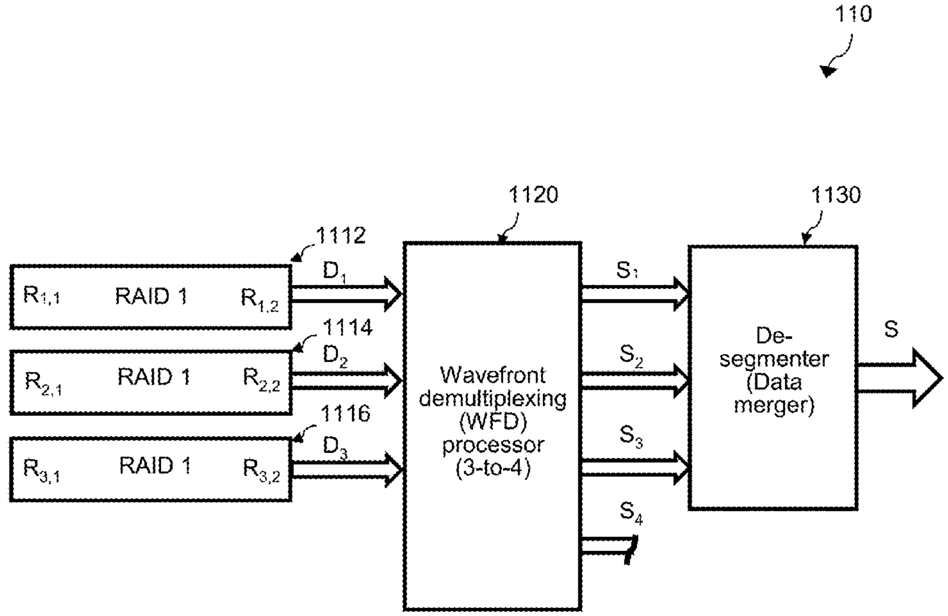

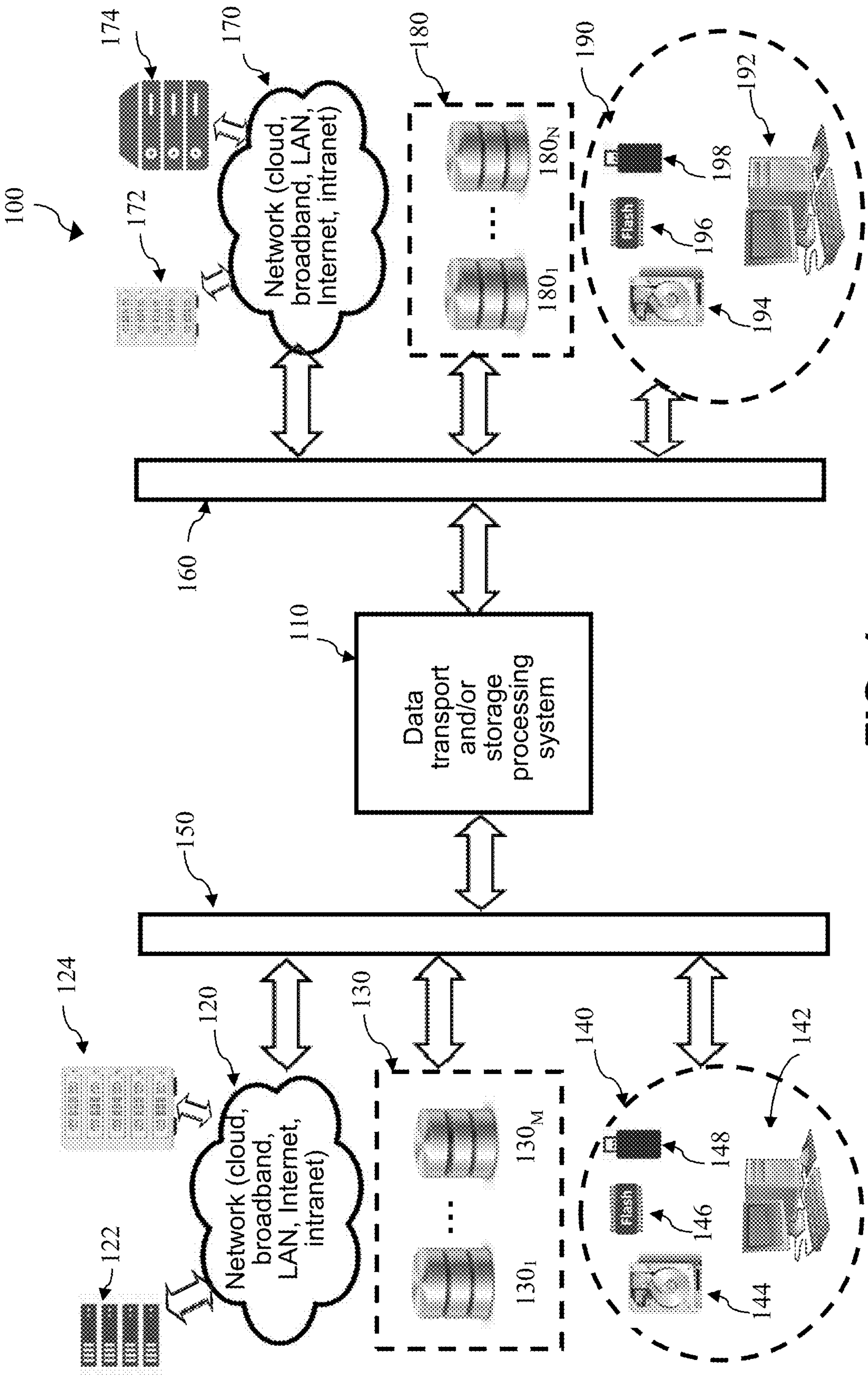
100
172
174
170
Network (cloud, broadband, LAN, Internet, intranet)
180
180_1
…
180_N
190
194
196
Flash
198
192
160
110
Data transport and/or storage processing system
150
124
122
120
Network (cloud, broadband, LAN, Internet, intranet)
130
130_1
…
130_M
140
144
146
Flash
148
142

FIG. 1

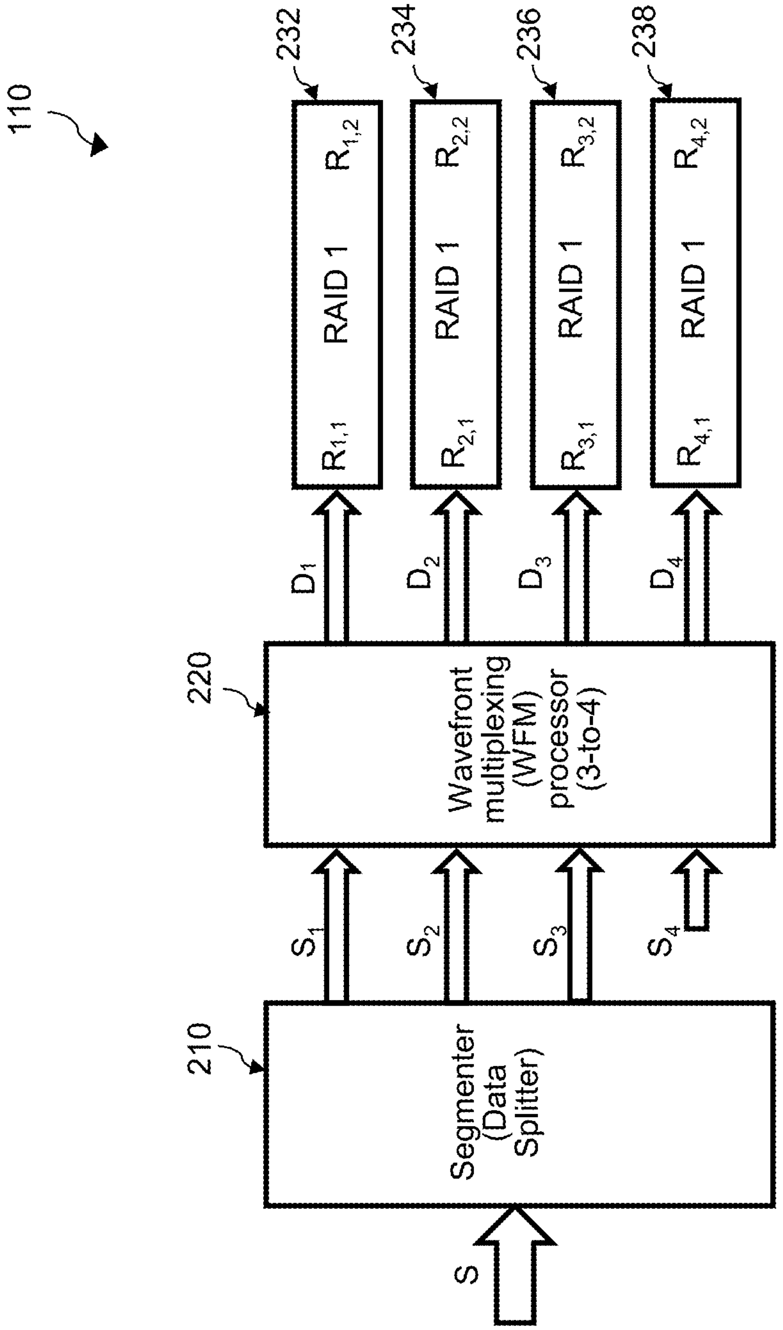
110
210
Segmenter (Data Splitter)
S
S_1
S_2
S_3
S_4
220
Wavefront multiplexing (WFM) processor (3-to-4)
D_1
D_2
D_3
D_4
232
234
236
238
RAID 1
$R_{1,1}$
$R_{1,2}$
RAID 1
$R_{2,1}$
$R_{2,2}$
RAID 1
$R_{3,1}$
$R_{3,2}$
RAID 1
$R_{4,1}$
$R_{4,2}$

FIG. 2

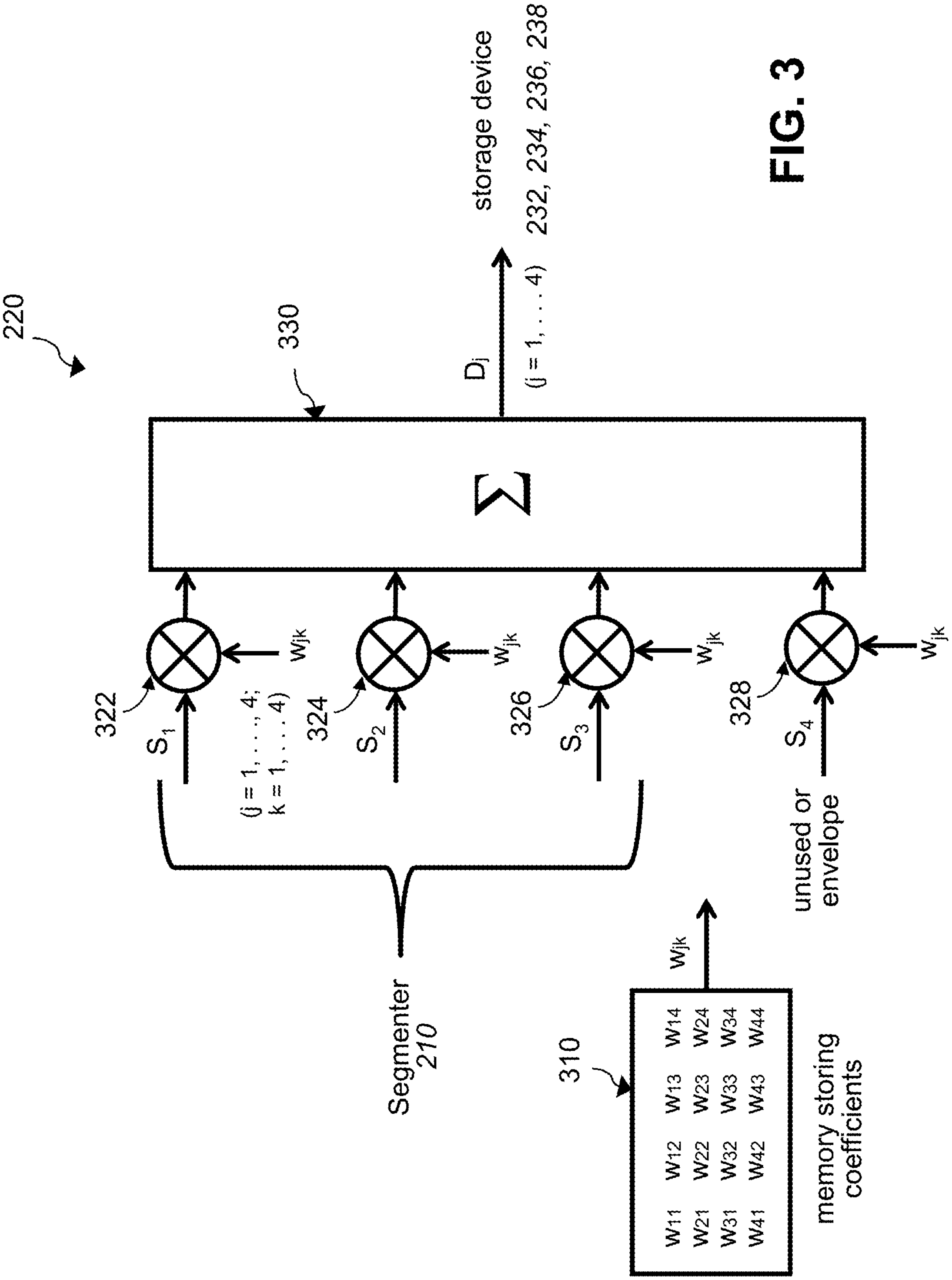
220
330
Σ
D_j
$(j = 1, \ldots 4)$
storage device
232, 234, 236, 238
322
324
326
328
S_1
S_2
S_3
S_4
w_{jk}
w_{jk}
w_{jk}
w_{jk}
$(j = 1, \ldots, 4;$
$k = 1, \ldots 4)$
Segmenter
210
unused or
envelope
w_{jk}
310
W_{11} W_{12} W_{13} W_{14}
W_{21} W_{22} W_{23} W_{24}
W_{31} W_{32} W_{33} W_{34}
W_{41} W_{42} W_{43} W_{44}
memory storing
coefficients

FIG. 3

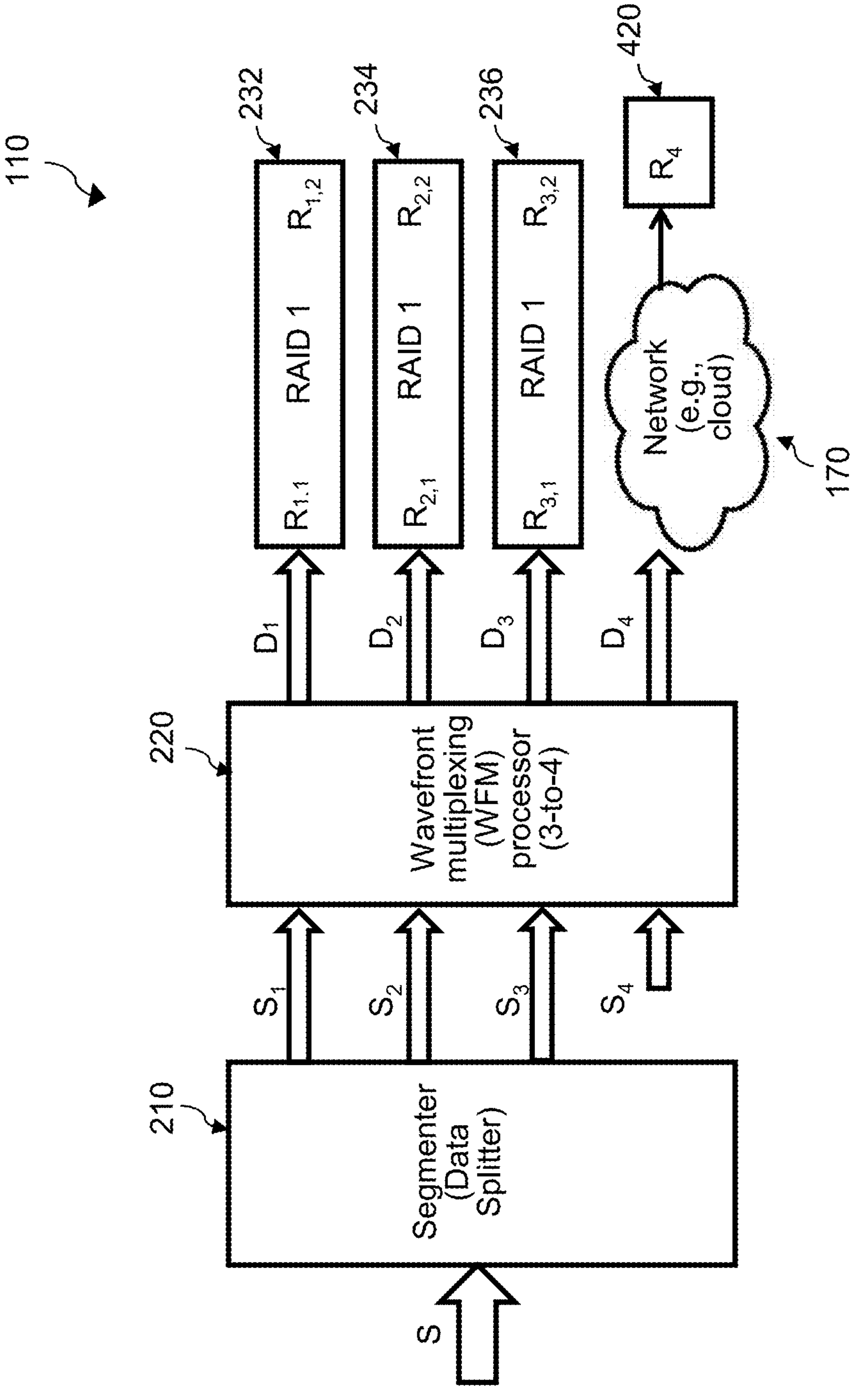
110
S
Segmenter (Data Splitter)
210
S_1
S_2
S_3
S_4
Wavefront multiplexing (WFM) processor (3-to-4)
220
D_1
D_2
D_3
D_4
232
$R_{1,1}$ RAID 1 $R_{1,2}$
234
$R_{2,1}$ RAID 1 $R_{2,2}$
236
$R_{3,1}$ RAID 1 $R_{3,2}$
Network (e.g., cloud)
170
R_4
420

FIG. 4

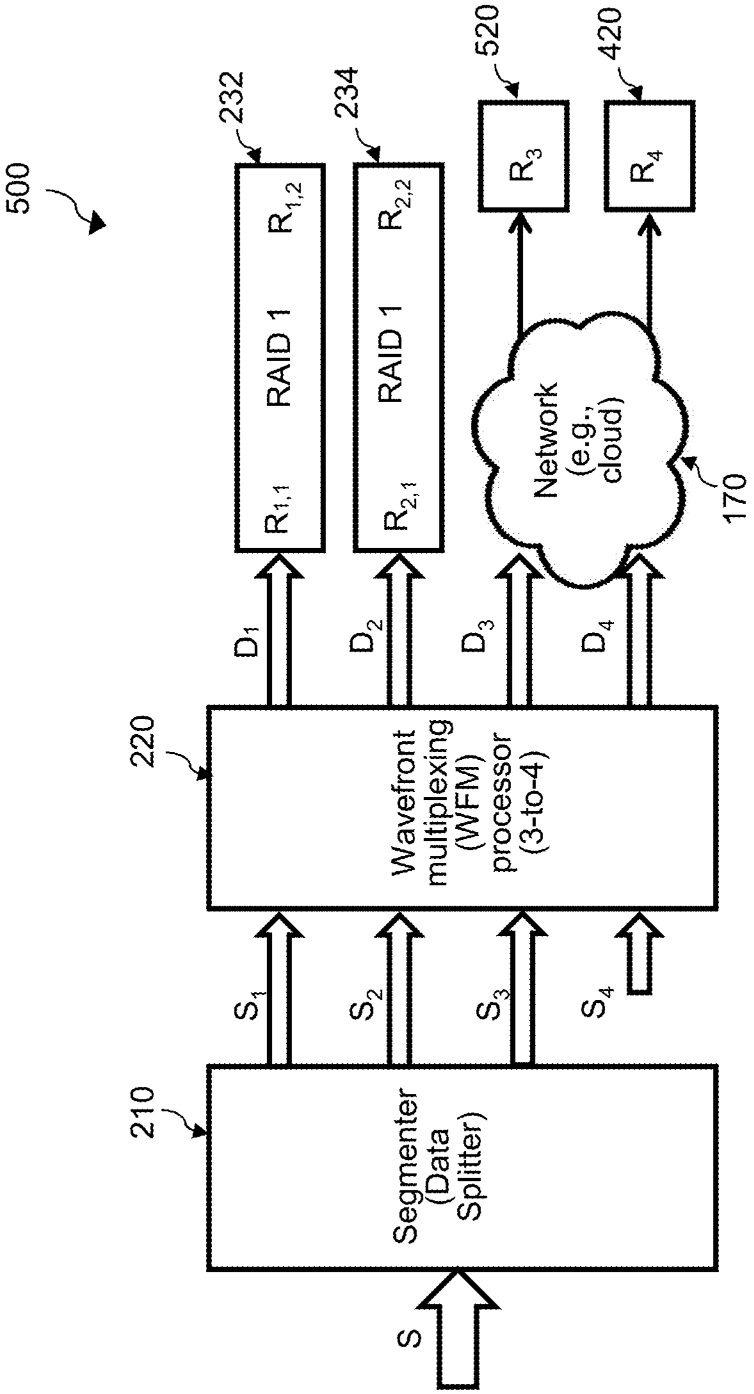
500
210
Segmenter (Data Splitter)
S
S_1
S_2
S_3
S_4
220
Wavefront multiplexing (WFM) processor (3-to-4)
D_1
D_2
D_3
D_4
232
$R_{1,1}$
RAID 1
$R_{1,2}$
234
$R_{2,1}$
RAID 1
$R_{2,2}$
Network (e.g., cloud)
170
520
R_3
420
R_4

FIG. 5

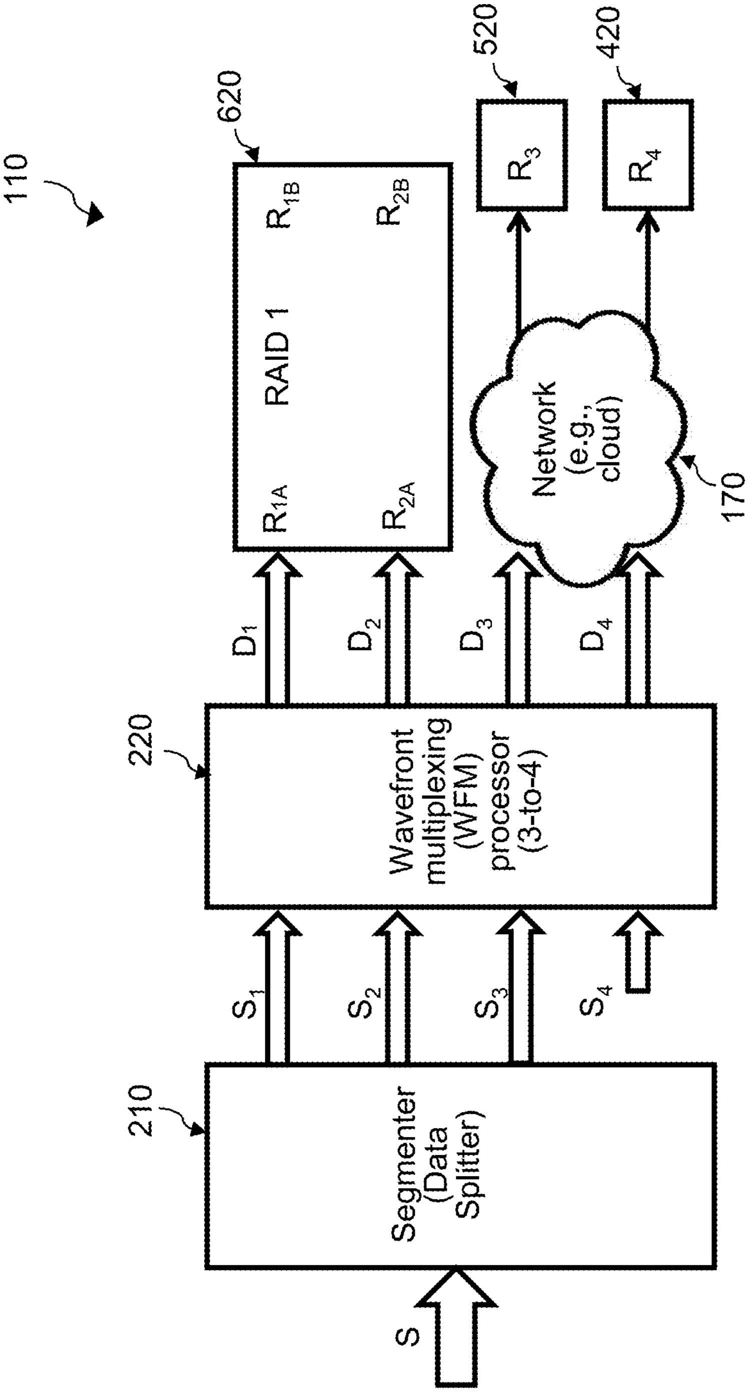
110
620
RAID 1
R_{1A}
R_{1B}
R_{2A}
R_{2B}
520
R_3
420
R_4
Network (e.g., cloud)
170
D_1
D_2
D_3
D_4
220
Wavefront multiplexing (WFM) processor (3-to-4)
S_1
S_2
S_3
S_4
210
Segmenter (Data Splitter)
S

FIG. 6

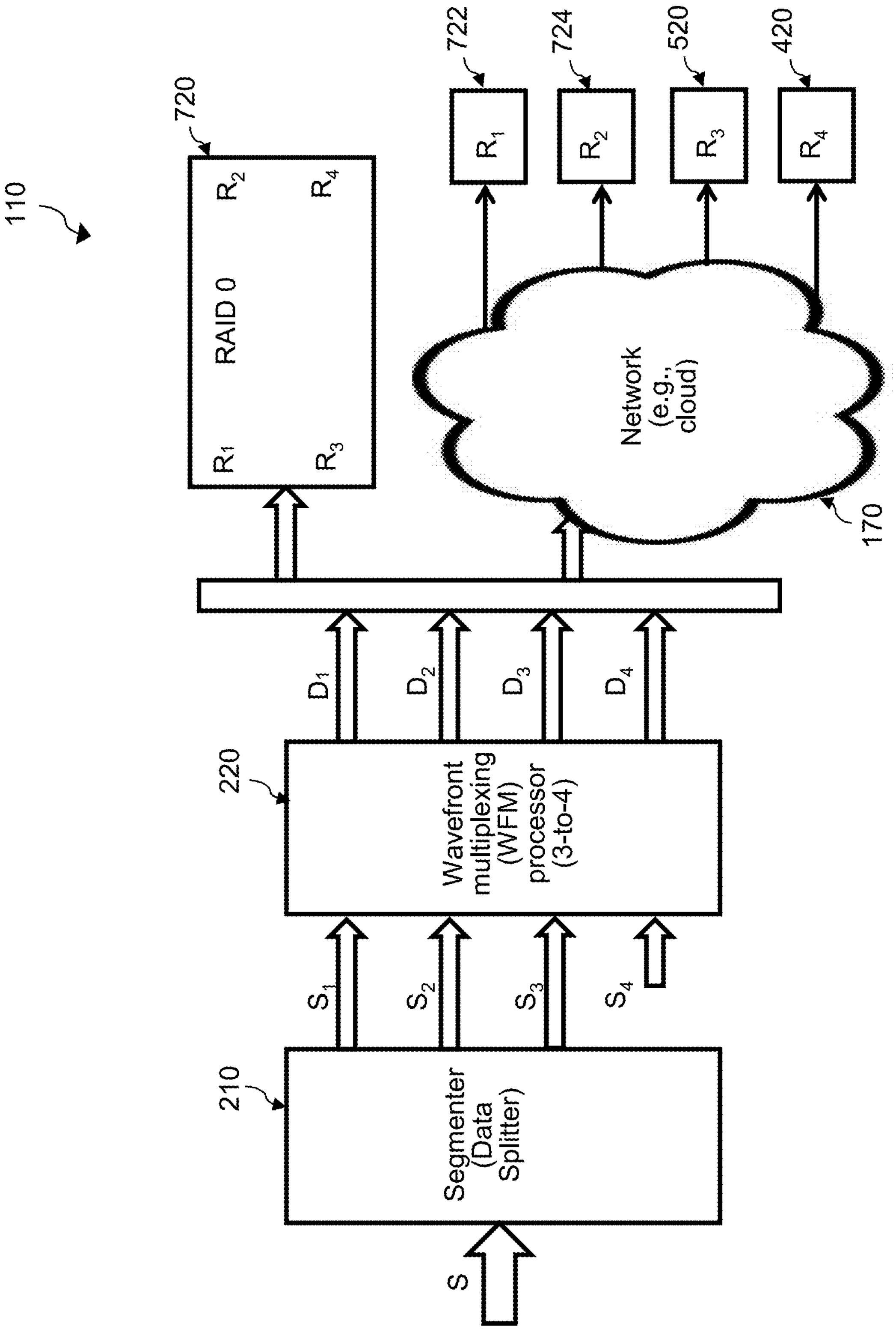
110
S
Segmenter (Data Splitter)
210
S_1
S_2
S_3
S_4
Wavefront multiplexing (WFM) processor (3-to-4)
220
D_1
D_2
D_3
D_4
RAID 0
720
R_1
R_2
R_3
R_4
Network (e.g., cloud)
170
722
R_1
724
R_2
520
R_3
420
R_4

FIG. 7

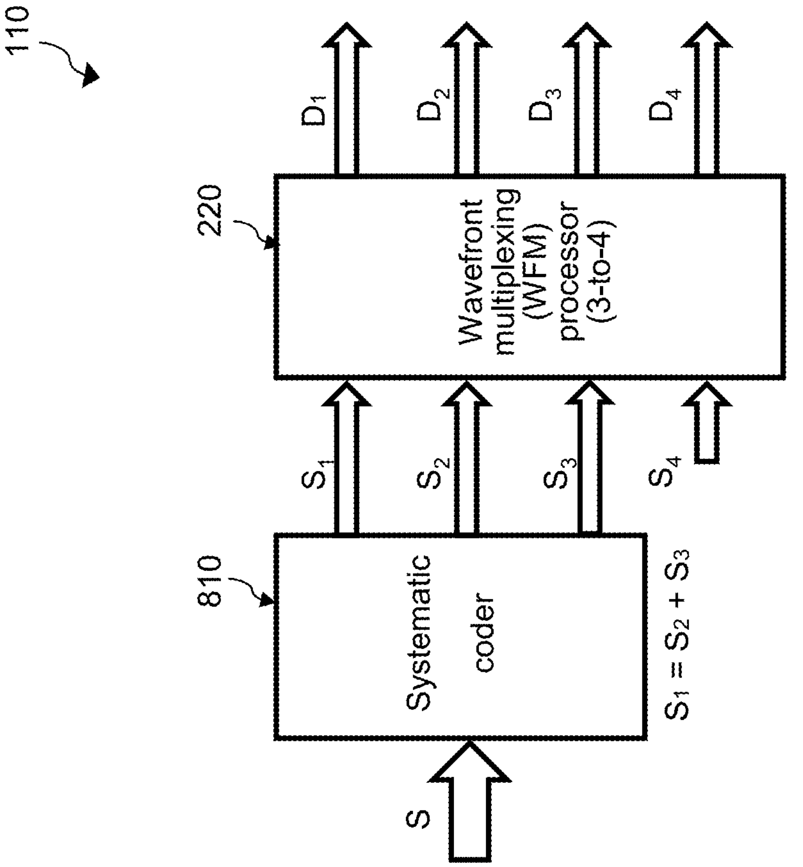
110
220
Wavefront multiplexing (WFM) processor (3-to-4)
D_1
D_2
D_3
D_4
S_1
S_2
S_3
S_4
810
Systematic coder
S
$S_1 = S_2 + S_3$

FIG. 8

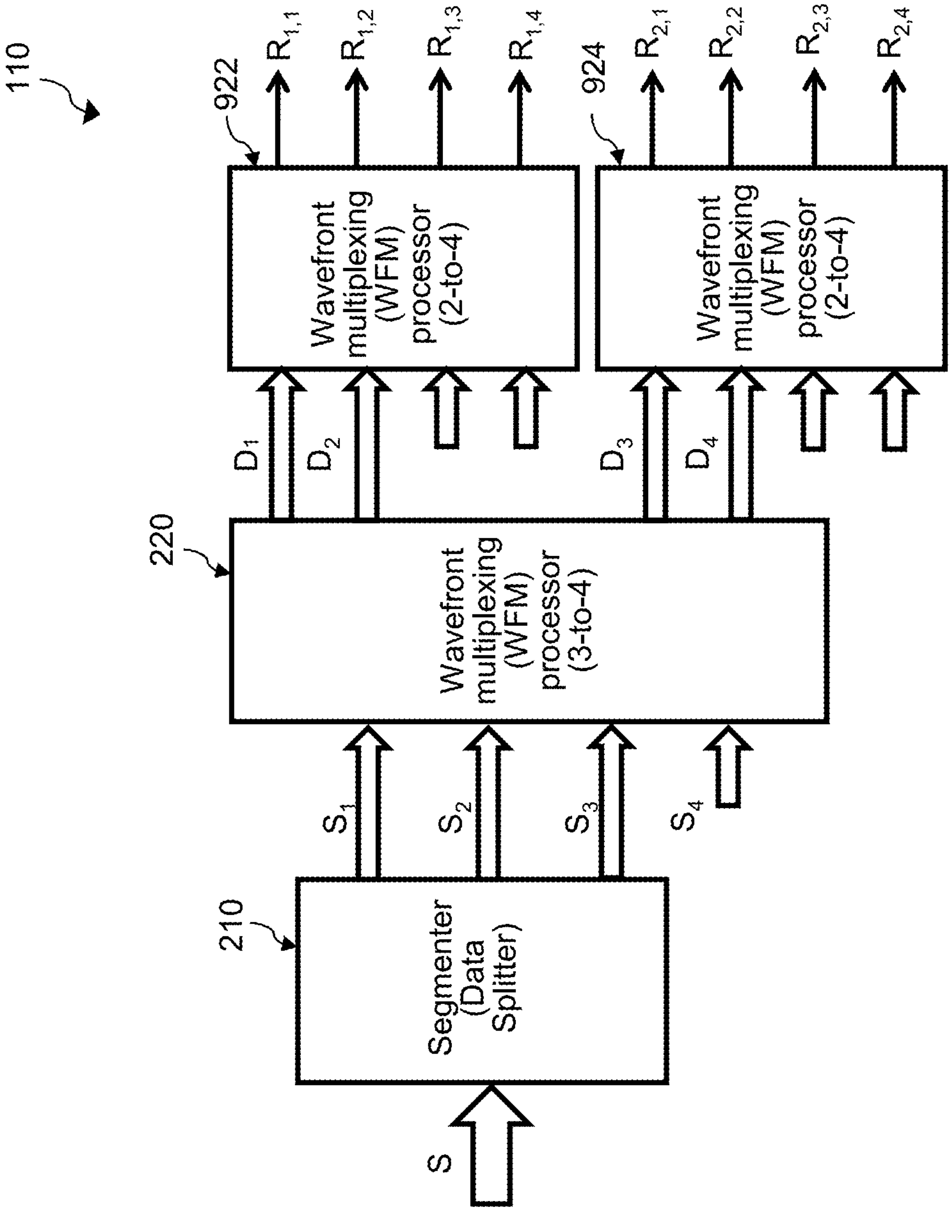
110
S
Segmenter (Data Splitter)
210
S_1
S_2
S_3
S_4
Wavefront multiplexing (WFM) processor (3-to-4)
220
D_1
D_2
D_3
D_4
Wavefront multiplexing (WFM) processor (2-to-4)
922
Wavefront multiplexing (WFM) processor (2-to-4)
924
$R_{1,1}$
$R_{1,2}$
$R_{1,3}$
$R_{1,4}$
$R_{2,1}$
$R_{2,2}$
$R_{2,3}$
$R_{2,4}$

FIG. 9

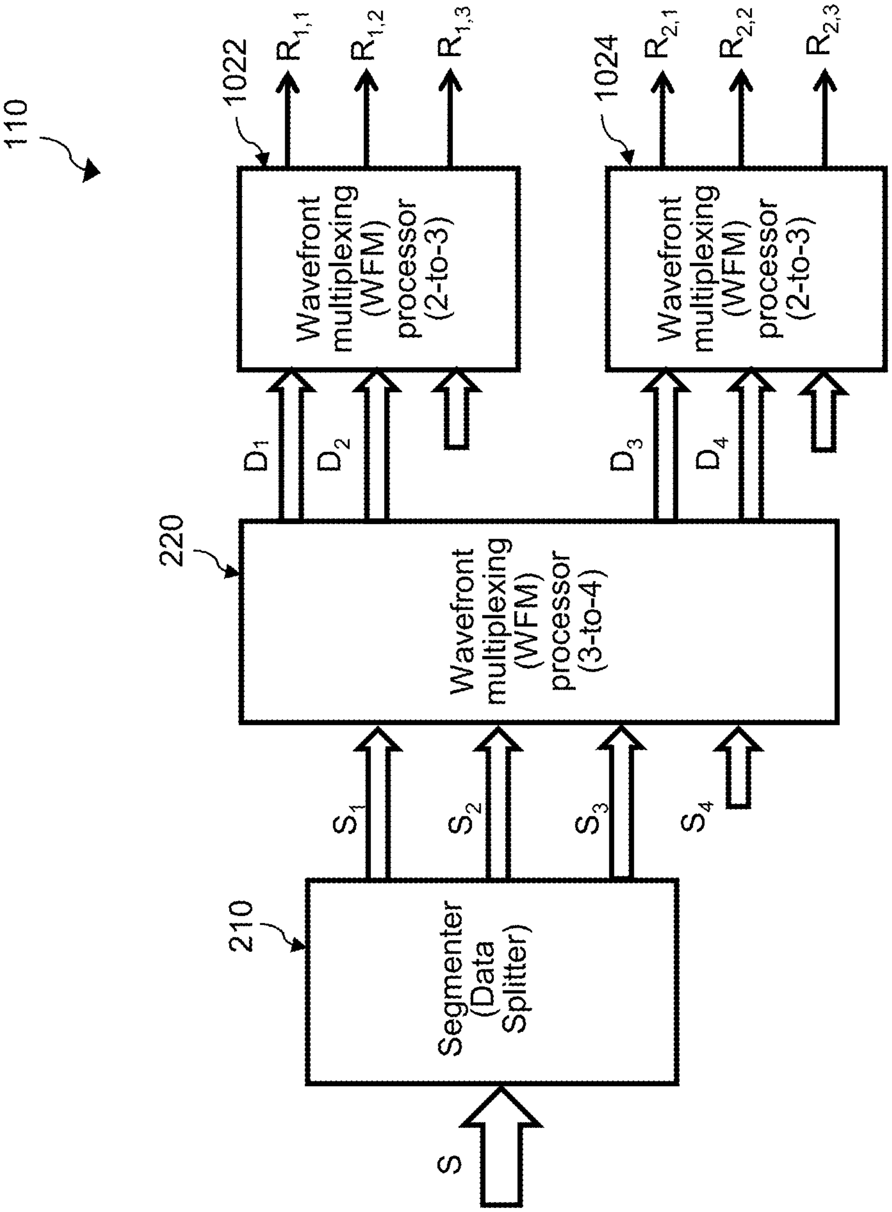
110
S
210
Segmenter (Data Splitter)
S1
S2
S3
S4
220
Wavefront multiplexing (WFM) processor (3-to-4)
D1
D2
D3
D4
1022
Wavefront multiplexing (WFM) processor (2-to-3)
R1,1
R1,2
R1,3
1024
Wavefront multiplexing (WFM) processor (2-to-3)
R2,1
R2,2
R2,3

FIG. 10

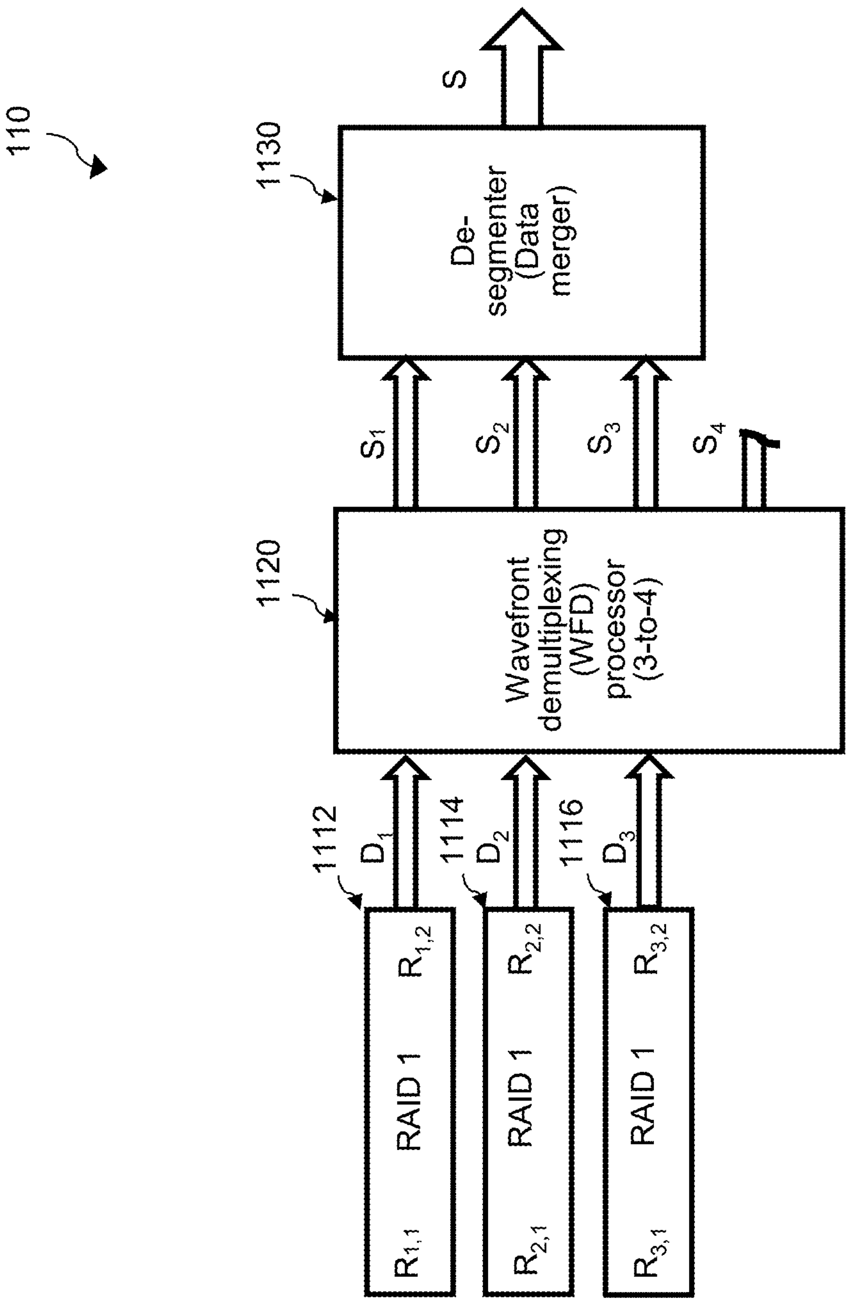
110
1130
De-segmenter (Data merger)
S
1120
Wavefront demultiplexing (WFD) processor (3-to-4)
S_1
S_2
S_3
S_4
1112
1114
1116
D_1
D_2
D_3
$R_{1,1}$ RAID 1 $R_{1,2}$
$R_{2,1}$ RAID 1 $R_{2,2}$
$R_{3,1}$ RAID 1 $R_{3,2}$

FIG. 11

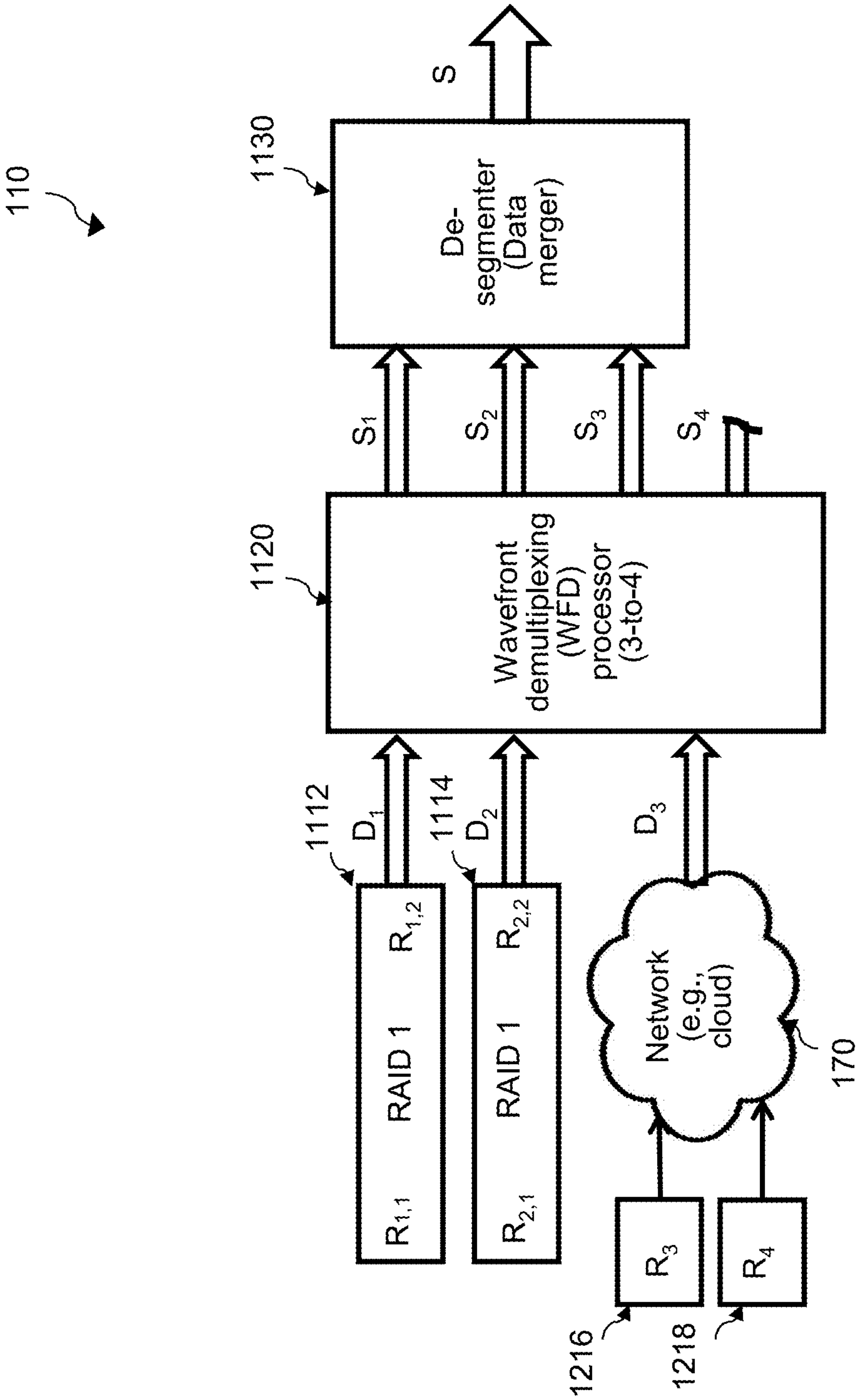
110
1130
De-segmenter (Data merger)
S
1120
Wavefront demultiplexing (WFD) processor (3-to-4)
S1
S2
S3
S4
1112
D1
1114
D2
D3
R1,1
RAID 1
R1,2
R2,1
RAID 1
R2,2
Network (e.g., cloud)
170
R3
R4
1216
1218

FIG. 12

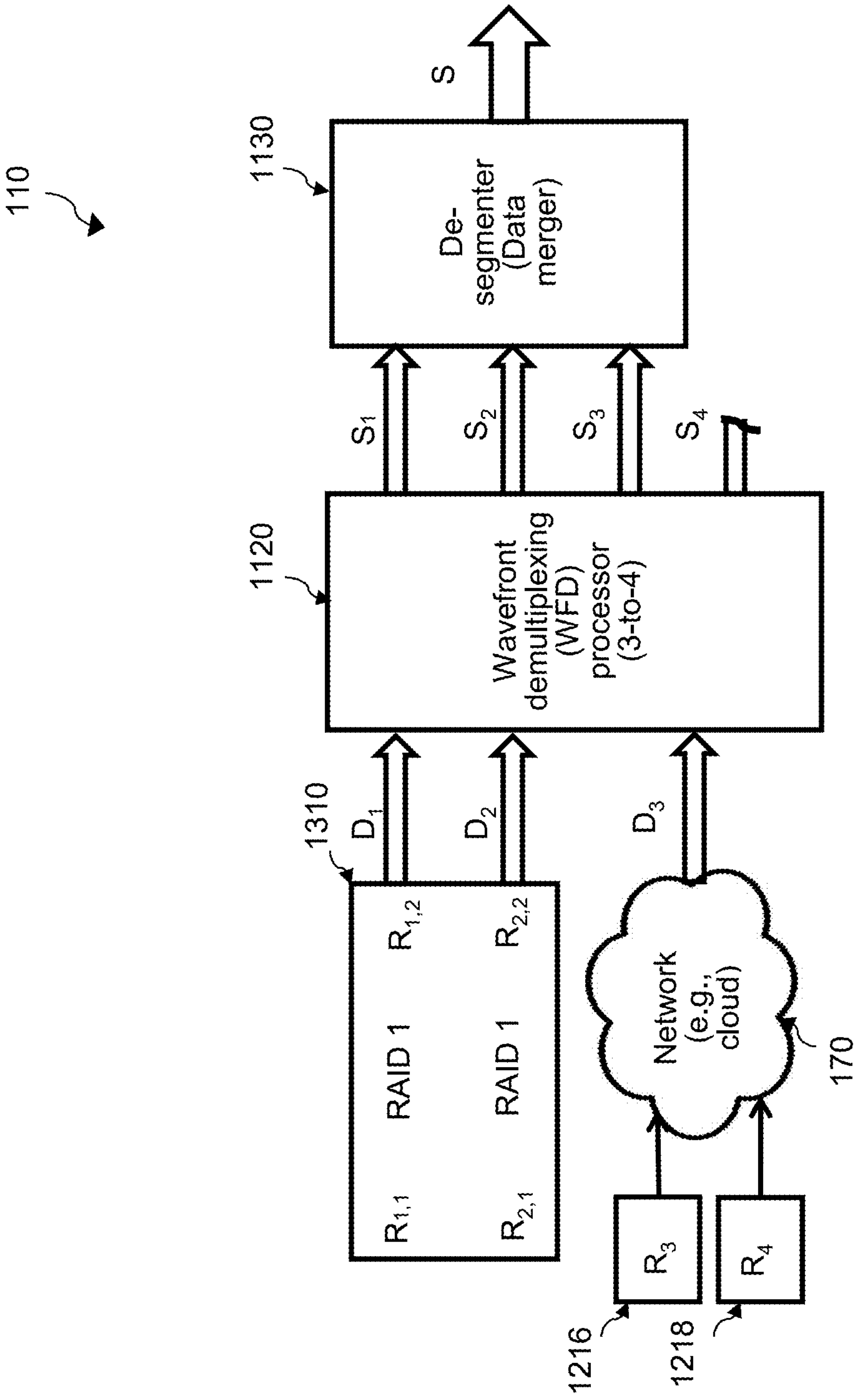
110
1130
De-segmenter (Data merger)
S
S_1
S_2
S_3
S_4
1120
Wavefront demultiplexing (WFD) processor (3-to-4)
1310
D_1
D_2
D_3
$R_{1,1}$
RAID 1
$R_{1,2}$
$R_{2,1}$
RAID 1
$R_{2,2}$
Network (e.g., cloud)
170
R_3
R_4
1216
1218

FIG. 13

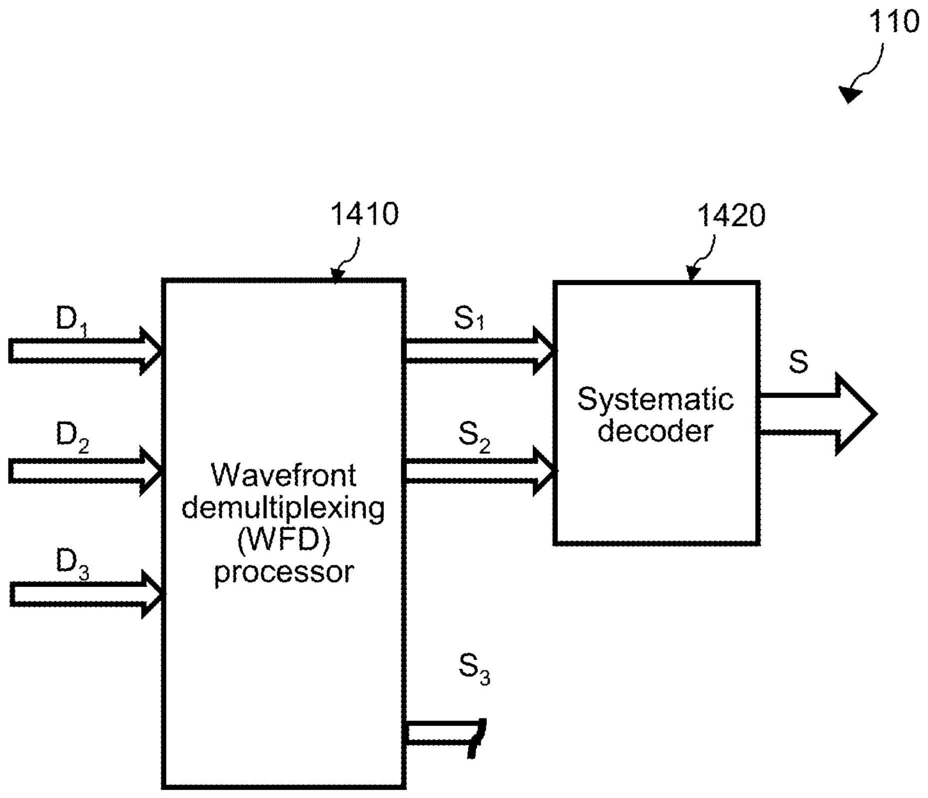
110
1410
1420
D_1
D_2
D_3
Wavefront demultiplexing (WFD) processor
S_1
S_2
S_3
Systematic decoder
S

FIG. 14

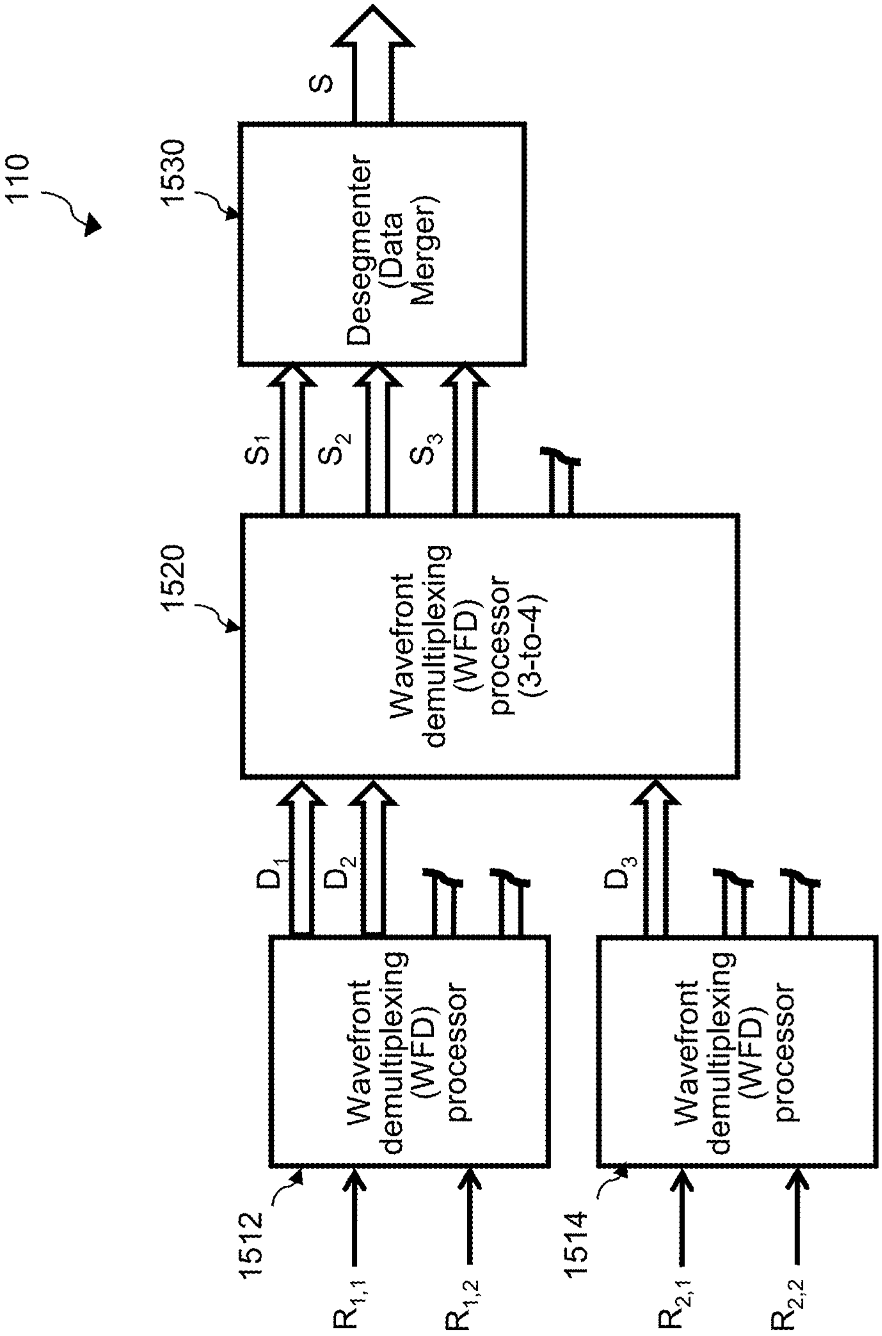
110
1530
S
Desegmenter (Data Merger)
S_1
S_2
S_3
1520
Wavefront demultiplexing (WFD) processor (3-to-4)
D_1
D_2
D_3
Wavefront demultiplexing (WFD) processor
Wavefront demultiplexing (WFD) processor
1512
1514
$R_{1,1}$
$R_{1,2}$
$R_{2,1}$
$R_{2,2}$

FIG. 15

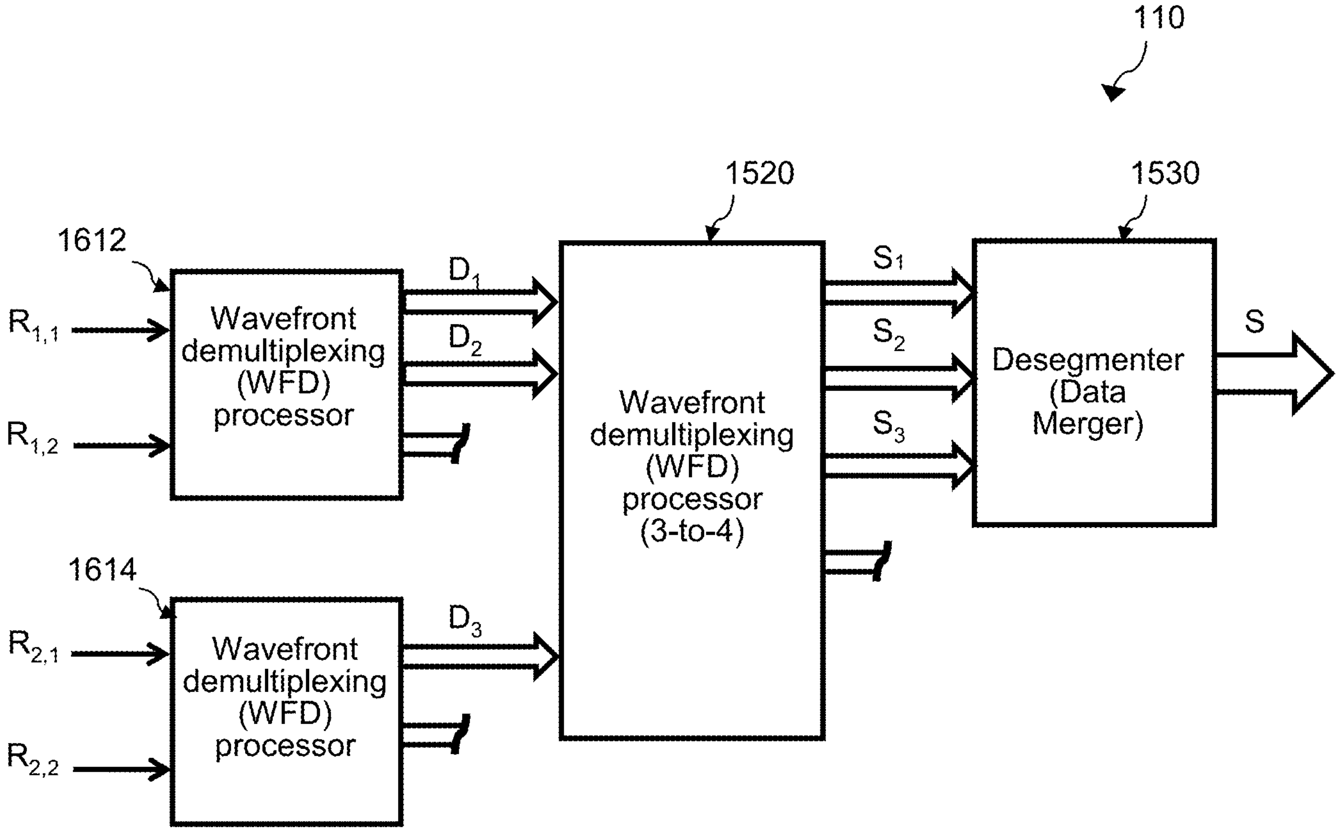
110
1612
$R_{1,1}$
$R_{1,2}$
Wavefront demultiplexing (WFD) processor
1614
$R_{2,1}$
$R_{2,2}$
Wavefront demultiplexing (WFD) processor
D_1
D_2
D_3
1520
Wavefront demultiplexing (WFD) processor (3-to-4)
S_1
S_2
S_3
1530
Desegmenter (Data Merger)
S

FIG. 16

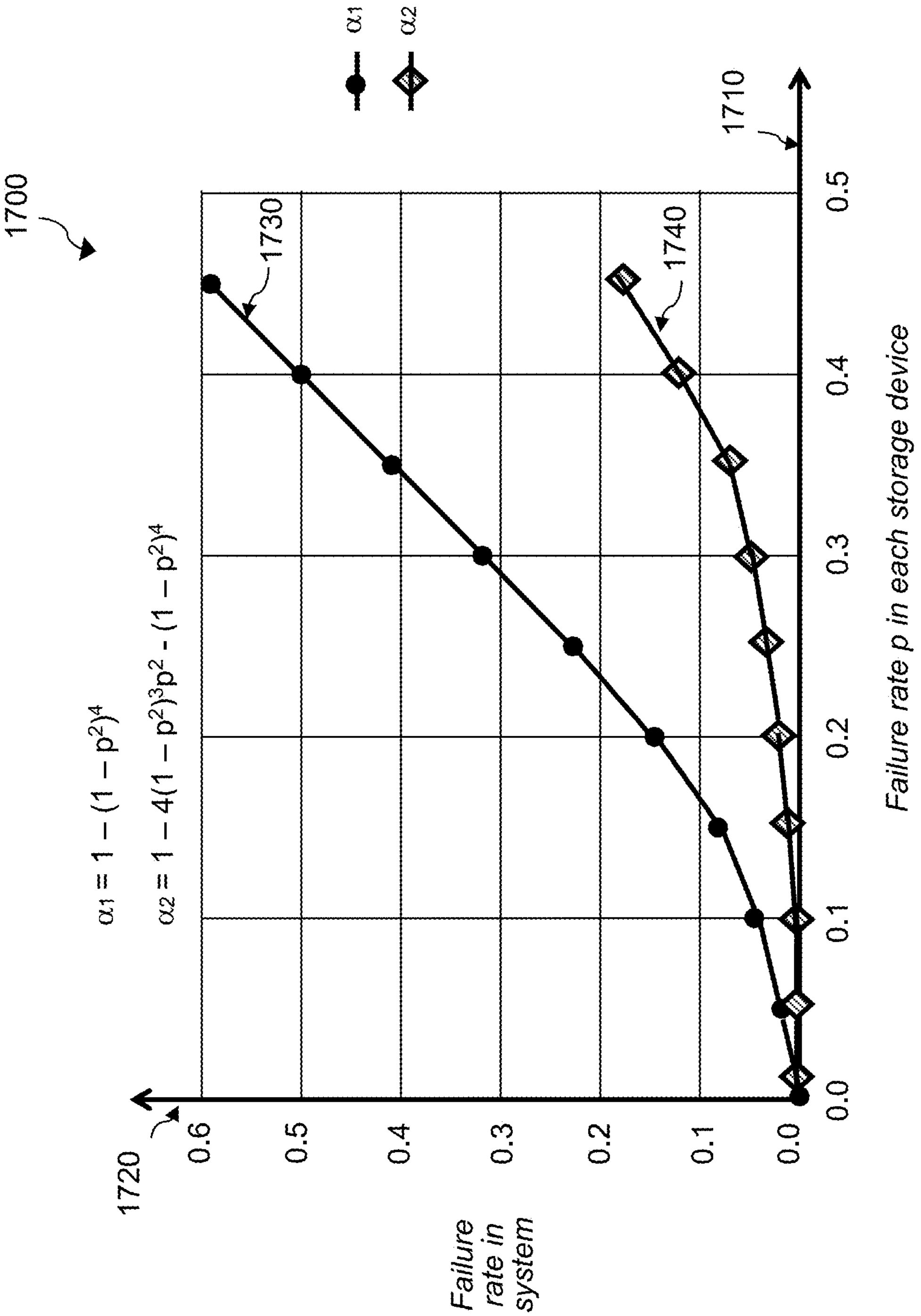
1700
$\alpha_1 = 1 - (1 - p^2)^4$
$\alpha_2 = 1 - 4(1 - p^2)^3p^2 - (1 - p^2)^4$
Failure rate in system
1720
0.6
0.5
0.4
0.3
0.2
0.1
0.0
0.0
0.1
0.2
0.3
0.4
0.5
1710
Failure rate p in each storage device
1730
1740
α_1
α_2

FIG. 17

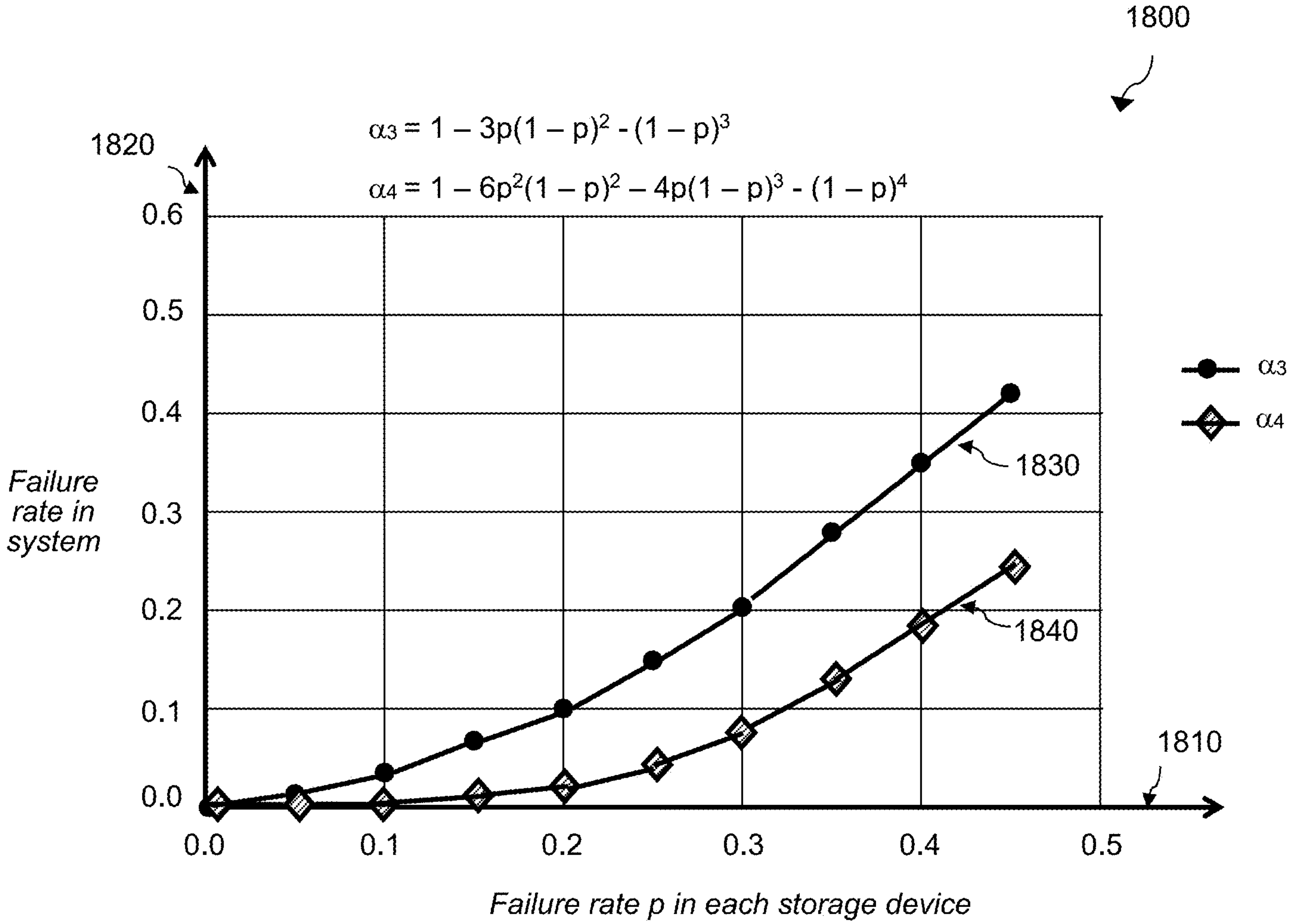

$\alpha_3 = 1 - 3p(1-p)^2 - (1-p)^3$

$\alpha_4 = 1 - 6p^2(1-p)^2 - 4p(1-p)^3 - (1-p)^4$

FIG. 18

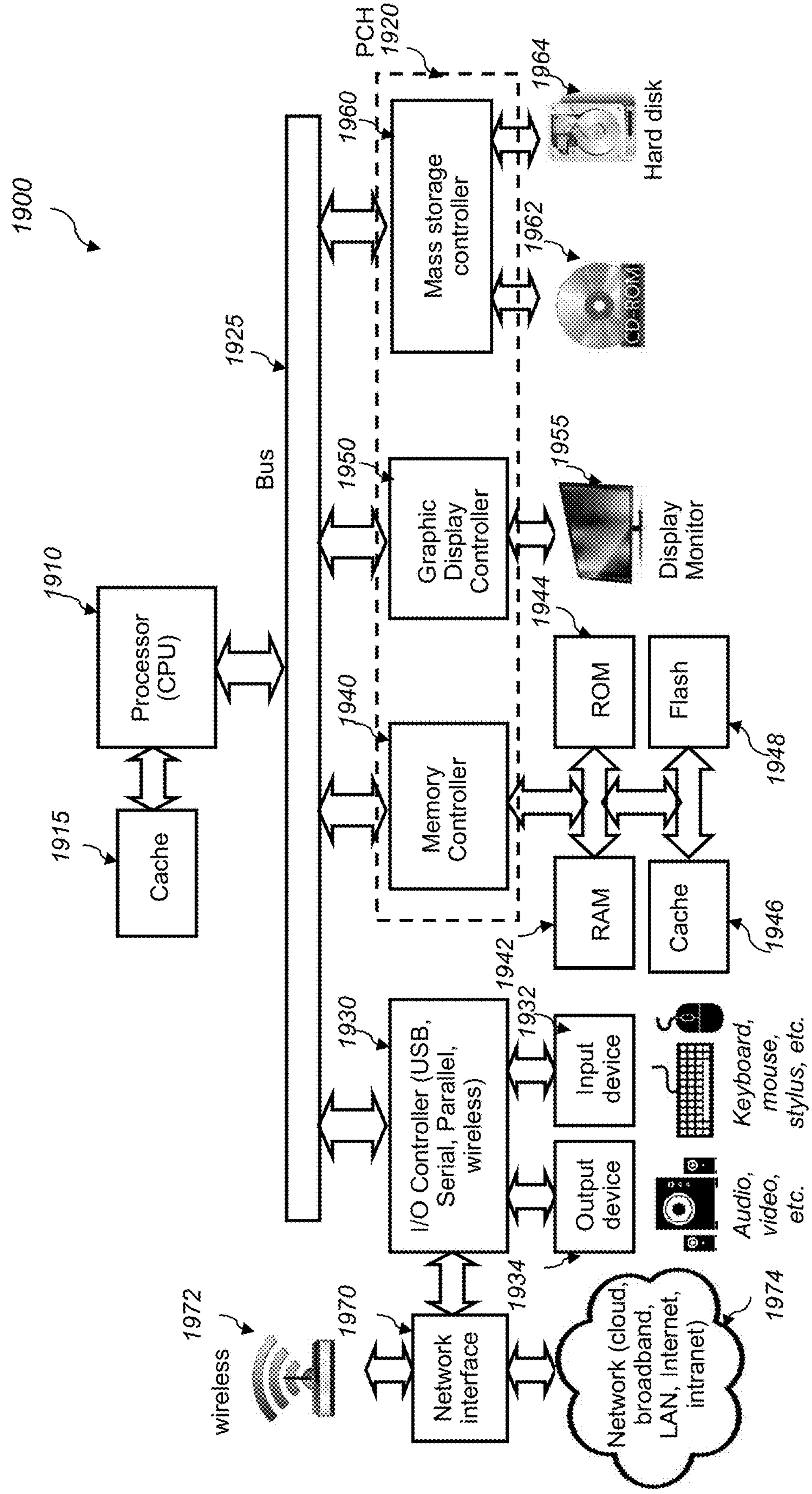
1900
1910
Processor (CPU)
1915
Cache
1925
Bus
PCH 1920
1930
I/O Controller (USB, Serial, Parallel, wireless)
1940
Memory Controller
1950
Graphic Display Controller
1960
Mass storage controller
1964
Hard disk
1962
CD-ROM
1955
Display Monitor
1944
ROM
Flash
1948
1942
RAM
Cache
1946
1932
Input device
Keyboard, mouse, stylus, etc.
Output device
Audio, video, etc.
1934
1970
Network interface
1972
wireless
Network (cloud, broadband, LAN, Internet, intranet)
1974

FIG. 19

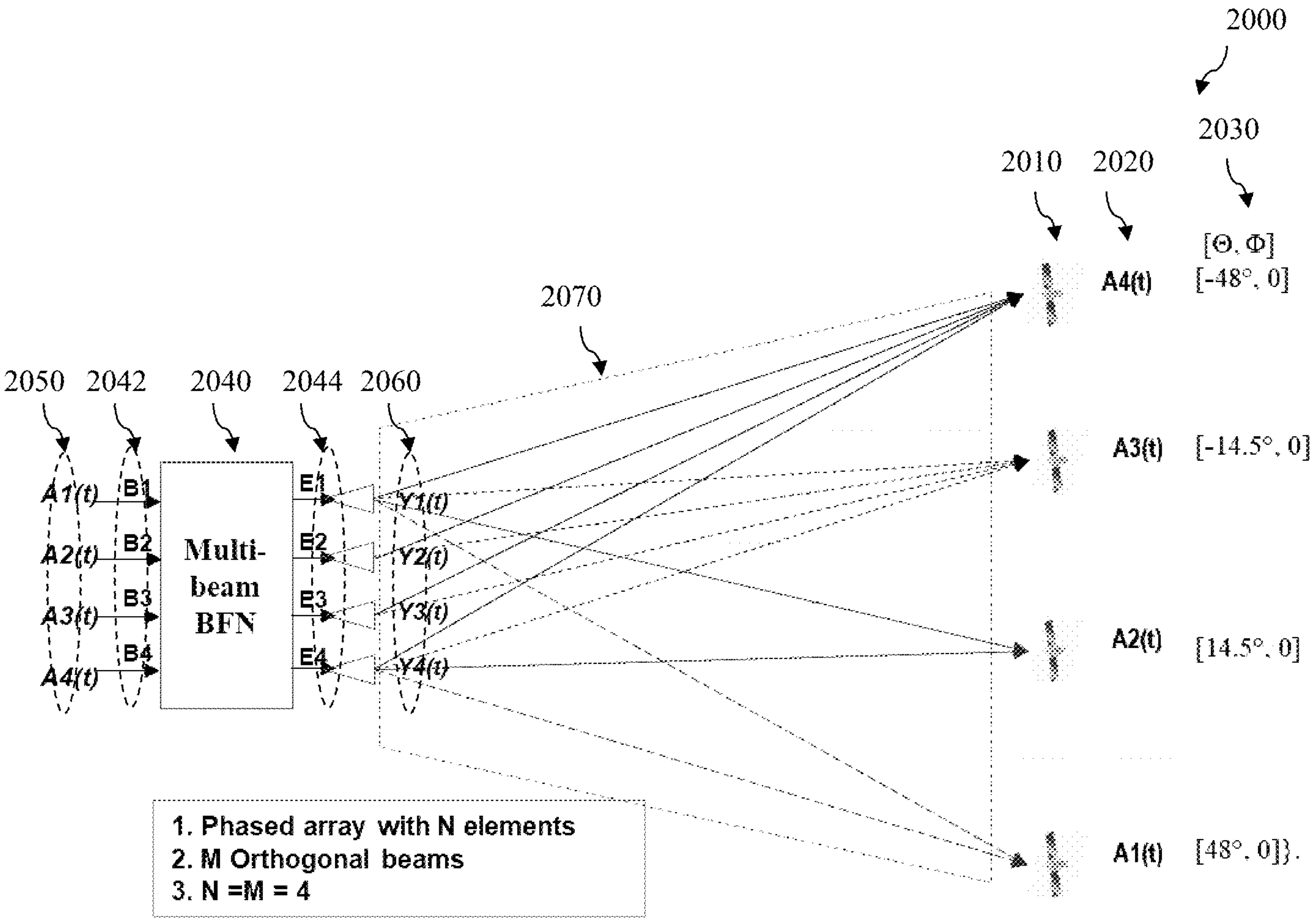
2000
2030
2010
2020
[Θ, Φ]
A4(t) [-48°, 0]
A3(t) [-14.5°, 0]
A2(t) [14.5°, 0]
A1(t) [48°, 0]}.
2070
2050
2042
2040
2044
2060
A1(t)
A2(t)
A3(t)
A4(t)
B1
B2
B3
B4
Multi-beam BFN
E1
E2
E3
E4
Y1(t)
Y2(t)
Y3(t)
Y4(t)
1. Phased array with N elements
2. M Orthogonal beams
3. N =M = 4

FIG. 20

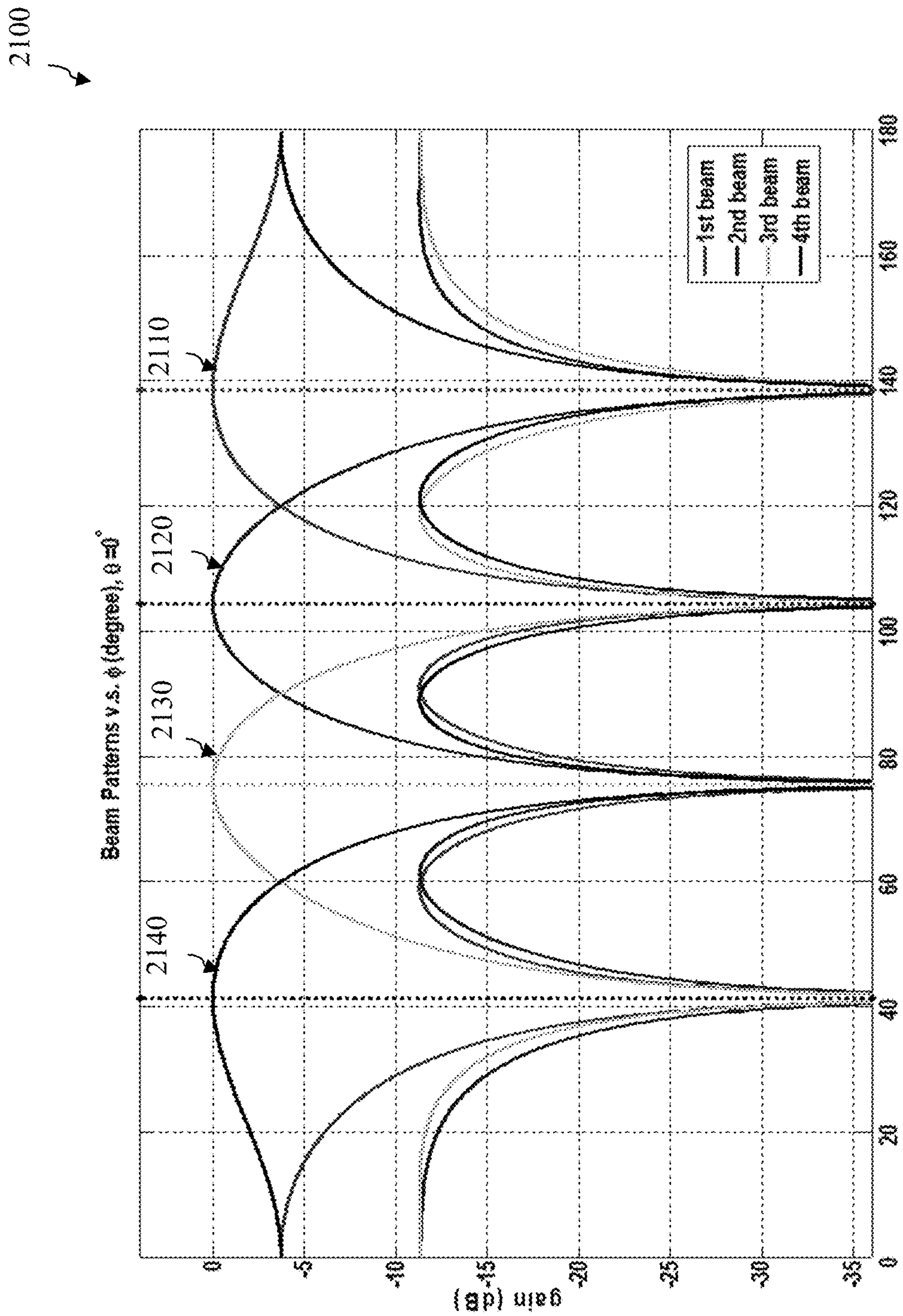
2100
Beam Patterns v.s. ϕ (degree), θ =0°
2140
2130
2120
2110
gain (dB)
0
-5
-10
-15
-20
-25
-30
-35
0
20
40
60
80
100
120
140
160
180
ϕ (degree)
1st beam
2nd beam
3rd beam
4th beam

FIG. 21

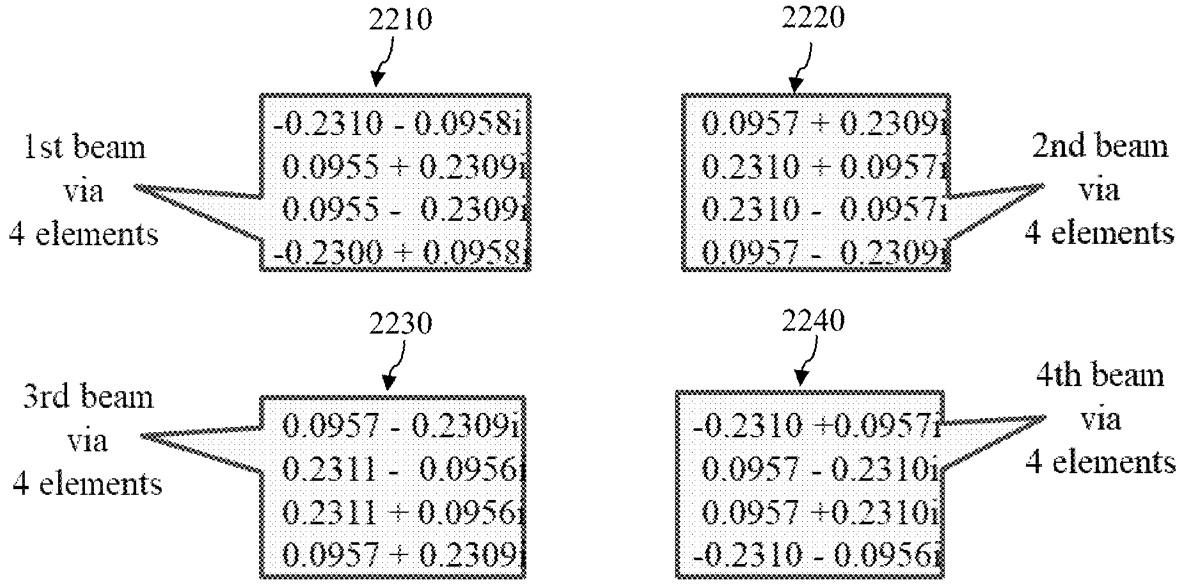
2210
-0.2310 - 0.0958i
0.0955 + 0.2309i
0.0955 - 0.2309i
-0.2300 + 0.0958i
1st beam via 4 elements
2220
0.0957 + 0.2309i
0.2310 + 0.0957i
0.2310 - 0.0957i
0.0957 - 0.2309i
2nd beam via 4 elements
2230
0.0957 - 0.2309i
0.2311 - 0.0956i
0.2311 + 0.0956i
0.0957 + 0.2309i
3rd beam via 4 elements
2240
-0.2310 +0.0957i
0.0957 - 0.2310i
0.0957 +0.2310i
-0.2310 - 0.0956i
4th beam via 4 elements

FIG. 22

$$\overset{2060}{\begin{bmatrix} y1(t) \\ y2(t) \\ y3(t) \\ y4(t) \end{bmatrix}} = \overset{2310}{[\boldsymbol{BWVs}]} * \overset{2050}{\begin{bmatrix} A1(t) \\ A2(t) \\ A3(t) \\ A4(t) \end{bmatrix}}$$

Ai(t): signals for i^{th} beam

yj(t): signals for j^{th} element

$$\overset{2310}{[\boldsymbol{BWVs}]} = \begin{bmatrix} -0.2310 - 0.0958i & 0.0957 + 0.2309i & 0.0957 - 0.2309i & -0.2310 + 0.0956i \\ 0.0955 + 0.2309i & 0.2310 + 0.0957i & 0.2311 - 0.0956i & 0.0956 - 0.2310i \\ 0.0955 - 0.2309i & 0.2310 - 0.0957i & 0.2311 + 0.0956i & 0.0956 + 0.2310i \\ -0.2300 + 0.0958i & 0.0957 - 0.2309i & 0.0957 + 0.2309i & -0.2310 - 0.0956i \end{bmatrix}$$

$$\begin{array}{cccc} \text{BWV1} & \text{BWV2} & \text{BWV3} & \text{BWV4} \\ \text{Beam 1} & \text{Beam 2} & \text{Beam 3} & \text{Beam 4} \\ \text{4 elements} & \text{4 elements} & \text{4 elements} & \text{4 elements} \end{array}$$

FIG. 23

2400

1. **4 to 4 K-muxing; [K-muxing] = [BWVs]**

$$[yj(t)] = [\text{K-muxing}]*[Ai(t)], \text{ or } \quad \begin{bmatrix} y1(t) \\ y2(t) \\ y3(t) \\ y4(t) \end{bmatrix} = [BWVs]* \begin{bmatrix} A1(t) \\ A2(t) \\ A3(t) \\ A4(t) \end{bmatrix}$$

   - Ai(t) = ith input data; i = 1 to 4 and yj(t) = jth output data; j = 1 to 4

2. **4 to 4 K-demuxing; [K-demuxing] = [P]**
   - yj(t) = jth input data; j = 1 to 4 ***propagating to 4 different directions for recovering A1(t), A2(t), A3(t) and A4(t)***
   - Ai(t) = ith output data; i = 1 to 4
     - A1(t) will be delivered by the 4 element array to a 1st direction at angle [$\theta 1, \phi 1$]
       - A1(t)= w11* y1(t) +w12 * y2(t) + w13* y3(t) +w14 * y4(t)
     - A2(t) will be delivered by the 4 element array to a 2nd direction at angle [$\theta 2, \phi 2$]
       - A2(t)= w21* y1(t) +w22 * y2(t) + w23* y3(t) +w24 * y4(t)
     - A3(t) will be delivered by the 4 element array to a 3rd direction at angle [$\theta 3, \phi 3$]
       - A3(t)= w31* y1(t) +w32 * y2(t) + w33* y3(t) +w34 * y4(t)
     - A4(t) will be delivered by the 4 element array to a 4th direction at angle [$\theta 2, \phi 2$]
       - A4(t)= w41* y1(t) +w42 * y2(t) + w43* y3(t) +w44 * y4(t)

FIG. 24

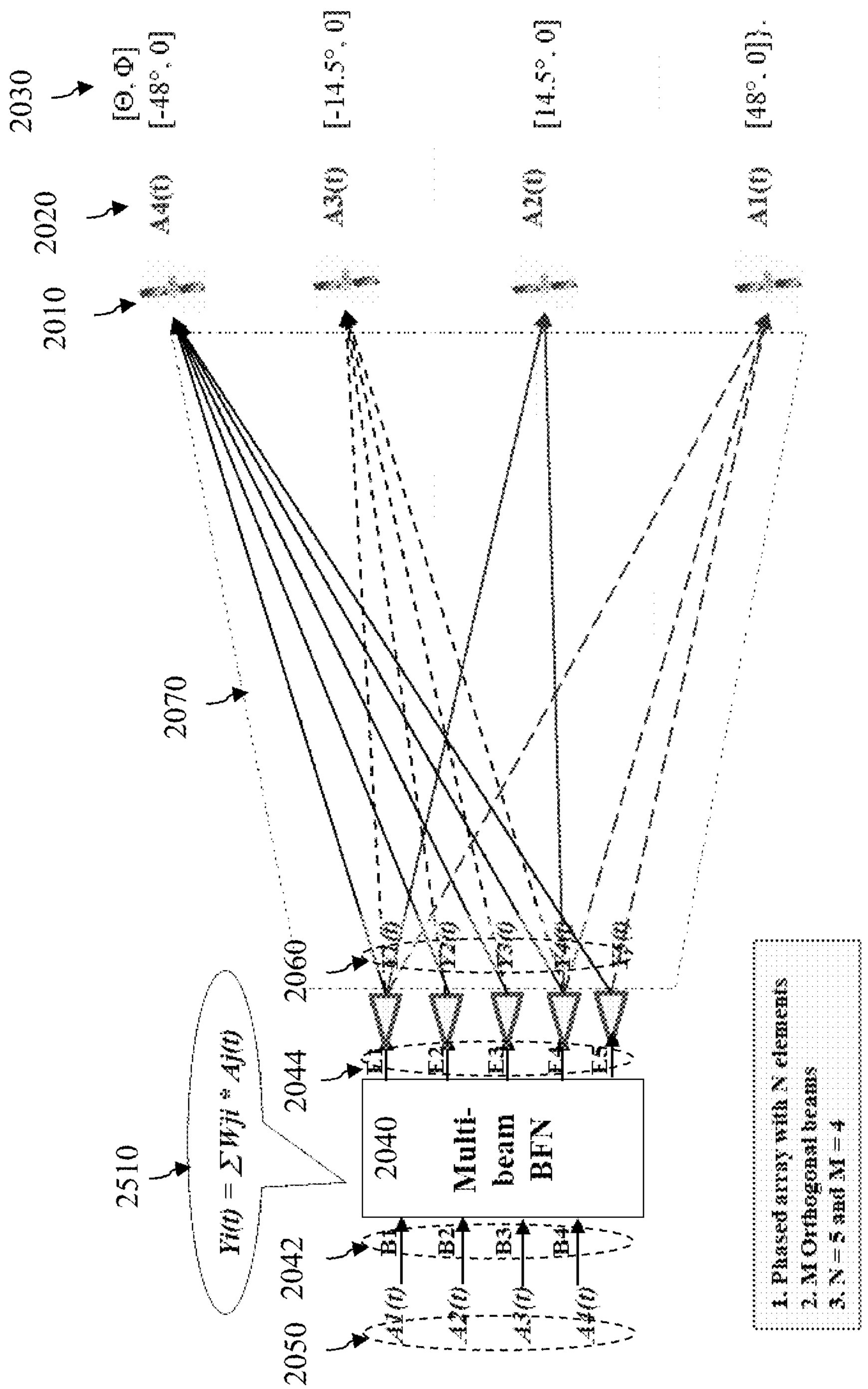
2030
[Θ, Φ]
[-48°, 0]
[-14.5°, 0]
[14.5°, 0]
[48°, 0]}.
2020
A4(t)
A3(t)
A2(t)
A1(t)
2010
2070
2060
Y1(t)
Y2(t)
Y3(t)
Y4(t)
Y5(t)
2044
E1
E2
E3
E4
E5
2040
Multi-beam BFN
2510
Yi(t) = ΣWji * Aj(t)
2042
B1
B2
B3
B4
2050
A1(t)
A2(t)
A3(t)
A4(t)
1. Phased array with N elements
2. M Orthogonal beams
3. N = 5 and M = 4

FIG. 25

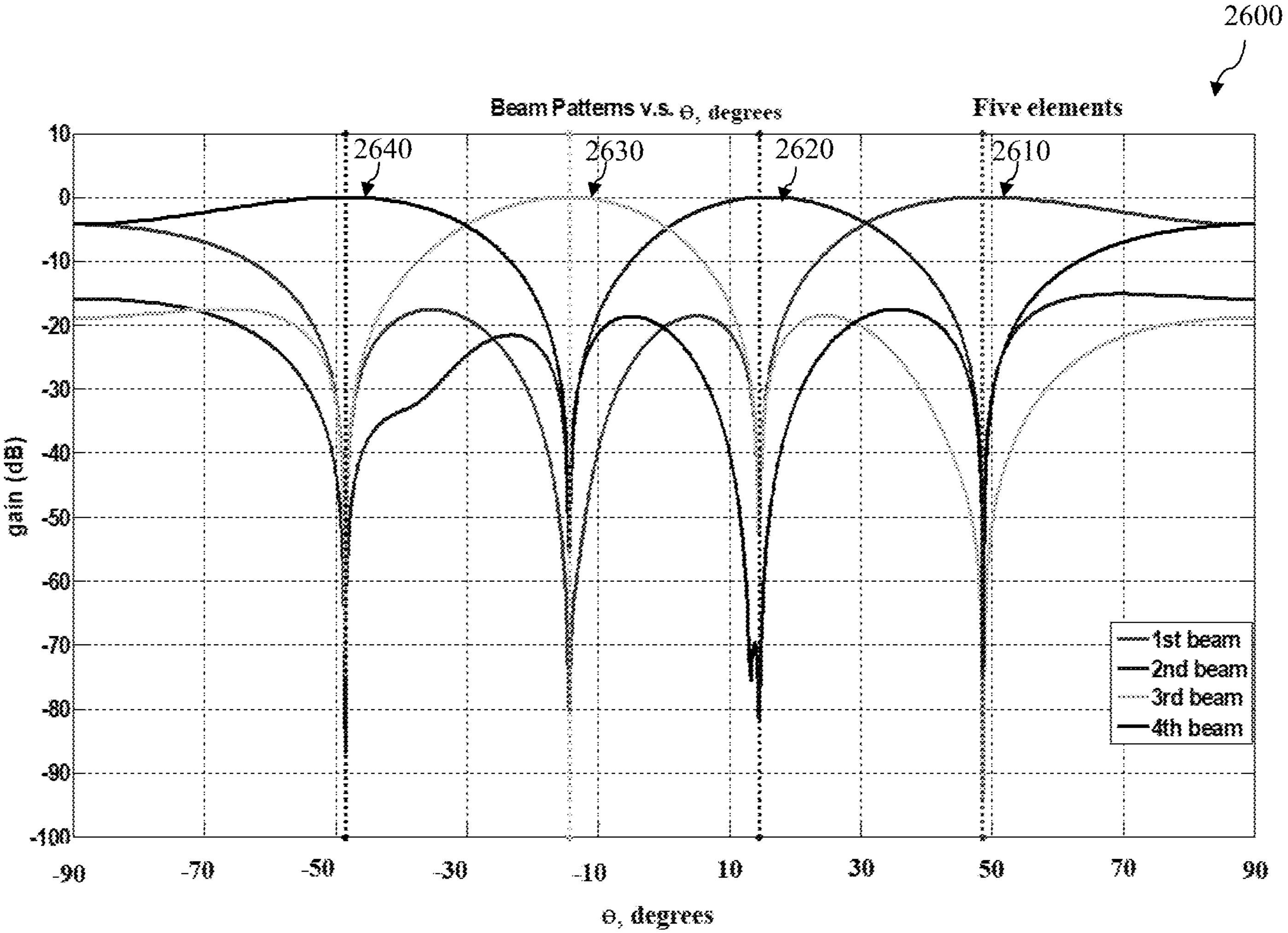
2600
Beam Patterns v.s. θ, degrees
Five elements
2640
2630
2620
2610
gain (dB)
10
0
-10
-20
-30
-40
-50
-60
-70
-80
-90
-100
-90
-70
-50
-30
-10
10
30
50
70
90
θ, degrees
1st beam
2nd beam
3rd beam
4th beam

FIG. 26

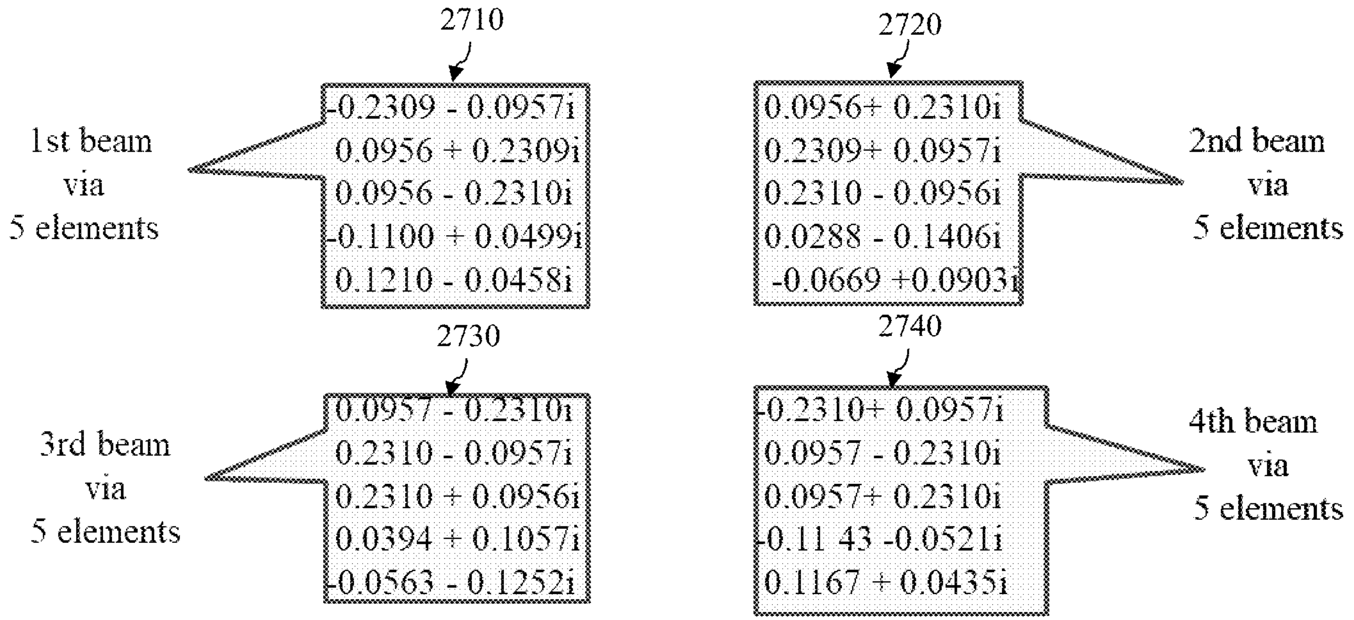
2710
-0.2309 - 0.0957i
0.0956 + 0.2309i
0.0956 - 0.2310i
-0.1100 + 0.0499i
0.1210 - 0.0458i
1st beam via 5 elements
2720
0.0956+ 0.2310i
0.2309+ 0.0957i
0.2310 - 0.0956i
0.0288 - 0.1406i
-0.0669 +0.0903i
2nd beam via 5 elements
2730
0.0957 - 0.2310i
0.2310 - 0.0957i
0.2310 + 0.0956i
0.0394 + 0.1057i
-0.0563 - 0.1252i
3rd beam via 5 elements
2740
-0.2310+ 0.0957i
0.0957 - 0.2310i
0.0957+ 0.2310i
-0.11 43 -0.0521i
0.1167 + 0.0435i
4th beam via 5 elements

FIG. 27

$$\overset{2060}{\begin{bmatrix} y1(t) \\ y2(t) \\ y3(t) \\ y4(t) \\ y5(t) \end{bmatrix}} = \overset{2310}{[\boldsymbol{BWVs}]} * \overset{2060}{\begin{bmatrix} A1(t) \\ A2(t) \\ A3(t) \\ A4(t) \end{bmatrix}}$$

Ai(t): signals for i^{th} beam

yj(t): signals for j^{th} element

$$\overset{2310}{[\boldsymbol{BWVs}]} = \begin{array}{cccc} \left[\begin{matrix} -0.2309-0.0957i \\ 0.0956+0.2309i \\ 0.0956-0.2310i \\ -0.1100+0.0499i \\ 0.1210-0.0458i \end{matrix}\right. & \begin{matrix} 0.0956+0.2310i \\ 0.2309+0.0957i \\ 0.2310-0.0956i \\ 0.0288-0.1406i \\ -0.0669+0.0903i \end{matrix} & \begin{matrix} 0.0957-0.2310i \\ 0.2310-0.0957i \\ 0.2310+0.0956i \\ 0.0394+0.1057i \\ -0.0563-0.1252i \end{matrix} & \left.\begin{matrix} -0.2310+0.0957i \\ 0.0957-0.2310i \\ 0.0957+0.2310i \\ -0.1143-0.0521i \\ 0.1167+0.0435i \end{matrix}\right] \\ \text{BWV1} & \text{BWV2} & \text{BWV3} & \text{BWV4} \\ \text{Beam 1} & \text{Beam 2} & \text{Beam 3} & \text{Beam 4} \\ \text{5 elements} & \text{5 elements} & \text{5 elements} & \text{5 elements} \end{array}$$

FIG. 28

2900

1. **4 to 4 K-muxing; [K-muxing] = [BWVs]**

[yj(t)] = [K-muxing]*[Ai(t)], or $\begin{bmatrix} y1(t) \\ y2(t) \\ y3(t) \\ y4(t) \\ y5(t) \end{bmatrix} = [BWVs]^* \begin{bmatrix} A1(t) \\ A2(t) \\ A3(t) \\ A4(t) \end{bmatrix}$

- Ai(t) = ith input data; i = 1 to 4 and yj(t) = jth output data; j = 1 to 5

2. **4 to 4 K-demuxing; [K-demuxing] = [P]**

- yj(t) = jth input data; j = 1 to 5 ***propagating to 4 different directions for recovering A1(t), A2(t), A3(t) and A4(t)***
- Ai(t) = ith output data; i = 1 to 4
  - A1(t) will be delivered by the 4 element array to a 1st direction at angle $[\theta1,\phi1]$
    - A1(t)= w11* y1(t) +w12 * y2(t) + w13* y3(t) +w14 * y4(t) +w15 * y5(t)
  - A2(t) will be delivered by the 4 element array to a 2nd direction at angle $[\theta2,\phi2]$
    - A2(t)= w21* y1(t) +w22 * y2(t) + w23* y3(t) +w24 * y4(t) +w25 * y5(t)
  - A3(t) will be delivered by the 4 element array to a 3rd direction at angle $[\theta3,\phi3]$
    - A3(t)= w31* y1(t) +w32 * y2(t) + w33* y3(t) +w34 * y4(t) +w35 * y5(t)
  - A4(t) will be delivered by the 4 element array to a 4th direction at angle $[\theta2,\phi2]$
    - A4(t)= w41* y1(t) +w42 * y2(t) + w43* y3(t) +w44 * y4(t) + w45 * y5(t)

FIG. 29

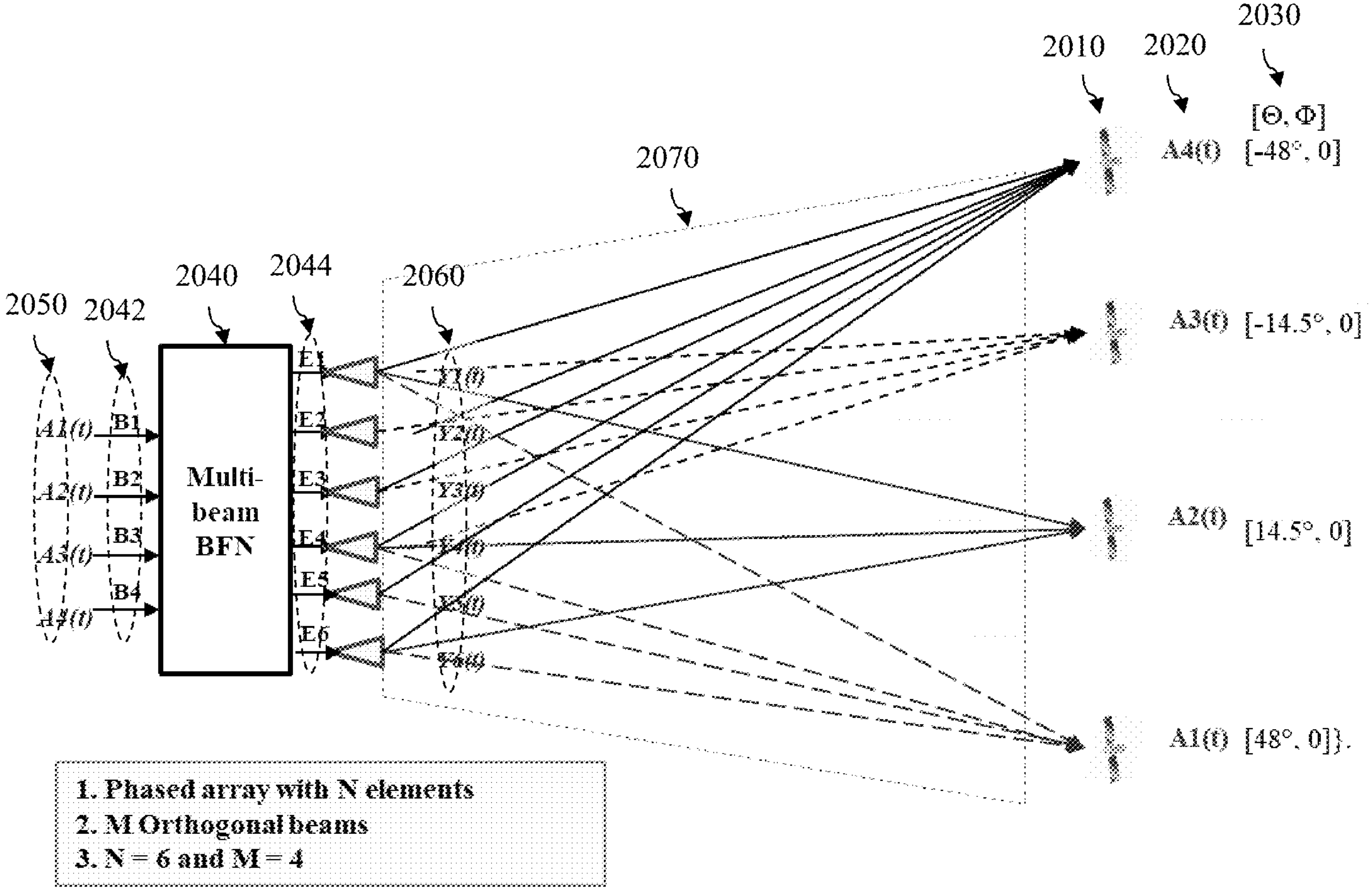
2050
2042
2040
2044
2060
2070
2010
2020
2030
A1(t)
A2(t)
A3(t)
A4(t)
B1
B2
B3
B4
Multi-beam BFN
E1
E2
E3
E4
E5
E6
Y1(t)
Y2(t)
Y3(t)
Y4(t)
Y5(t)
Y6(t)
[Θ, Φ]
A4(t) [-48°, 0]
A3(t) [-14.5°, 0]
A2(t) [14.5°, 0]
A1(t) [48°, 0]}.
1. Phased array with N elements
2. M Orthogonal beams
3. N = 6 and M = 4

FIG. 30

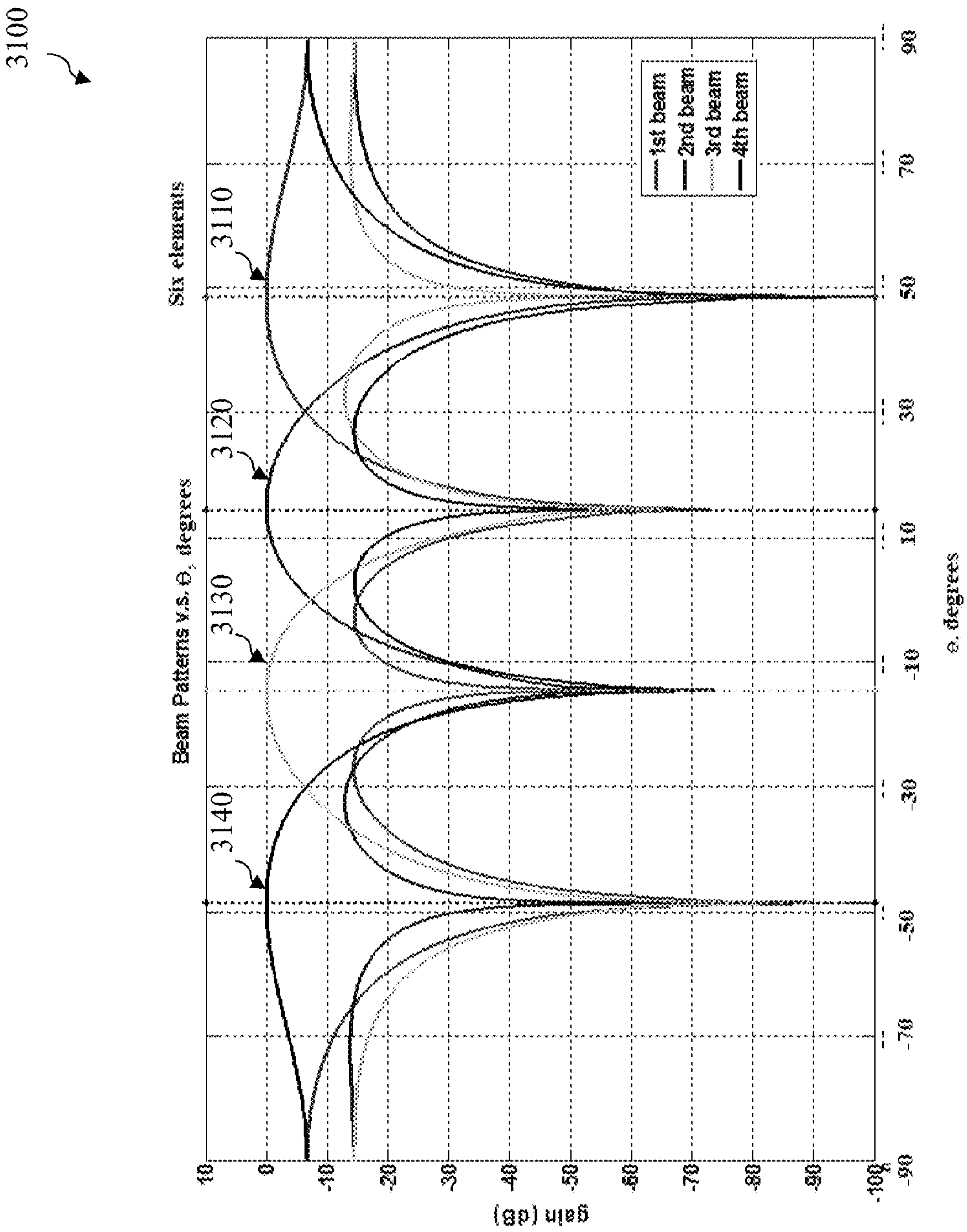
3100
Beam Patterns v.s. Θ, degrees
Six elements
3110
3120
3130
3140
1st beam
2nd beam
3rd beam
4th beam
gain (dB)
10
0
-10
-20
-30
-40
-50
-60
-70
-80
-90
-100
θ, degrees
-90
-70
-50
-30
-10
10
30
50
70
90

FIG. 31

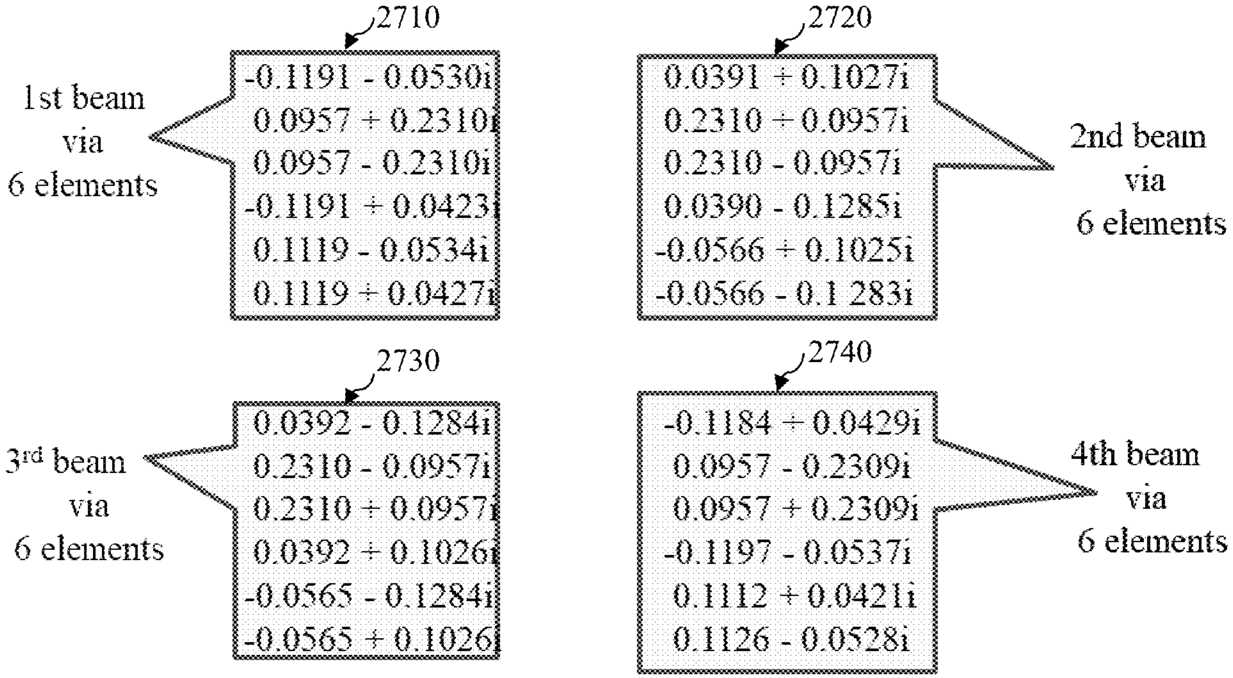
2710
-0.1191 - 0.0530i
0.0957 + 0.2310i
0.0957 - 0.2310i
-0.1191 + 0.0423i
0.1119 - 0.0534i
0.1119 + 0.0427i
1st beam via 6 elements
2720
0.0391 + 0.1027i
0.2310 + 0.0957i
0.2310 - 0.0957i
0.0390 - 0.1285i
-0.0566 + 0.1025i
-0.0566 - 0.1 283i
2nd beam via 6 elements
2730
0.0392 - 0.1284i
0.2310 - 0.0957i
0.2310 + 0.0957i
0.0392 + 0.1026i
-0.0565 - 0.1284i
-0.0565 + 0.1026i
3rd beam via 6 elements
2740
-0.1184 + 0.0429i
0.0957 - 0.2309i
0.0957 + 0.2309i
-0.1197 - 0.0537i
0.1112 + 0.0421i
0.1126 - 0.0528i
4th beam via 6 elements

FIG. 32

$$\overset{2060}{\begin{bmatrix} y1(t) \\ y2(t) \\ y3(t) \\ y4(t) \\ y5(t) \\ y6(t) \end{bmatrix}} = \overset{2310}{[\boldsymbol{BWVs}]} * \overset{2050}{\begin{bmatrix} A1(t) \\ A2(t) \\ A3(t) \\ A4(t) \end{bmatrix}}$$

Ai(t): signal for i^{th} beam

yj(t): signals for j^{th} element

$$\overset{2310}{[\boldsymbol{BWVs}]} = \begin{array}{cccc} \left[\begin{matrix} -0.1191 - 0.0530i \\ 0.0957 + 0.2310i \\ 0.0957 - 0.2310i \\ -0.1191 + 0.0423i \\ 0.1119 - 0.0534i \\ 0.1119 + 0.0427i \end{matrix}\right. & \begin{matrix} 0.0391 + 0.1027i \\ 0.2310 + 0.0957i \\ 0.2310 - 0.0957i \\ 0.0390 - 0.1285i \\ -0.0566 + 0.1025i \\ -0.0566 - 0.1283i \end{matrix} & \begin{matrix} 0.0392 - 0.1284i \\ 0.2310 - 0.0957i \\ 0.2310 + 0.0957i \\ 0.0392 + 0.1026i \\ -0.0565 - 0.1284i \\ -0.0565 + 0.1026i \end{matrix} & \left.\begin{matrix} -0.1184 + 0.0429i \\ 0.0957 - 0.2309i \\ 0.0957 + 0.2309i \\ -0.1197 - 0.0537i \\ 0.1112 + 0.0421i \\ 0.1126 - 0.0528i \end{matrix}\right] \\ \text{BWV1} & \text{BWV2} & \text{BWV3} & \text{BWV4} \\ \text{1st beam} & \text{2nd beam} & \text{3rd beam} & \text{4th beam} \\ \text{6 elements} & \text{6 elements} & \text{6 elements} & \text{6 elements} \end{array}$$

FIG. 33

3400

1. **4 to 4 K-muxing; [K-muxing] = [BWVs]**

[yj(t)] = [K-muxing]*[Ai(t)], or

$$\begin{bmatrix} y1(t) \\ y2(t) \\ y3(t) \\ y4(t) \\ y5(t) \\ y6(t) \end{bmatrix} = [BWVs]^{*} \begin{bmatrix} A1(t) \\ A2(t) \\ A3(t) \\ A4(t) \end{bmatrix}$$

   - Ai(t) = ith input data; i = 1 to 4 and yj(t) = jth output data; j = 1 to 6

2. **4 to 4 K-demuxing; [K-demuxing] = [P]**
   - yj(t) = jth input data; j = 1 to 6 ***propagating to 4 different directions for recovering A1(t), A2(t), A3(t) and A4(t)***
   - Ai(t) = ith output data; i = 1 to 4
     - A1(t) will be delivered by the 4 element array to a 1st direction at angle [θ1,ϕ1]
       - A1(t)= w11*y1(t)+w12*y2(t)+w13*y3(t)+w14*y4(t)+w15*y5(t)+w16*y6(t)
     - A2(t) will be delivered by the 4 element array to a 2nd direction at angle [θ2,ϕ2]
       - A2(t)= w21*y1(t)+w22*y2(t)+w23*y3(t)+w24*y4(t)+w25*y5(t)+w26*y6(t)
     - A3(t) will be delivered by the 4 element array to a 3rd direction at angle [θ3,ϕ3]
       - A3(t)=w31*y1(t) +w32*y2(t)+w33*y3(t)+w34*y4(t)+w35*y5(t)+w36*y6(t)
     - A4(t) will be delivered by the 4 element array to a 4th direction at angle [θ2,ϕ2]
       - A4(t)= w41*y1(t)+w42*y2(t)+w43*y3(t) +w44*y4(t)+w45*y5(t)+w46*y6(t)

FIG. 34

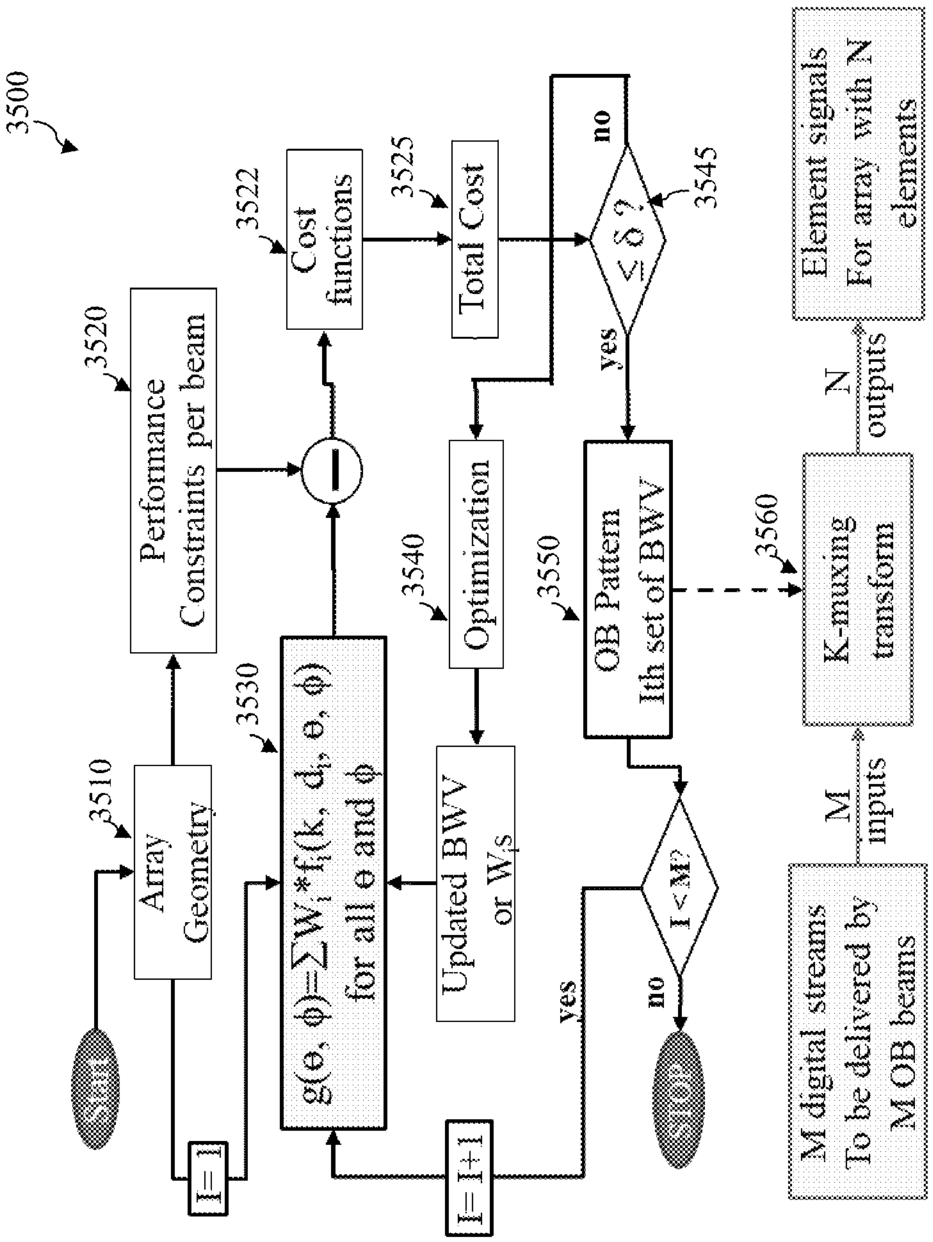
3500
Start
3510
Array Geometry
I = 1
3520
Performance Constraints per beam
3530
$g(\theta, \phi)=\sum W_i * f_i(k, d_i, \theta, \phi)$ for all θ and φ
3522
Cost functions
3525
Total Cost
3545
≤ δ ?
no
yes
3540
Optimization
Updated BWV or W_is
3550
OB Pattern Ith set of BWV
I < M?
yes
no
I = I+1
STOP
3560
K-muxing transform
M digital streams To be delivered by M OB beams
M inputs
N outputs
Element signals For array with N elements

FIG. 35

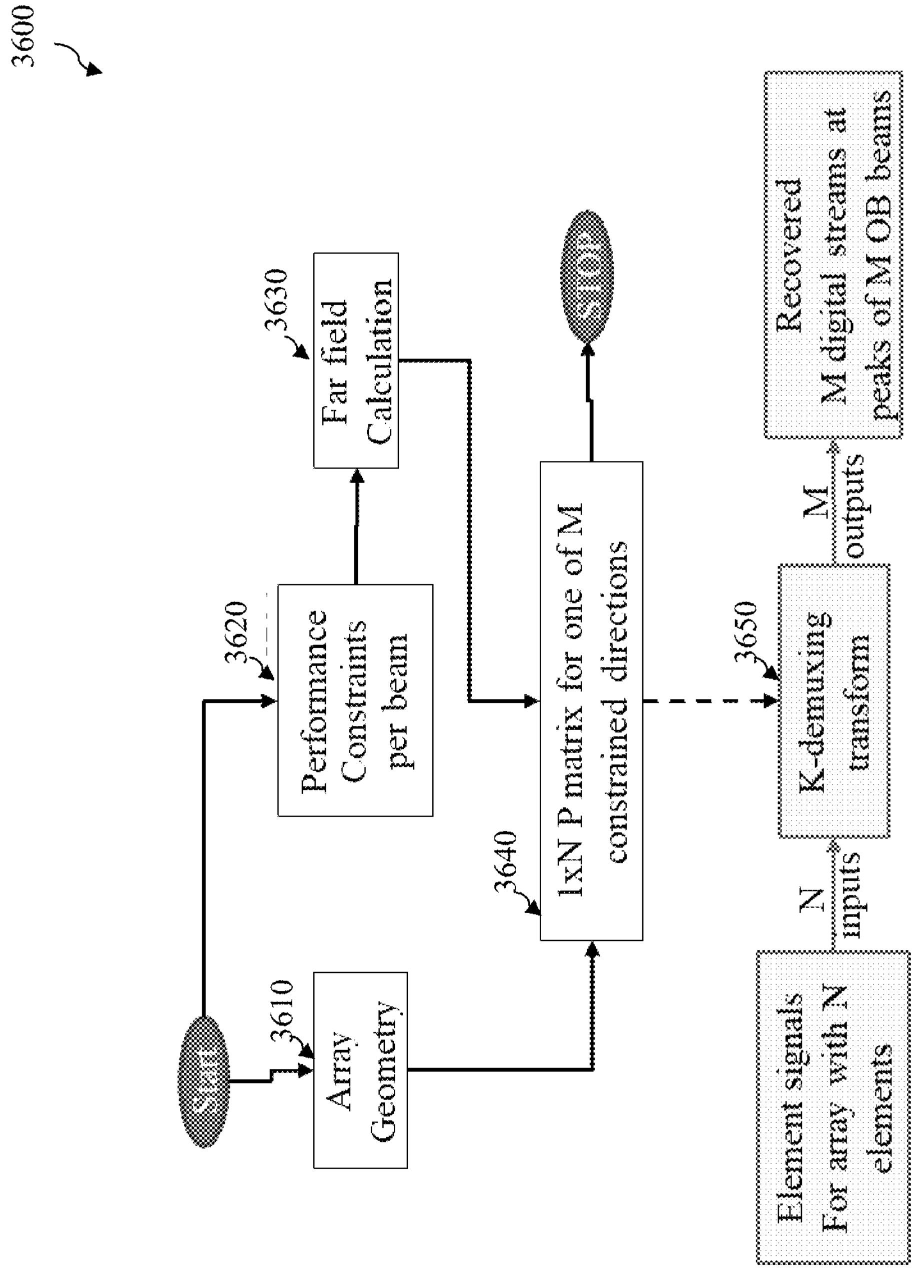
3600
Start
3610
Array Geometry
3620
Performance Constraints per beam
3630
Far field Calculation
3640
1xN P matrix for one of M constrained directions
STOP
Element signals For array with N elements
N inputs
3650
K-demuxing transform
M outputs
Recovered M digital streams at peaks of M OB beams

FIG. 36

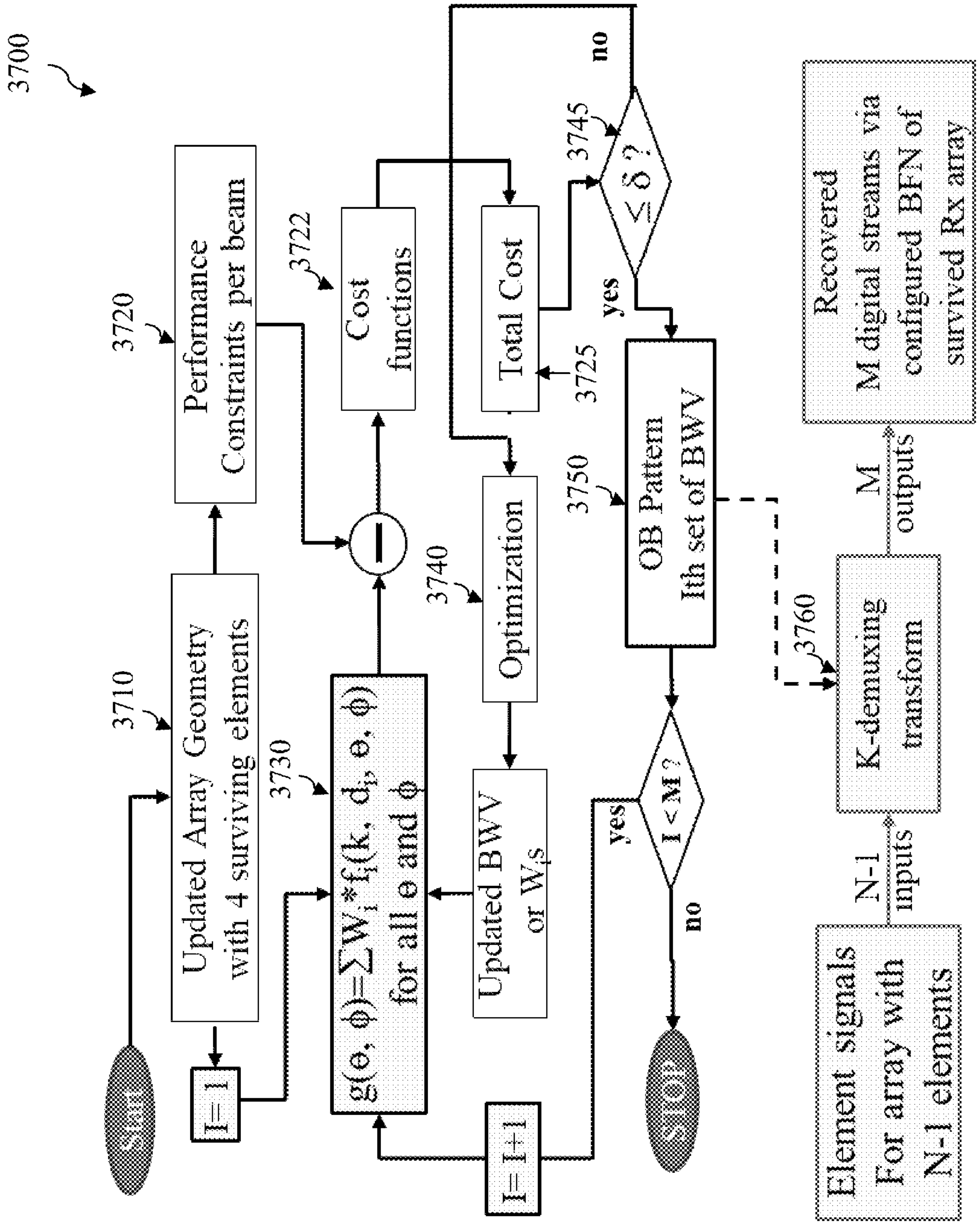
3700
Start
Updated Array Geometry with 4 surviving elements
3710
Performance Constraints per beam
3720
I= 1
$g(\theta, \phi)=\sum W_i * f_i(k, d_i, \theta, \phi)$ for all θ and ϕ
3730
Cost functions
3722
Total Cost
3725
Optimization
3740
Updated BWV or W_s
≤ δ ?
3745
no
yes
OB Pattern Ith set of BWV
3750
I < M ?
yes
no
I= I+1
STOP
K-demuxing transform
3760
Element signals For array with N-1 elements
N-1 inputs
M outputs
Recovered M digital streams via configured BFN of survived Rx array

FIG. 37

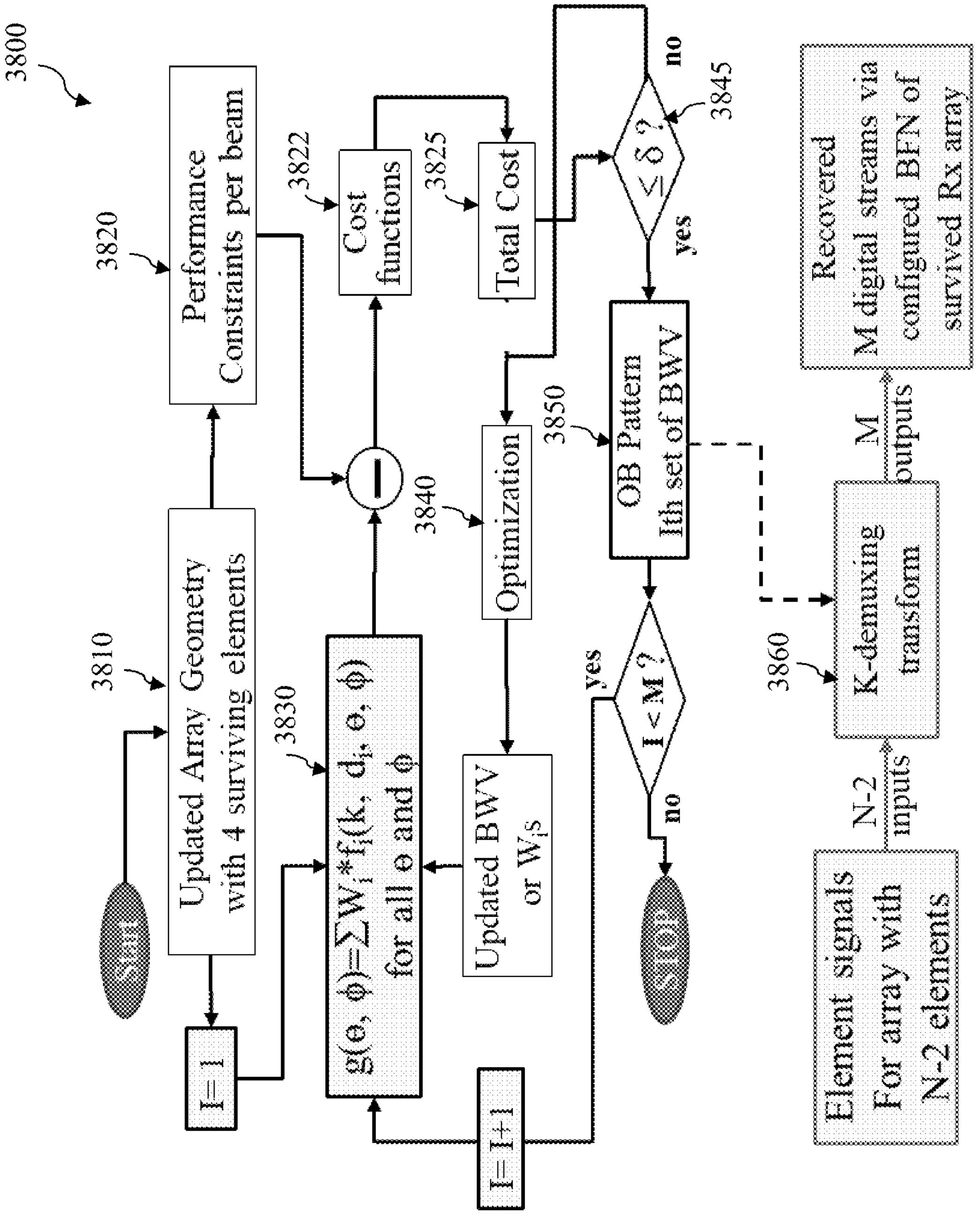
3800
Start
3810
Updated Array Geometry with 4 surviving elements
3820
Performance Constraints per beam
I= 1
3830
$g(\theta, \phi)=\sum W_i * f_i(k, d_i, \theta, \phi)$ for all θ and ϕ
−
3822
Cost functions
3825
Total Cost
3840
Optimization
Updated BWV or W_is
3845
$\leq \delta$?
no
yes
3850
OB Pattern Ith set of BWV
I < M ?
yes
no
I= I+1
STOP
3860
K-demuxing transform
Element signals For array with N-2 elements
N-2 inputs
M outputs
Recovered M digital streams via configured BFN of survived Rx array

FIG. 38

COMPOSITE DATA TRANSPORT AND STORAGE VIA WAVEFRONT MULTIPLEXING

RELATED APPLICATIONS

This application is a continuation of application Ser. No. 15/933,322, filed on Mar. 22, 2018, entitled "COMPOSITE DATA TRANSPORT AND STORAGE VIA WAVEFRONT MULTIPLEXING", which claims the benefit of Provisional Patent Application No. 62/475,026, filed on Mar. 22, 2017. This application is related to U.S. Pat. No. 8,098,612 issued on Jan. 17, 2012, entitled "APPARATUS AND METHOD FOR REMOTE BEAM FORMING FOR SATELLITE BROADCASTING SYSTEMS"; U.S. Pat. No. 8,111,646 issued on Feb. 7, 2012, entitled "COMMUNICATION SYSTEM FOR DYNAMICALLY COMBINING POWER FROM A PLURALITY OF PROPAGATION CHANNELS IN ORDER TO IMPROVE POWER LEVELS OF TRANSMITTED SIGNALS WITHOUT AFFECTING RECEIVER AND PROPAGATION SEGMENTS"; U.S. patent application Ser. No. 14/712,145, filed on May 14, 2015, entitled "SURVIVABLE CLOUD DATA STORAGE AND TRANSPORT"; and U.S. patent application Ser. No. 14/512,959, filed on Oct. 13, 2014, entitled "Enveloping for Cloud Computing via Wavefront Muxing", all of which are expressly incorporated by reference herein in their entireties.

TECHNICAL FIELD

One disclosed aspect of the embodiments is directed to the field of data communication. In particular, the embodiment is directed to data transport and communication using wavefront multiplexing (WFM) technology.

BACKGROUND

Long before the beginning or digital age, people had manually stored data while the 'data storage' from time to time might suffer loss due to lack of availability and privacy protection. With the advancement of digital technology, data storage has been an indispensable function in many aspects of modern era. The need for availability and privacy protection remains central to evolving data storage design.

Data not only resides in storage but also appears in transition among communication terminals and users. To provide quality of service and quality of experience, it is also of significant value to transport data that is highly available and securely protected. The service of data transport should meet requirements of availability and privacy protection to satisfy user's demand for quality and experience.

Repetition coding is one approach to providing availability against the event of data loss. One application of repetition code is RAID (redundant array of independent disks). Among variations of RAID, RAID 1 creates one redundant piece of a data stream. For one data stream, RAID thus creates two identical copies to be stored. The space overhead of RAID 1 is 50%, which is high in state-of-the-art storage, and it bears low level privacy protection if no encoding or other measure is further applied to the stored copy.

SUMMARY

One disclosed aspect of the embodiments is a method and apparatus to provide data transport and communication using wavefront multiplexing (WFM) technique. For signal transmission, a pre-processing device performs a wavefront multiplexing (WFM) transform on M input streams corresponding to M orthogonal beams to generate N output streams using a weight matrix having M beam weight vectors (BWVs) associated with the M orthogonal beams. An antenna array having N elements transmits the N output streams to a plurality of receivers. For signal reception, an antenna array having N elements receives N input streams from a plurality of transmitters. A post-processing device performs a wavefront de-multiplexing (WFD) transform on the N input streams corresponding to M orthogonal beams to generate M output streams using a weight matrix having M beam weight vectors (BWVs) associated with the M orthogonal beams. M and N are positive integers and $1<M\leq N$. The M BWVs are calculated using an optimization procedure based on performance constraints.

BRIEF DESCRIPTION OF THE DRAWINGS

Embodiments may best be understood by referring to the following description and accompanying drawings that are used to illustrate embodiments. In the drawings:

FIG. **1** is a diagram illustrating a system using a data transport and/or storage processing system according to one embodiment.

FIG. **2** is a diagram illustrating a data transport and/or storage processing system for transmitting or writing data to a storage system according to one embodiment.

FIG. **3** is a diagram illustrating an architecture for the data transport and/or storage processing system according to one embodiment.

FIG. **4** is a diagram illustrating a data transport and/or storage processing system for transmitting or writing data to three local storage systems and one cloud storage device according to one embodiment.

FIG. **5** is a diagram illustrating a data transport and/or storage processing system for transmitting or writing data to two local storage systems and two cloud storage devices according to one embodiment.

FIG. **6** is a diagram illustrating a data transport and/or storage processing system for transmitting or writing data to a storage system having two devices and two cloud storage devices according to one embodiment.

FIG. **7** is a diagram illustrating a data transport and/or storage processing system for transmitting or writing data to a storage system and four cloud storage devices according to one embodiment.

FIG. **8** is a diagram illustrating a data transport and/or storage processing system for transmitting or writing data using a systematic coder according to one embodiment.

FIG. **9** is a diagram illustrating a data transport and/or storage processing system for transmitting or writing data using a cascaded structure for the WFM processor according to one embodiment.

FIG. **10** is a diagram illustrating a data transport and/or storage processing system for transmitting or writing data using a cascaded structure for the WFM processor according to one embodiment.

FIG. **11** is a diagram illustrating a data transport and/or storage processing system for receiving or reading data from a storage system according to one embodiment.

FIG. **12** is a diagram illustrating a data transport and/or storage processing system for receiving or reading data from a storage system and a cloud storage according to one embodiment.

FIG. **13** is a diagram illustrating a data transport and/or storage processing system for receiving or reading data from a storage system and a cloud storage according to one embodiment.

FIG. **14** is a diagram illustrating a data transport and/or storage processing system for receiving or reading data using a systematic decoder according to one embodiment.

FIG. **15** is a diagram illustrating a data transport and/or storage processing system for receiving or reading data using a cascaded structure for the WFD processor according to one embodiment.

FIG. **16** is a diagram illustrating a data transport and/or storage processing system for receiving or reading data using a cascaded structure for the WFD processor according to one embodiment.

FIG. **17** is a diagram illustrating a data writing system using cascaded K-muxing according to one embodiment.

FIG. **18** is a diagram illustrating a data reading system using cascaded K-de-muxing according to one embodiment.

FIG. **19** is a diagram illustrating a WF processor according to one embodiment.

FIG. **20** is a diagram illustrating a 4-element array forming 4 concurrent beams with OB radiation patterns according to one embodiment.

FIG. **21** is a diagram illustrating simulated radiation patterns of 4 shaped beams according to one embodiment.

FIG. **22** is a diagram illustrating 4×4 matrices corresponding to 4 optimized Beam Weight Vectors (BWVs) according to one embodiment.

FIG. **23** is a diagram illustrating 4 optimized Beam Weight Vectors (BWVs) according to one embodiment.

FIG. **24** is a diagram illustrating K-muxing and K-de-muxing transforms for BWVs from a 4-element linear array according to one embodiment.

FIG. **25** is a diagram illustrating OB radiation patterns from 4 concurrent beams generated by a 5-element array according to one embodiment.

FIG. **26** is a diagram illustrating simulated radiation patterns using beam-shaping algorithms and performance constraints of the directions of 4 shaped beams according to one embodiment.

FIG. **27** is a diagram illustrating the BWVs for 4 OB beams from a 5-element array according to one embodiment.

FIG. **28** is a diagram illustrating the BWVs generated by an optimizing processing for a 5-element array according to one embodiment.

FIG. **29** is a diagram illustrating K-muxing and K-de-muxing transforms for BWVs from a 5-element linear array according to one embodiment.

FIG. **30** is a diagram illustrating OB radiation patterns from 4 concurrent beams generated by a 6-element array according to one embodiment.

FIG. **31** is a diagram illustrating simulated radiation patterns using beam-shaping algorithms and performance constraints of the directions of 4 shaped beams according to one embodiment.

FIG. **32** is a diagram illustrating the BWVs for 4 OB beams from a 6-element array according to one embodiment.

FIG. **33** is a diagram illustrating the BWVs generated by an optimizing processing for a 6-element array according to one embodiment.

FIG. **34** is a diagram illustrating K-muxing and K-de-muxing transforms for BWVs from a 6-element linear array according to one embodiment.

FIG. **35** is a flowchart illustrating a method to calculate the BWVs for an array with N elements generating concurrent M beams according to one embodiment.

FIG. **36** is a flowchart illustrating a method to calculate various propagation vectors for different beams of an array with N elements according to one embodiment.

FIG. **37** is a flowchart illustrating an alternate method to reconstitute the M beam signals based on N element signals (N=5 and M=4) according to one embodiment.

FIG. **38** is a flowchart illustrating an alternate method to reconstitute the M beam signals based on N element signals (N=6 and M=4) according to one embodiment.

DETAILED DESCRIPTION

One disclosed aspect of the embodiments is a method and apparatus to provide data communication using wavefront multiplexing (WFM) technique. The technique allows signal transmissiona and reception via orthogonal beams.

For signal transmission, a pre-processing device performs a wavefront multiplexing (WFM) transform on M input streams corresponding to M orthogonal beams to generate N output streams using a weight matrix having M beam weight vectors (BWVs) associated with the M orthogonal beams. An antenna array having N elements transmits the N output streams to a plurality of receivers. For signal reception, an antenna array having N elements receives N input streams from a plurality of transmitters. A post-processing device performs a wavefront de-multiplexing (WFD) transform on the N input streams corresponding to M orthogonal beams to generate M output streams using a weight matrix having M beam weight vectors (BWVs) associated with the M orthogonal beams. M and N are positive integers and $1<M\leq N$. The M BWVs are calculated using an optimization procedure based on performance constraints.

Wavefront multiplexing (WF muxing, or K-muxing) and wavefront demultiplexing (WF demuxing or K-demuxing) are multi-dimension data processing methods. Both K-muxing and K-demuxing define transformation of multi-dimensional signals or data streams that feature particular distribution patterns (or 'wavefronts') in K-space. K-muxing and K-demuxing enable redundancy to enhance availability and provide scrambled signals or data streams designed toward privacy protection. The data transport and communication may store data in storage sites. The storage sites may include at least one of a network attached storage (NAS) device, a direct access storage (DAS) device, a storage area network (SAN) device, redundant array of independent disks (RAIDs), a cloud storage, a hard disk, a solid-state memory device, and a device capable of storing data.

In the following description, numerous specific details are set forth. However, it is understood that embodiments may be practiced without these specific details. In other instances, well-known circuits, structures, and techniques have not been shown to avoid obscuring the understanding of this description. One disclosed feature of the embodiments may be described as a process which is usually depicted as a flowchart, a flow diagram, a structure diagram, or a block diagram. One embodiment may be described by a schematic drawing depicting a physical structure. It is understood that the schematic drawing illustrates the basic concept and may not be scaled or depict the structure in exact proportions.

The term "writing" refers to the act of storing data on or transmitting or sending data through multiple physical and logical dimensions. The term "reading" refers to the act of retrieving data from or receiving data through multiple physical and logical dimensions. Physical dimensions may refer to computers, mobile devices, data centers and so on. Logical dimensions may refer to allocated or virtualized resources for data storage or data transport. Both physical and logical dimensions may also refer to communication channels in general.

One aspect of the embodiments relates to distributed data storages with built-in redundancy for a single stream data subdivided into multiple (M) data substreams or M independent data streams, converted into K-muxed domain with M+N output wavefront components (WFCs), and stored these M+N WFC output data as M+N separated data storage sets, where N, and M are non-negative integers. As a result, the stored data sets are WFCs in the format of linear combinations of the data sets, instead of the data sets themselves. The coefficients involved in K-muxing and K-demuxing may take complex values. Hence the vector of coefficients involved in K-muxing and K-demuxing may include, but not limited to, column vectors in Hadamard transformation, Fourier transformation, etc. The matrix comprising coefficients involved in K-muxing and K-demuxing features subsets of M rows that have full rank in order to satisfy the redundancy requirements.

In general, the input ports of a K-muxing transform are referred to as "slices" and the output ports are referred to as "WFCs". For instance, the first and the third input ports to a 16-to-16 K-muxing transform are referred as the slice 1 and the slice 3, respectively. Similarly the 13th and the 16th output ports are called the WFC 13 and the WFC16, respectively. Collectively, the output data from a K-muxing transform also referred as the K-muxed data are outputted from all the WFC ports. A first input stream connected to slice 1 of the 16-to-16 K muxing transform shall appear in all the WFC ports with a unique wavefront called wavefront 1 indicated as wavefront vector 1 or WFV1 over a 16-dimensional space; each dimension representing an output from a unique WFC port. Similarly, a second input stream connected to slice 16 of the 16-to-16 K muxing transform shall also appear in all the WFC ports with another unique wavefront called wavefront 16 indicated as wavefront vector 16 or WFV16.

Existing redundancy-generation coding such as erasure code often appears as systematic code, which preserves original data streams in addition to computed parity data streams. The preserved original data streams should be protected, unless otherwise further processed by measures such as encryption. On the other hand, K-muxing renders each WFC unintelligible to protect every data stream to be stored or transported.

Assume, in a writing process, a data stream's M substreams ($S_1, S_2, \ldots, S_M$) are transformed to M+N WFCs ($D_1, D_2, \ldots, D_{M+N}$) via K-muxing. Each WFC D_i can be further coded by a coding function that generates coded components (CCs) $R_{i,1}, R_{i,2}, \ldots, R_{i,L}$ to be stored in or transported through multiple physical and logical dimensions. To 'read' the substreams ($S_1, S_2, \ldots, S_M$), the set of CCs $\{) R_{i,1}, R_{i,2}, \ldots, R_{i,L}\}$ (or its subset) associated with D_i can be used to first decode D_i via a decoding function; and then a subset (with size no less than M) of the WFCs $\{D_1, D_2, \ldots, D_{M+N}\}$ can be used to reconstitute $S_1, S_2, \ldots, S_M$ via K-demuxing followed by the recovery of the original data stream. Hence, in the writing process, K-muxing can be performed, proceeding the execution of the coding function. In the corresponding reading process, decoding takes place first, followed by K-demuxing.

Assume, in a writing process, a data stream is transformed by a K-muxer, generating WFCs $D_1, D_2, \ldots, D_{M+N}$. A coding function can be enabled to take all WFCs ($D_1, D_2, \ldots, D_{M+N}$) as input, generating CCs $R_1, R_2, \ldots, R_L$), where L is an integer, as output to be stored in or transported through multiple physical and logical dimensions. In the corresponding reading process, a decoding function can be enabled to take the set of CCs $\{R_1, R_2, \ldots R_L\}$ or its subset as input, recovering the set of WFCs $\{D_1, D_2, \ldots, D_{M+N}\}$ or its subset as output. A K-demuxer can then be enabled to take the set of WFCs $\{D_1, D_2, \ldots, D_{M+N}\}$ or its subset as input and then reconstitute the original data stream.

One can also arrange the K-muxer and coding function as follows. Assume, in a writing process, a data stream is transformed by a K-muxer, generating WFCs $D_1, D_2, \ldots, D_{M+N}$. Several coding functions can be enabled in parallel, each of which takes one subset of the set $\{D_1, D_2, \ldots, D_{M+N}\}$ as input denoted by $\{D_{i,1}, D_{i,2}, \ldots, D_{i,Q}\}$, where Q is an integer, and generates a set of CCs $\{R_{i,1}, R_{i,2}, \ldots, R_{i,L}\}$ to be stored in and transported through multiple physical and logical dimensions. In the corresponding reading process, all or some decoding functions can be enabled, each of which can take one subset of some CC set $\{R_{i,1}, R_{i,2}, \ldots, R_{i,L}\}$ as input and generate a set of WFCs $\{D_{i,1}, D_{i,2}, \ldots, D_{i,Q}\}$ or its subset as output. A K-demuxer can then be enabled to take the set of WFCs $\{D_1, D_2, \ldots, D_{M+N}\}$ or its subset (with size no less than M) as input and then reconstitute the original data stream.

The K-muxer and coding function can also be arranged in different orders. Assume, in a writing process, a data stream is encoded by a coding function, generating CCs $R_1, R_2, \ldots, R_M$. A K-muxer can be enabled to take all CCs ($R_1, R_2, \ldots, R_M$) as input, generating M+N WFCs ($D_1, D_2, \ldots, D_{M+N}$) as output to be stored in or transported through multiple physical and logical dimensions. In the corresponding reading process, a K-demuxer can be enabled to take a subset (with size no less than M) of the WFCs ($D_1, D_2, \ldots, D_{M+N}$) as input, generating the set of CCs $\{R_1, R_2, \ldots, R_M\}$ or its subset as output. A decoding function can then be enabled to take the set of CCs $\{R_1. R_2, \ldots, R_M\}$ or its subset as input and then reconstitute the original data stream.

One can also arrange the K-muxer and coding function as follows. Assume, in a writing process, a data stream is encoded by a coding function, generating CCs $R_1, R_2, \ldots, R_L$. Several K-muxers can be enabled in parallel, each of which takes one subset of the set $\{R_1, R_2, \ldots, R_L\}$ as input denoted by $\{R_{i,1}, R_{i,2}, \ldots, R_{i,M}\}$ and generates a set of WFCs $\{D_{i,1}, D_{i,2}, \ldots, D_{i,(M+N)}\}$ to be stored in and transported through multiple physical and logical dimensions. In the corresponding reading process, all or some K-demuxers can be enabled, each of which can take one subset (with size no less than M) of some WFC set $\{D_{i,1}, D_{i,2}, \ldots, D_{i,(M+N)}\}$ as input and generate a set of CCs $\{R_{i,1}, R_{i,2}, \ldots, R_{i,M}\}$ or its subset as output. A decoding function can then be enabled to take the set of CCs $\{R_1, R_2, \ldots, R_M\}$ or its subset as input and then reconstitute the original data stream.

K-muxers and K-demuxers can also be cascaded in designated order according to the requirements of resource allocation, as disclosed in this disclosure.

FIG. **1** is a diagram illustrating a system **100** using a data transport and/or storage processing system according to one embodiment. The system **100** includes a data transport and/or storage processing system **110**, a source network **120**, a source storage system **130**, a source computer system **140**, a destination network **170**, a destination storage system **180**, and a destination computer system **190**. Note that the source device may be the same as the destination device. For example, the source network **120** may be the same as the destination network **170**. The system **100** may contain more or less than the above components. The system **100** may function to transport data and write or transmit data to a storage system, such as the destination storage system **180**. The system **100** may also function to transport data and read or receive data from a storage system, such as the source storage system **130**. In addition, the system **100** may function to read or receive data from one end and to write or transmit data to another end, including both source devices and destination devices.

The data transport and/or storage processing system may receive or read a stream of data from the source network **120**, the source storage system **130**, or the source computer system **140**. The data or stream of data may be an original stream of data or content that has not been processed by the processing system **110**, or it may have already been processed by the processing system **110** and is now ready to be reconstituted to produce the original data or stream of data.

The source network **120** may be any type of network, wired or wireless, including broadband, local area network (LAN), the Internet, intranet, or cloud. The network **120** may connect to any device that have storage capability or produce content that may be transmitted. In one embodiment, the network **120** may be connected to storage devices **122** and **124**. The storage devices **122** and **124** may be any one of a network attached storage (NAS) device, a direct access storage (DAS) device, or a storage area network (SAN) device. The NAS device may use any suitable data transmission methods, such as Transmission Control Protocol/Internet Protocol (TCP/IP), Ethernet. The DAS device may employ any of the interfaces such as small computer system interface (SCSI), serial attached SCSI (SAS), Advanced Technology Attachment (ATA), etc. The SAN device may use any suitable interface for data transmission such as Fiber Channel, IP.

The source storage system **130** may be a highly reliable storage system such as a group of redundant array of independent disks (RAIDs) $\mathbf{130}_1, \ldots, \mathbf{130}_M$. The RAIDs **130** may be any type of RAIDs that provide data redundancy, fault tolerance, or performance improvement. Any suitable level may be configured. For example, RAID 0 provides striping that distributes contents of files among the disks, RAID 1 provides data mirroring in which data is written identically to two drives, thereby producing a “mirrored set” of drives.

The source computer system **140** may be any suitable computer system having storage capability, including a server, a desktop computer **142**, a laptop computer, a mobile device such as panel computer or telephone, video or image capture device, etc. It may include storage devices such as hard disk **144**, solid-state drive **146**, or thumb drive **148**.

The data from the source network **120**, the source RAIDs **130**, or the source computer system **140** are transferred to the processing system **110** via a bus or channel **150**.

The processing system **110** processes the data and transmits, sends, writes, or stores the processed data to a destination device, including the destination network **170**, the destination storage device **180**, and the destination computer system **190**. Similar to their source counterparts, the destination network **170** may connect to storage devices **172** and **174**. The storage devices **172** and **174** may be any one of a NAS device, a DAS device, or a SAN device. The destination storage device **180** may have RAIDs $\mathbf{180}_1, \ldots, \mathbf{180}_N$; and the destination computer system **190** may have a desktop computer **192**, a hard drive **194**, a solid-state drive (flash devices) **196**, and a thumb drive **198**. The writing or storing data into these destination devices may be performed in a distributed manner. In other words, output data streams from the processing system **110** may be distributed over any combination of these destination devices. For example, if there are 4 output streams from the processing system **110**, three may be stored in the RAIDs **180**, and one may be stored in a cloud storage device.

The system **100** may operate in a writing mode or a reading mode. In the writing mode, a source stream S is available to be processed and written or stored in any of the destination devices **170**/**180**/**190**. There are a number of embodiments in the writing mode, shown in FIGS. **2**, **4**-**10**. In the reading mode, a number of storage streams are available from a least a storage device **120**/**130**/**140** to be processed to recover or reconstitute the source stream S. There are a number of embodiments in the reading mode, shown in FIGS. **11**-**16**. In essence, the process in the reading mode of the data streams D_1's operates in reverse of the process that writes the data streams D_1's to the storage device(s).

FIG. **2** is a diagram illustrating the data transport and/or storage processing system **110** for transmitting or writing data to a storage system according to one embodiment. The processing system **110** may include a segmenter **210** and a WFM processor **220**. The processing system **110** may include more or less than the above components. For clarity, components of the storage system **170**/**180**/**190** are shown in FIG. **2** as RAID 1 **232**, **234**, **236**, and **238**. In other embodiments, any of the storage devices **170**/**180**/**190** may be used.

The segmenter **210** is a pre-processor that pre-processes the source stream S, which comes from a source device (e.g., the source network **120**, the source storage system **130**, or the source computer system **140**) to produce the M input streams. In the illustrative example shown in FIG. **2**, M=3. In other words, the segmenter **210** splits the source stream S into 3 data streams or segments S_1, S_2, and S_3. The splitting may be performed using a pre-determined method such as permutation.

The WFM processor **220** performs WFM on the M input streams to generate N output streams as the WF components (WFC). In the illustrative example in FIG. **2**, M=3 and N=4. So, the WFM processor **220** performs the WFM on the 3 input streams or segments S_1, S_2, and S_3 to generate 4 output streams D_1, D_2, D_3, and D_4. The WFM is essentially a matrix multiplication of the input vector $S=(S_1, S_2, S_3)^T$ (T indicates a transpose vector) and the coefficient matrix $[w_{ij}]$ as follows:

$$\begin{bmatrix} D_1 \\ D_2 \\ D_3 \\ D_4 \end{bmatrix} = \begin{bmatrix} w_{11} & w_{12} & w_{13} \\ w_{21} & w_{22} & w_{23} \\ w_{31} & w_{32} & w_{33} \\ w_{41} & w_{42} & w_{43} \end{bmatrix} \begin{bmatrix} S_1 \\ S_2 \\ S_3 \end{bmatrix}. \tag{1}$$

Equation (1) gives rise to the following:

$$D_1 = w_{11}S_1 + w_{12}S_2 + w_{13}S_3 \tag{2a}$$

$$D_2 = w_{21}S_1 + w_{22}S_2 + w_{23}S_3 \tag{2b}$$

$$D_3 = w_{31}S_1 + w_{32}S_2 + w_{33}S_3 \tag{2c}$$

$$D_4 = w_{41}S_1 + w_{42}S_2 + w_{43}S_3 \tag{2d}$$

As seen from the above equations, each of the output streams D_i's (i=1, 2, 3, 4), may be considered as a linear combination of the coefficients w_{ij}'s (i=1, 2, 3, 4; j=1, 2, 3), and the input streams S_j's (j=1, 2, 3). To solve for S_j's (j=1, 2, 3), we need only three independent equations. Since there are 4 equations, one is extraneous and may be ignored. For example, the output D_4 may not be used. Alternatively, all 4 may be used with one is redundant, used for increasing fault tolerance in case one of the three outputs is in error or lost. Suppose D_4 is not used, the above set of equations reduces to (2a), (2b) and (2c) which can be solved by a number of methods such as substitution, elimination, or Kramer's rule, as are well known by one skilled in the art.

The three column vectors of the matrix in (1) represent three 'wavefronts' that feature three distribution patterns of segments S_1, S_2 and S_3 respectively. Each coefficient w_{ij} can take real or complex value. As discussed above, any sub-matrix comprising three rows of the matrix in (1) has full rank in order to fulfill the redundancy requirements: any three wavefront components (WFCs) of D_1, D_2, D_3 and D_4 are sufficient to recover three segments S_1, S_2 and S_3.

Another way to envision this transformation is to assume there are 4 input streams S_1, S_2, S_3, and S_4, and the input vector [S] is a column vector with 4 components where S_4 is set to zero. The coefficient matrix therefore may be organized as a 4×4 matrix. The matrix multiplication may be performed as follows:

$$\begin{bmatrix} D_1 \\ D_2 \\ D_3 \\ D_4 \end{bmatrix} = \begin{bmatrix} w_{11} & w_{12} & w_{13} & w_{14} \\ w_{21} & w_{22} & w_{23} & w_{24} \\ w_{31} & w_{32} & w_{33} & w_{34} \\ w_{41} & w_{42} & w_{43} & w_{44} \end{bmatrix} \begin{bmatrix} S_1 \\ S_2 \\ S_3 \\ 0 \end{bmatrix}. \tag{3}$$

The output from each WFC is processed by RAID 1 that performs mirroring, namely replication. Data storage sites or devices **232**, **234**, **236**, and **238** perform 'mirroring' functions such that $D_i=R_{i,1}=R_{i,2}$, i=1, 2, 3, 4. Four sets $\{R_{i,1}, R_{i,2}\}$, i=1, 2, 3, 4, may be stored in four physical and logical dimensions such as four separate network-attached storage (NAS) sites or devices. These NAS sites may be local NAS sites, on private cloud or on public cloud. One such distribution may feature three local NAS sites and the remaining one in a storage site on public cloud. The local distribution of three WFM data sites will be sufficient for reconstituting the stored data, while the one on cloud provides additional redundancy.

The WFM processor **220** may also be re-configured to take a known data stream as a 4^{th} input (not shown). This 'injected' data stream may appear as a dominating 'envelope' over the four WFCs D_1, D_2, D_3 and D_4. Systems, methods and apparatus for digital enveloping have been discussed extensively in the U.S. patent application Ser. No. 14/512,959, filed on Oct. 13, 2014. The WFM processor **220** may perform WFM on the M input streams including an envelope to generate the N output streams including an enveloped output stream which is substantially identical to the envelope.

FIG. **3** is a diagram illustrating an architecture for the data transport and/or storage processing system **220** according to one embodiment. The architecture correspond to the 4×4 matrix shown in Equation (2) above. The processing system **220** includes a storage device **310** such as a memory that stores the coefficients w_{ik}'s (j, k=1, . . . , 4), multipliers **322**, **324**, **326**, and **328** and an adder **330**. For fully parallel operations, four sets of the 4 multipliers and one adder will be needed. Any combination of devices may be employed. For example, a single multiplier and a 2-input adder may be used where the multiplier performs multiplication sequentially and the adder acts like an accumulator to accumulate the partial products. The input S_4 may be unused or us an envelope for envelope processing as discussed above. The four multipliers **322**, **324**, **326**, and **328** and the adder **330** may form a linear combiner that perform a linear combination of the coefficients w_{ik}'s and the input streams S_k's as discussed above.

It should also be noted that while the architecture **220** is shown for the WFM processor, it is also applicable for the WFD processor because both types of processor involve a matrix multiplication. The differences are the types of inputs and outputs and the matrix coefficients in the memory **310**.

FIG. **4** is a diagram illustrating the data transport and/or storage processing system **110** for transmitting or writing data to three local storage systems and one cloud storage device according to one embodiment. The processing system **110** in FIG. **4** is similar to the system **110** in FIG. **2** except that the RAID 1 device **238** is replaced by the network cloud **170** and a storage device R_4 **420**.

The WFM processor **220** performs WFM on the three input streams S_1, S_2 and S_3 and generates the four output streams WFCs D_1, D_2, D_3 and D_4 as given in equation (1) above. The three output streams D_1, D_2, D_3 are written or stored in three local storage devices **232**, **234**, and **236**, respectively (e.g., local NAS sites). The output stream D_4 may be stored in a public storage R_4 **420** via cloud **170**. As discussed above, the data stored locally are sufficient to recover the segmented streams S_1, S_2, and S_3. In case one is lost or the corresponding NAS site fails, the data D_4 may be retrieved from the cloud storage **420**. It then can be used together with the remaining two data streams to recover the segmented streams S_1, S_2, and S_3.

FIG. **5** is a diagram illustrating the data transport and/or storage processing system **110** for transmitting or writing data to two local storage systems and two cloud storage devices according to one embodiment. The processing system **110** in FIG. **5** is similar to the system **110** in FIG. **2** except that the RAID 1 device **238** and RAID 1 device **236** are replaced by the network cloud **170** and two storage devices R_3 **520** and R_4 **420**.

As discussed above, the two data streams D_1 and D_2 stored in the local NAS devices **232** and **234** are not sufficient to recover the segmented streams S_1, S_2, and S_3. One data stream stored on the cloud devices R_3 **520** and R_4 **420** may be retrieved to be used together with the two data streams D_1 and D_2 to recover the segmented streams S_1, S_2, and S_3.

FIG. **6** is a diagram illustrating a data transport and/or storage processing system for transmitting or writing data to a storage system having two devices and two cloud storage devices according to one embodiment. The processing system **110** in FIG. **6** is similar to the processing system **110** in FIG. **5** except that the two NAS sites RAID 1 device **232** and RAID 1 device **234** are replaced by a local NAS site **620** that stores D_1 and D_2 in a RAID 1 manner (i.e., mirroring).

As above, the two data streams D_1 and D_2 stored in the local NAS device **620** are not sufficient to recover the segmented streams S_1, S_2, and S_3. One data stream stored on the cloud devices R3 **520** and R4 **420** may be retrieved to be used together with the two data streams D_1 and D_2 to recover the segmented streams S_1, S_2, and S_3.

FIG. **7** is a diagram illustrating the data transport and/or storage processing system **110** for transmitting or writing data to a storage system and four cloud storage devices according to one embodiment. The processing system **110** is similar to the processing system **110** in FIGS. **2**, **4**-**6** except in the destination storage devices. In FIG. **7**, the 4 output streams D_1, D_2, D_3, and D_4 are stored in local NAS site **720** in a RAID 0 configuration and are also stored in four storage devices R_1 **722**, R_2 **724**, R_3 **520**, and R_4 **420**.

In the local NAS site **720**, four storage devices store all four but not redundantly. Therefore, while there is no local redundancy, any three of the data streams may be retrieved to reconstitute the segmented streams S_1, S_2, and S_3. If one or two of the devices fail, the data streams may be retrieved from the corresponding cloud storage devices.

FIG. **8** is a diagram illustrating the data transport and/or storage processing system **110** for transmitting or writing data using a systematic coder according to one embodiment. The processing system **110** includes a systematic code **810** and the WFM processor **220**. The WFM processor **220** is similar to the WFM processor **220** in FIG. **2** and therefore does not need further description. Similarly, the writing or storing the four output streams D_1, D_2, D_3, and D_4 may be any one of the previously described schemes in FIGS. **2-7** and therefore is not described further.

The systematic coder **810** transforms or converts the source stream S into three input streams S_1, S_2, and S_3. The systematic coder **810** encodes the source stream S with a systematic code and then splits the encoded stream into three input streams S_1, S_2, and S_3. A systematic code may be any error-correcting code in which the data in the source stream is embedded in the encoded data. For example, checksums and hash functions may be combined with the source stream. As another example, S_3 may be the parity data stream as a numerical combination of S_1 and S_2. Any two of the three input streams S_1, S_2, and S_3 may be used to reconstitute the source stream S.

FIG. **9** is a diagram illustrating the data transport and/or storage processing system **110** for transmitting or writing data using a cascaded structure for the WFM processor according to one embodiment. The processing system **110** in FIG. **9** is similar to the processing system **110** in FIG. **2** except that the WFM operation is performed by additional WFM processors arranged in a serially cascaded configuration.

The cascaded structure includes two levels of WFM processors. In the first level, a first WFM processor performs WFM on M input streams to generate N output streams. In the second level, a second WFM processor performs WFM on the N output streams to produce storage streams to be stored in a storage device. In the illustrative example in FIG. **9**, the first level WFM processor is the WFM processor **220** and the second WFM processor includes two WFM processors **922** and **924** each operating on a subset of N data streams. Specifically, the WFM processor **220** performs WFM on the input streams S_1, S_2, and S_3 to produce the four output streams D_1, D_2, D_3, and D_4. The WFM processor **922** performs WFM on two streams D_1 and D_2, to generate four storage streams $R_{i,1}$, $R_{i,2}$, $R_{i,3}$, and $R_{i,4}$. The WFM processor **924** performs WFM on two streams D_3 and D_4, to generate four storage streams $R_{2,1}$, $R_{2,2}$, $R_{2,3}$, and $R_{2,4}$.

The WFM performed by the WFM processor **922** and **924** is similar to that performed by the WFM **220** except the number of inputs and the matrix coefficients are different. The WFM processor **922** performs the WFM as a matrix multiplication as follows:

$$\begin{bmatrix} R_{1,1} \\ R_{1,2} \\ R_{1,3} \\ R_{1,4} \end{bmatrix} = \begin{bmatrix} \rho_{11} & \rho_{12} \\ \rho_{21} & \rho_{22} \\ \rho_{31} & \rho_{32} \\ \rho_{41} & \rho_{42} \end{bmatrix} \begin{bmatrix} D_1 \\ D_2 \end{bmatrix}. \tag{4}$$

Similarly as in FIG. **2**, the coefficient ρ_{ij}'s may take real or complex values. Any sub-matrix comprising two rows of the matrix in (4) has full rank in order to fulfill the redundancy requirements: any two WFCs of $R_{1,1}$, $R_{1,2}$, $R_{1,3}$ and $R_{1,4}$ are sufficient to recover two WFCs D_1 and D_2. The WFM processor **924** may follow a similar configuration: Any two WFCs of $R_{2,1}$, $R_{2,2}$, $R_{2,3}$ and $R_{2,4}$ are sufficient to recover two WFCs D_3 and D_4.

The writing or storing of the storage streams $R_{1,1}$, $R_{1,2}$, $R_{1,3}$ and $R_{1,4}$ and $R_{2,1}$, $R_{2,2}$, $R_{2,3}$ and $R_{2,4}$ is similar to the embodiments described earlier in FIGS. **2**, **4-6**.

FIG. **10** is a diagram illustrating the data transport and/or storage processing system **110** for transmitting or writing data using a cascaded structure for the WFM processor according to one embodiment. The processing system **110** in FIG. **10** is similar to the processing system **110** in FIG. **9** except that the WFM processors in the second level each generates three storage streams. The processing system **110** includes the segmenter **210**, the WFM processor **220**, and two WFM processors **1022** and **1034**.

The WFM processor **1022** performs WFM on two streams D_1 and D_2, to generate three storage streams $R_{1,1}$, $R_{1,2}$, and $R_{1,3}$. The WFM processor **924** performs WFM on two streams D_3 and D_4, to generate three storage streams $R_{2,1}$, $R_{2,2}$, and $R_{2,3}$.

The WFM performed by the WFM processor **1022** and **1024** is similar to that performed by the WFM **220** except the number of inputs and the matrix coefficients are different. The WFM processor **1022** performs the WFM as a matrix multiplication as follows:

$$\begin{bmatrix} R_{1,1} \\ R_{1,2} \\ R_{1,3} \end{bmatrix} = \begin{bmatrix} \sigma_{11} & \sigma_{12} \\ \sigma_{21} & \sigma_{22} \\ \sigma_{31} & \sigma_{32} \end{bmatrix} \begin{bmatrix} D_1 \\ D_2 \end{bmatrix}. \tag{5}$$

Similarly as in FIG. **9**, the coefficient ρ_{ij}'s may take real or complex values. Any sub-matrix comprising two rows of the matrix in (5) has full rank in order to fulfill the redundancy requirements: any two WFCs of $R_{1,1}$, $R_{1,2}$, and $R_{1,3}$ are sufficient to recover two WFCs D_1 and D_2. The WFM processor **1024** may follow a similar configuration: Any two WFCs of $R_{2,1}$, $R_{2,2}$, and $R_{2,3}$ are sufficient to recover two WFCs D_3 and D_4.

The writing or storing of the storage streams $R_{1,1}$, $R_{1,2}$, and $R_{1,3}$ and $R_{2,1}$, $R_{2,2}$, and $R_{2,3}$ is similar to the embodiments described earlier in FIGS. **2**, **4-6**.

FIG. **11** is a diagram illustrating the data transport and/or storage processing system **110** for receiving or reading data from a storage system according to one embodiment. The processing system **110** includes storage devices **1112**, **1114**, and **1116**, WF de-multiplexing (WFD) processor **1120**, and a de-segmenter **1130**. The processing system **110** may include more or less than the above components. For clarity, components of the storage system **120**/**130**/**140** are shown in FIG. **11** as RAID **1112**, **1114**, and **1116**. In other embodiments, any of the storage devices **120**/**130**/**140** may be used.

The storage devices **1112**, **1114**, and **1116** represent any of the source storage devices **120**, **130** and **140** shown in FIG. **1**. In the illustrative example shown in FIG. **11**, they are NAS storage devices configured as RAID 1. The storage device **1112** stores mirrored data in $R_{1,1}$ and $R_{1,2}$ which include the stream D_1. The storage device **1114** stores mirrored data in $R_{2,1}$ and $R_{2,2}$ which include the stream D_2. The storage device **1116** stores mirrored data in $R_{3,1}$ and $R_{3,2}$ which include the stream D_3.

The WFD processor **1120** performs WFD on M input streams to generate N output streams. In the illustrative example in FIG. **11**, M=3 and N=4. The WFD processor **1120** performs WFD on the 3 input streams D_1, D_2, and D_3, and generates 4 output streams S_1, S_2, S_3, and S_4. The WFD essentially is the reverse operation of the WFM. To successfully recover the original source stream S, at least three NAS sites should be available. This operation is a matrix multiplication of the column vector $(D_1, D_2, D_3)^T$ using the following equations to recover the column vector $(S_1, S_2, S_3, S_4)^T$:

$$S_1 = w_{11'}D_1 + w_{12'}D_2 + w_{13'}D_3 \tag{6a}$$

$$S_2 = w_{21'}D_1 + w_{22'}D_2 + w_{23'}D_3 \tag{6b}$$

$$S_3 = w_{31'}D_1 + w_{32'}D_2 + w_{33'}D_3 \tag{6c}$$

$$S_4 = w_{41'}D_1 + w_{42'}D_2 + w_{43'}D_3 \tag{6d}$$

The WFD processor **1120** may generate one redundant data stream S_4. This data stream S_4 may be left unused or is used for integrity check against possible compromised stored/transported data streams.

When the M input streams are known to be generated using an envelope, the first WFD processor performs WFD on the M input streams including an envelope to generate the N output streams including a de-enveloped output stream.

The de-segmenter **1130** acts as a post-processor to de-segment or to merge the output streams S_1, S_2, S_3, and S_4 into the source stream S. The de-segmentation is the reverse of the known segmentation in the writing or storing process.

FIG. **12** is a diagram illustrating the data transport and/or storage processing system **110** for receiving or reading data from two local storage systems and two cloud storage devices according to one embodiment. The processing system **110** is configured to correspond to the configuration shown in FIG. **5**. The storage system **120/130/140** in FIG. **12** is similar to the storage system **170/180/190** shown in FIG. **5**. This configuration includes two local storage systems such as NAS devices **1112** and **1114** and two cloud storage devices R_3 **1216** and R_4 **1218** via the cloud **120**.

The WFD processor **1120** performs WFD on M input streams to generate N output streams. In the illustrative example in FIG. **12**, M=3 and N=4. The WFD processor **1120** performs WFD on the 3 input streams D_1, D_2, and D_3, and generates 4 output streams S_1, S_2, S_3, and S_4. The WFD essentially is the reverse operation of the WFM. As in the configuration in FIG. **11**, the WFD processor **1120** may generate one redundant data stream S_4. This data stream S_4 may be left unused or is used for integrity check against possible compromised stored/transported data streams. The de-segmenter **1130** acts as a post-processor to de-segment or to merge the output streams S_1, S_2, S_3, and S_4 into the source stream S. The de-segmentation is the reverse of the known segmentation in the writing or storing process.

FIG. **13** is a diagram illustrating the data transport and/or storage processing system **110** for receiving or reading data from a local storage system and two cloud storage devices according to one embodiment. The processing system **110** is configured to correspond to the configuration shown in FIG. **6**. The storage system **120/130/140** in FIG. **12** is similar to the storage system **170/180/190** shown in FIG. **6**. This configuration includes a local storage site **1310** having two storage systems such as NAS devices as RAID 1 to store data streams R_1 and R_2 in mirrored format and two cloud storage devices R_3 **1216** and R_4 **1218** via the cloud **120**.

The WFD processor **1120** performs WFD on M input streams to generate N output streams. In the illustrative example in FIG. **12**, M=3 and N=4. The WFD processor **1120** performs WFD on the 3 input streams D_1, D_2, and D_3, and generates 4 output streams S_1, S_2, S_3, and S_4. The WFD essentially is the reverse operation of the WFM. As in the configuration in FIG. **11**, the WFD processor **1120** may generate one redundant data stream S_4. This data stream S_4 may be left unused or is used for integrity check against possible compromised stored/transported data streams. The de-segmenter **1130** acts as a post-processor to de-segment or to merge the output streams S_1, S_2, S_3, and S_4 into the source stream S. The de-segmentation is the reverse of the known segmentation in the writing or storing process.

FIG. **14** is a diagram illustrating the data transport and/or storage processing system **110** for receiving or reading data using a systematic decoder according to one embodiment. The processing system **110** includes a WFD processor **1410** and a systematic decoder **1420**. The configuration in FIG. **14** corresponds to the reverse process of the configuration in FIG. **8**.

The WFD processor **1120** performs WFD on M input streams to generate N output streams. In the illustrative example in FIG. **11**, M=3 and N=2. The WFD processor **1410** performs WFD on the 3 input streams D_1, D_2, and D_3, and generates 3 output streams S_1, S_2, and S_3. The WFD essentially is the reverse operation of the WFM. To successfully recover the original source stream S, at least three NAS sites should be available. This operation is a matrix multiplication of the column vector $(D_1, D_2, D_3)^T$ using the following equations to recover the column vector $(S_1, S_2, S_3)^T$:

$$S_1 = w_{11'}D_1 + w_{12'}D_2 + w_{13'}D_3 \tag{7a}$$

$$S_2 = w_{21'}D_1 + w_{22'}D_2 + w_{23'}D_3 \tag{7b}$$

$$S_3 = w_{31'}D_1 + w_{32'}D_2 + w_{33'}D_3 \tag{7c}$$

FIG. **15** is a diagram illustrating the data transport and/or storage processing system **110** for receiving or reading data using a cascaded structure for the WFD processor according to one embodiment. The processing system **110** includes a WFD processor **1520**, two WFD processors **1512** and **1514**, and a de-segmenter **1530**. The processing system **110** may include more or less than the above components.

The cascade structure includes two levels. In the first level, the two WFD processors **1512** and **1514** perform WFD on the retrieved data streams $R_{1,1}$, $R_{1,2}$, $R_{2,1}$, and $R_{2,2}$ to generate the input streams D_1, D_2, and D_3. The WFD processor **1512** operates on the two storage streams $R_{1,1}$ and $R_{1,2}$ and generates 4 outputs, two of which are D_1 and D_2; the other two outputs may be unused or may be used for integrity check against possible compromised stored/transported data streams. As discussed above, the WFD may be performed by a matrix multiplication using the inverse matrix of:

$$\begin{bmatrix} \rho_{11} & \rho_{12} \\ \rho_{21} & \rho_{22} \end{bmatrix}$$

The WFD processor **1514** operates on the two storage streams $R_{2,1}$ and $R_{2,2}$ and generates 3 outputs, one of which is D_3; the other two outputs may be unused or may be used for integrity check against possible compromised stored/transported data streams.

In the second level, the WFD processor **1520** perform WFD on the three input streams D_1, D_2, and D_3 to generate 3 output streams S_1, S_2, and S_3. As discussed above, the WFD may be performed as a matrix multiplication using the inverse matrix of the matrix used to generate D_1, D_2, and D_3 in the writing or storing process.

The de-segmenter **1530** acts as a post-processor to de-segment or to merge the output streams S_1, S_2, and S_3 into the source stream S. The de-segmentation is the reverse of the known segmentation in the writing or storing process.

FIG. **16** is a diagram illustrating the data transport and/or storage processing system **110** for receiving or reading data using a cascaded structure for the WFD processor according to one embodiment. The processing system **110** in FIG. **16** is similar to the processing system **110** in FIG. **15** except the number of output streams in the first level WFD processors. The processing system **110** includes WFD processors **1612** and **1614** in the first level, the WFD processor **1520** in the second level, and the de-segmenter **1530**. The WFD processor **1612** operates on the two streams $R_{1,1}$ and $R_{1,2}$ and generates 3 outputs, two of which are D_1 and D_2; the other output may be unused or may be used for integrity check against possible compromised stored/transported data streams. The WFD processor **1614** operates on the two storage streams $R_{2,1}$ and $R_{2,2}$ and generates 2 outputs, one of which is D_3; the other output may be unused or may be used for integrity check against possible compromised stored/transported data streams.

FIG. **17** is a diagram illustrating curves **1700** representing failure rate of a distribute storage system according to one embodiment. The curves **1700** include two curves **1730** and **1740** plotted on a coordinate system having a horizontal axis **1710** and a vertical axis **1720**. The horizontal axis **1710** represents the failure rate p in each storage device. The vertical axis **1720** represents the failure rate in the system

One can compare the storage scheme with RAID 10 in terms of the array failure rate. Suppose each of the four NAS sites has a failure rate p over the next three years. If these sites are arranged in RAID 10 configuration, the corresponding array failure rate over the next three years is $\alpha_1=1-(1-p^2)^4$. If these sites are arranged in the configuration disclosed in FIG. **2** and FIG. **11**, the corresponding array failure rate over the next three years is $\alpha_2=1-4(1-p^2)^3p^2-(1-p^2)^4$. The disclosed configuration thus has better availability as $\alpha_1>\alpha_2$ given typical p values ($p<1/2$), and has better privacy protection as every NAS stores data sub-streams is identical to WFCs.

The failure rate α_1 **1730** for conventional RAID 10 configuration is higher than the failure rate α_2 **1740** for WFMed RAID 11 configurations. At a case where individual device failure rate p at 0.4 for next 3 years, the calculated failure rate α_1 for a conventional RAID 10 configuration will be at 0.5 or 50% probability while the calculated failure rate α_2 for a WFMed RAID 11 configuration will be at 0.13 or 13% probability.

FIG. **18** is a diagram illustrating curves representing failure rate of a distribute storage system according to one embodiment.

One can compare the storage scheme with systematic code governed solely by coder **810** (in FIG. **8**) in terms of the array failure rate shown in FIG. **14**. Suppose each of the four NAS sites has a failure rate p over the next three years. If these sites are arranged in 2-plus-1 systematic coding configuration, the corresponding array failure rate over the next three years is $\alpha_3=1-3p(1-p)^2-(1-p)^3$. If these sites are arranged in the configuration disclosed in FIG. **8** and FIG. **14**, the corresponding array failure rate over the next three years is $\alpha_4=1-6p^2(1-p)^2-4p(1-p)^3-(1-p)^4$. The disclosed configuration thus has better availability as $\alpha_3>\alpha_4$ given typical p values, and has better privacy protection as every NAS stores data sub-stream is identical to WFCs.

The curves represent failure rates **1800** of distributed storage systems α_3 and α_4 as functions of the failure rate of individual storage devices or storage disks, p. The vertical axis **1820** is the failure rate in a system, while the horizontal axis **1810** is the failure rate p in each storage devices. The failure rate α_3 **1830** for a systematic coder **810** (in FIG. **8**) configuration for a redundancy is higher than the failure rate **1840** for WFMed systematic coder configuration for 2 redundancies. At a case where individual device failure rate p at 0.4 for next 3 years, the calculated failure rate α_3 for a conventional systematic coder **810** configuration will be at 0.35 or 35% probability while the calculated failure rate α_4 for a WFM systematic coder configuration will be at 0.18 or 18% probability.

FIG. **19** is a diagram illustrating a WF processor **1900** according to one embodiment. The processing system **1900** shown in FIG. **19** may represent the processing system **110**, or the individual processors within the processing system **110**, the system **1700** or its individual processors (e.g., **1710**, **1720**, or **1760**), or the system **1800** or its individual processors (e.g., **1810**, **1820**, or **1860**). Not all of the components in FIG. **19** are present for a particular processor. For brevity, the following refers to the processing system **1900**, but it is noted that the architecture of the processing system **1900** may change depending on the particular function.

The processing system **1900** includes a central processing unit (CPU) or a processor **1910**, a cache **1915**, a platform controller hub (PCH) **1920**, a bus **1925**. The PCH **1920** may include an input/output (I/O) controller **1930**, a memory controller **1940**, a graphic display controller (GDC) **1950**, and a mass storage controller **1960**. The system **1900** may include more or less than the above components. In addition, a component may be integrated into another component. As shown in FIG. **19**, all the controllers **1930**, **1940**, **1950**, and **1960** are integrated in the PCH **1920**. The integration may be partial and/or overlapped. For example, the GDC **1950** may be integrated into the CPU **1910**, the I/O controller **1930** and the memory controller **1940** may be integrated into one single controller, etc.

The CPU or processor **1910** is a programmable device that may execute a program or a collection of instructions to carry out a task. It may be a general-purpose processor, a digital signal processor, a microcontroller, or a specially designed processor such as one design from Applications Specific Integrated Circuit (ASIC). It may include a single core or multiple cores. Each core may have multi-way multi-threading. The CPU **1910** may have simultaneous multithreading feature to further exploit the parallelism due to multiple threads across the multiple cores. In addition, the CPU **1910** may have internal caches at multiple levels.

The cache **1915** is a first level (L1) external cache memory. It is typically implemented by fast static random access memory (RAM). Other cache levels may appear externally, such as the cache **1946**. Some or all cache levels (L1, L2, and L3) may all be integrated inside the CPU **1910**.

The bus **1925** may be any suitable bus connecting the CPU **1910** to other devices, including the PCH **1920**. For example, the bus **1925** may be a Direct Media Interface (DMI).

The PCH **1920** in a highly integrated chipset that includes many functionalities to provide interface to several devices such as memory devices, input/output devices, storage devices, network devices, etc.

The I/O controller **1930** controls input devices (e.g., stylus, keyboard, and mouse, microphone, image sensor) and output devices (e.g., audio devices, speaker, scanner, printer). It also has interface to a network interface card **1970** which provides interface to a network **1974** and wireless controller **1972**. The network interface card (NIC) **1970** transmits and receives the data packets to and from a wired, wireless network **1972** or **1974**. The NIC **1970** may have one or more sockets for network cables and the type of socket depends on the type of network it will be used in. The network **1974** may be a LAN, a MAN, a WAN, an intranet, an extranet, or the Internet.

The memory controller **1940** controls memory devices such as the random access memory (RAM) **1942**, the read-only memory (ROM) **1944**, the cache memory **1946**, and the flash memory **1948**. The RAM **1942** may store instructions or programs, loaded from a mass storage device, that, when executed by the CPU **1910**, cause the CPU **1910** to perform operations as described above, such as WFM operations. It may also store data used in the operations, including the input data stream or the output data stream. The ROM **1944** may include instructions, programs, constants, or data that are maintained whether it is powered or not. This may include the matrix coefficients used in the envelope or de-envelope process, a catalog of the envelopes, boot program, self-test programs, etc. The cache memory **1946** may store cache data at level L2 or L3. The cache memory **1946** is typically implemented by fast static RAM to allow fast access from the CPU **1910**. The flash memory **1948** may store programs, instructions, constants, tables, coefficients, envelopes as in the ROM **1944**. It may be erased and programmed as necessary.

The GDC **1950** controls the display monitor **1955** and provides graphical operations. It may be integrated inside the CPU **1910**. It typically has a graphical user interface (GUI) to allow interactions with a user who may send a command or activate a function.

The mass storage controller **1960** controls the mass storage devices such as CD-ROM **1962** and hard disk **1964**.

Additional devices or bus interfaces may be available for interconnections and/or expansion. Some examples may include the Peripheral Component Interconnect Express (PCIe) bus, the Universal Serial Bus (USB), etc.

Relationship of a K-Muxing Transform and a Multibeam Array Digital Beam Forming (DBF) Matrix:

A multibeam array can form orthogonal beams (OB) through a transmit (Tx) digital beam forming (DBF) which is characterized by a M-to-N transform; where M is the number of beams with OB patterns and N is number of array elements. In general, both N and M are positive integers and N≥M>1. When N=M, there are adequate resources (i.e., array elements) to form N orthogonal beams. When N>M, there are N−M redundant elements in forming N orthogonal beams. The redundancy degree is N−M. In other words, when N>M, the signal reconstitution for signal reception is possible even when N−M elements are non-functional.

The set of the N beams with OB patterns, or simply N OB beams, is to communication to N different targets in N discrete directions with the following features: (1) the peak of a first OB beam is always at nulls of all other N−1 beams, and (2) the peaks of all other OB beams are at nulls of the first OB beam. The two features above for the first OB beam are true for all other n−1 OB beams. The performance constraints for optimization in generating the Tx digital beam forming (DBF) include N target directions.

K-muxing may use the same mathematical transformation which are used as the beam weighting vectors (BWV) for generating concurrent beams with OB radiation patterns from a multibeam array.

Embodiments of the disclosure include procedures of generating sets of K-muxing and K-demuxing transforms for distributed data storage and transport via shape beam optimization in a Tx DBF for a multibeam array discretely communicating to multiple satellites, multiple basestations, or multiple distributed receivers using shaped beam with OB radiation patterns. When all N array elements are functional in transmit; an optimized Tx DBF matrix from beam ports to element ports may be utilized numerically as a M-to-N K-muxing transform. Similarly, a propagation matrix from the N array elements to various target directions from the Tx OB DBF array elements will become a N-to-M K-demuxing transform.

On the other hand, when not all N array elements are functional; the K-demuxing transform matrix will be optimized using a Rx DBF matrix re-configured using remaining N−nx functional elements only; where nx is an integer and is the number of unavailable elements. Three examples for the following relationships may be provided: (a) K-muxing transforms and multibeam array DBF matrices, (b) K-demuxing transforms and propagation matrices from multibeam arrays, (c) redundancy of incoherent K-demuxing transforms and reconfigured multibeam array Rx DBF matrices for data storage and transport, and (d) coherent K-muxing/K-demuxing transforms and reconfigured multibeam array Tx/Rx DBF matrices for private signal transmission.

In the following examples, linear arrays with equally spaced elements are used to exemplify the relationships. The elements are Omni directional, and performance constraints are specified in one-dimensional directions. However, the relationships are applicable to any array geometries including non-planar arrays with discrete elements with various directional gains and the performance constraints can be specified in any directions in a [u, v], [θ, ϕ], or other coordinates; where $u=\sin\theta\times\cos\phi$, and $v=\sin\theta\times\sin\phi$.

It will be given scenarios of a ground terminal with a multi-beam array antenna communicating to multiple satellites concurrently exemplifying what impacts on data streams from beam-forming-network as preprocessing and those from free space propagation as post-processing. It will be shown how to derive K-muxing and K-demuxing transforms. Many other scenarios will work equally for generating K-muxing and K-demuxing matrices. One such a scenario includes mobile terminals with multiple-beam antennas connecting to multiple base stations concurrently.

Example 1

A 4-element array forms 4 concurrent beams with OB radiation patterns in FIG. **20**. The peaks of the OB beam are at $[u, v]=\{[-\frac{3}{4}, 0], [-\frac{1}{4}, 0], [\frac{1}{4}, 0], [\frac{3}{4}, 0]\}$, or $[\Theta, \Phi]=\{[-48°, 0]\ [-14.5°, 0]\ [14.5°, 0]\ [48°, 0]\}$.

It depicts a scenario of communicating to 4 satellites **2010** concurrently from a multibeam transmitting array antenna, which features 4 array elements **2044** and a Tx multibeam beam-forming-network (BFN) **2040**. The multibeam antenna sends 4 beam signal streams **2050** concurrently to the 4 satellites **2010**. The 4 elements **2044** are aligned in a linear format with contiguous elements equally spaced at 0.5 wavelengths. The digital beam-forming-network (BFN) **2040** can be implemented as mechanisms for 4 Tx orthogonal beams. The target satellite directions **2020** are at u=±¼ and ±¾ (or Θ=±14.5° and ±48°).

It is well known that a 4-to-4 Butler matrix comprising 4 analogue hybrids can be used as a beam-forming network (BFN) for a Tx array with 4 contiguous elements. When the equally spaced elements are at 0.5 wavelength apart, the resulting 4 concurrently shaped beams usually feature 4 OB beams **2110**, **2120**, **2130**, **2140** as shown on FIG. **21**. The beam peak directions are at u=±¼ and ±¾ (or Θ=±14.5° and)±48° **2030** sending, a first signal stream **A1**(*t*) of the four beam signals **2050** to a first satellite at Θ=48°, a second signal stream A**2**(*t*) of the four beam signals **2050** to a second satellite at Θ=14.5°, a third signal stream A**3**(*t*) to a third satellite at Θ=−14.5°, and a fourth signal stream A**4**(*t*) to a 4th satellite at Θ=−48°, with low mutual interferences (usually better than −30 dB isolations).

A shaped beam is optimized as a weighted sum of individual element radiation patterns in digital beam forming networks (BFN). The weighting parameters are optimized to meet the performance constraints for the shaped beam. The weighting parameters for a 4-element array are in a weighting vector, referred to as the beam weight vector (BWV) for the shaped beam.

FIG. **21** shows simulated radiation patterns **2100** using beam-shaping algorithms and the performance constraints of the directions of 4 shaped beams at Θ=±14.5° and ±48°. The algorithms are to optimize 4 concurrent orthogonal beams **2110**, **2120**, **2130**, **2140** with minimized mutual interference.

Normalized radiation patterns of 4 shaped beams shown in FIG. **21** for the 4-element linear DBF array are dictated by the corresponding BWVs. They are shaped under OB performance constraints. The normalized beam peaks at 0 dB are indeed located at Θ=**±14.5**° and ±48°, respectively. The peak of any one of the 4 OB beams is located at a null of all other OB beams, and the peaks of all other OB beams are at nulls of the OB beam **2110**, **2120**, **2130**, **2140**. The depicted peak to null ratios shown are better than 35 dB; nearly the entire displayed range of the vertical axis. In fact, the real peak to null ratios shown are better than 60 dB (not shown).

Quantitatively, the Tx DBF matrix transforms 4 independent beam signals (**A1**(*t*), A**2**(*t*), A**3**(*t*), A**4**(*t*)) **2050** connected to 4 input ports **912**, to 4 element signals (y**1**(*t*), y**2**(*t*), y**3**(*t*), y**4**(*t*)) **2060** from the 4 output ports. The element signals are then connected to 4 radiating elements of the Tx array as shown in FIG. **20**.

$$y1(t) = w11*A1(t) + w12*A2(t) + w13*A3(t) + w14*A4(t) \tag{8a}$$

$$y2(t) = w21*A1(t) + w22*A2(t) + w23*A3(t) + w24*A4(t) \tag{8b}$$

$$y3(t) = w31*A1(t) + w32*A2(t) + w33*A3(t) + w34*A4(t) \tag{8c}$$

$$y4(t) = w41*A1(t) + w42*A2(t) + w43*A3(t) + w44*A4(t) \tag{8d}$$

where A**1**(*t*) is weighted by a first beam weight vector (BWV1) **2210**, A**2**(*t*) is weighted by a second beam weight vector (BWV2) **2220**, A**3**(*t*) is weighted by a third beam weight vector (BWV3) **2230**, A**4**(*t*) is weighted by a fourth beam weight vector (BWV4) **2240**.

$$BWV1 = [\,w11 \quad w21 \quad w31 \quad w41\,]^T \tag{9a}$$

$$BWV2 = [\,w12 \quad w22 \quad w32 \quad w42\,]^T \tag{9b}$$

$$BWV3 = [\,w13 \quad w23 \quad w33 \quad w43\,]^T \tag{9c}$$

$$BWV4 = [\,w14 \quad w24 \quad w34 \quad w44\,]^T \tag{9d}$$

The DBF matrix, [BWVs] **2310**, generated via an optimization processing for a 4-element linear array is a 4×4 matrix with complex parameters. The optimized 4 BWVs and a corresponding 4×4 matrix under the OB performance constraints are depicted in FIG. **22** and FIG. **23**. The matrix [BWVs] **2310** is repeated in the following:

$$[BWVs] = \begin{bmatrix} -0.231-0.096i & 0.096+0.231i & \begin{matrix}0.096-\\0.231i\end{matrix} & \begin{matrix}-0.231+\\0.096i\end{matrix} \\ 0.096+0.231i & 0.231+0.096i & \begin{matrix}0.231-\\0.096i\end{matrix} & \begin{matrix}0.096-\\0.231i\end{matrix} \\ 0.096-0.231i & 0.231-0.096i & \begin{matrix}0.231+\\0.096i\end{matrix} & \begin{matrix}0.096+\\0.231i\end{matrix} \\ -0.230+0.096i & 0.096-0.231i & \begin{matrix}0.096+\\0.231i\end{matrix} & \begin{matrix}-0.231-\\0.096i\end{matrix} \end{bmatrix} \tag{10}$$

And it can be rewritten as a row vector (a 1×4 matrix):

[BWVs]=[BWV1BWV2BWV3BWV4]

where each matrix element is a column vector (a 4×1 matrix)

$$BWV1 = 0.25[\exp(j157.5°)\exp(j67.5°)\exp(j-67.5°)\exp(j-157.5°)]^T \tag{12a}$$

$$BWV2 = 0.25[\exp(j67.5°)\exp(j22.5°)\exp(-j22.5°)\exp(-j67.5°)]^T \tag{12b}$$

$$BWV3 = 0.25[\exp(-j67.5°)\exp(-j22.5°)\exp(j22.5°)\exp(j67.5°)]^T \tag{12c}$$

$$BWV4 = 0.25[\exp(-j157.5°)\exp(-j67.5°)\exp(j67.5°)\exp(j157.5°)]^T \tag{12d}$$

Let us use the convention that an M×N matrix has M rows and N columns. BWV1 **2210** is a 4×1 matrix, and features a constant phase gradient of 135° (or)−225° among the adjacent components. Similarly, BWV2 **2220**, BWV3 **2230** and BWV4 **2240** show features of different constant phase gradients of 45°, −45° and −135° (or 225°) among adjacent components, respectively.

FIG. **24** illustrates **2400** which shows that a K-muxing transform can be derived from the DBF matrix for a set of 4 orthogonal beams, while the corresponding K-demuxing transform can be derived from M propagation vectors from the 4 elements in a linear Tx array for M various directions (M=4). The first direction at [Θ, Φ]=[48°, 0] is to recover A**1**(*t*). Similarly, the directions at [Θ, Φ]=[14.5°, 0], [−14.5°, 0], and [−48°, 0] are for A**2**(*t*), A**3**(*t*), and A**4**(*t*), respectively.

Assuming aligned along an x-axis direction, the N elements of the linear array are located, respectively, at $X_1=(x_1, 0, 0)$, $X_2=(x_2, 0, 0)$, . . . , $X_N=(X_N, 0, 0)$. A wave number, k, is defined as 2π/λ, where λ is the wavelength of a transmitted RF carrier. An ith propagation vector to an ith direction at $[\Theta_1, 0]$ from a 4-element linear array is written as

$$Pi=[\exp(jk^*x_1 \sin \Theta_i)\exp(jk^*x_2 \sin \Theta_i)\exp(j\,k^*x_3 \sin \Theta_i)\exp(jk^*x_4 \sin \Theta_i)] \tag{13}$$

where i=1, 2, 3, and 4.

The performance constraints do not have to be set at the $[\Theta_i, \phi]$ directions where $\phi=0$. For a more general N-element array geometry, and a propagation vector to an i^{th} direction at $[\Theta_i, \phi_i]$ can be expressed as:

$$Pi(\Theta_i,\phi_i)=[ph(X_1,\Theta_i,\phi_i),ph(X_2,\Theta_i,\varphi_i), \ldots ph(X_N,\Theta_i,\phi_i] \tag{14}$$

Referring to FIG. **21**, it is very clear when a first direction were not set at [Θ,φ]=[48°, 0], but say at [50°, 0], a recovered data or signal stream for A**1**(*t*) would be "contaminated" by leakages from other 3 beams. As a result, the recovered data streams can be expressed as:

$$A1'(t)=A1(t)+\delta 2A2(t)+\delta 3A3(t)+\delta 4A4(t) \tag{15}$$

The recovered data stream is contaminated by interferences. Additional post processing in a receiver is needed to estimate A**1**(*t*) from A**1**'(*t*), when A**2**(*t*), A**3**(*t*) and A**4**(*t*) become known to the receiver.

We summarize the above procedures in a more general formulation as follows mathematically.

$$\underline{Y} = [BWVs] * \underline{A} \tag{16a}$$

$$\underline{A'} = [P] * \underline{Y} \tag{16b}$$

$$\underline{A'} = [P] * [BWVs] * \underline{A} \tag{16c}$$

where: $\underline{Y}$ is a N×1 matrix, a vector representing a set of N element signals,

$\underline{A}$ is a M×1 matrix, representing a vector for a set of M beam signals,

$\underline{A'}$ a set of beam signals at receivers in M various directions

[BWVs] is a N×M matrix, representing a Tx beam forming function converting a set of M beam signals to a set of N element signals,

P_i is a 1×N matrix, a propagation vector from array elements to ith direction in a far field.

$[P]=[P_1\ P_2\ P_3, \ldots P_M]^T$ and is a M×N matrix, representing a set of propagation vectors converting a set of N element signals to a set of Tx beam signals at M various directions.

According to Equation (16c) under the following condition, $\underline{A'}$ will become $\underline{A}$,

$$[P]^*[\mathrm{BWVs}]=\underline{I} \tag{16d}$$

where $\underline{I}$ is an N×N identity matrix.

The [BWVs] 2310 for this example features a [N×M] matrix and can be used for a K-muxing operation. The number of elements, N, is set to 4, the number of shaped beams, M, is also set to 4. Similarly, the [P] is a [N×M] matrix and can be used for a K-demuxing operation.

Example 2

An example of OB radiation patterns **2600** from 4 concurrent beams generated by an array with 5 elements **2044** are depicted in FIG. **25**. The peaks of the OB beam are at [u, v]={[−¾, 0], [−¼, 0], [¼, 0], [¾, 0]}, or at [Θ, Φ]={[−48°, 0], [−14.5°, 0], [14.5°, 0], [48°, 0]} **2020**.

It depicts the same scenario of communicating to 4 satellites **2020** concurrently from a multibeam transmitting array antenna, which features 5 instead of 4 array elements as that in example 1 and a Tx multibeam beam-forming-network (BFN) **910**. The 5 elements **2044** are aligned in a linear format with contiguous elements equally spaced at 0.5 wavelengths. The Tx multibeam BFN **2040** features 4 input ports (or 4 beam ports **2042**), B1, B2, B3, and B4, and 5 output ports **2044** (or 5 element ports), E1, E2, E3, E4, and E5. The functions of the multibeam BFN **2040** include formulation of 5 element signals **2060** at the 5 output ports; each element signal as a weighted sum of 4 beam signals **2050** connected to 4 input ports **2042**.

The 4 beam signals **2050** A**1**(*t*), A**2**(*t*), A**3**(*t*), and A**4**(*t*) are connected to the 4 beam ports **2042** of the multibeam beam-forming-network (BFN). The 5 output signals from the 5 element ports **2044** of the multibeam BFN are 5 element signals **2060**; y**1**(*t*), y**2**(*t*), y**3**(*t*), y**4**(*t*), and y**5**(*t*). The radiated element signals will propagate in free space, and spatially combined in a far field. As a result of the free-space propagations **2070**, the radiated 4 beam signals **2050** by the 5 elements will be "untangled" and delivered individually and independently to 4 specified directions **2020**. The recovered signals **2020** at various directions **2030** shall be nearly identical to the beam signals **2050**.

The beam-forming-network (BFN) **2040** can be configured and implemented as mechanisms for 4 Tx orthogonal beams. The target satellite directions **2030** are at u=±¼ and ±¾ (or Θ=±14.5° and ±48°).

A 1^{st} shaped beam can be optimized as a weighted sum of individual element radiation patterns in digital beam forming networks. The weighting parameters are optimized to meet the performance constraints for the shaped beam. The weighting parameters for the 5-element array are in a weighting vector, referred to as the beam weight vector (BWV) for the shaped beam. FIG. **26** shows simulated radiation patterns using beam-shaping algorithms and the performance constraints of the directions of 4 shaped beams at Θ=±14.5° and ±48°. The algorithms are to optimize 4 concurrent orthogonal beams minimizing mutual interference. It is noticed that the vertical axis ranges from −100 to 10 dB depicting the radiation intensity variation over all coverage directions.

Normalized radiation patterns of 4 shaped beams **2600** shown in FIG. **27** for the 5-element linear DBF array are dictated by the corresponding BWVs. They are shaped under OB performance constraints. The normalized beam peaks at 0 dB are indeed located at Θ=±14.5° and ±48°, respectively. The peak of any one OB beam (**2610**, **2620**, **2630**, or **2640**) is located at a null of all other OB beams (**2610**, **2620**, **2630**, **2640**), and the peaks of all other OB beams (**2610**, **2620**, **2630**, **2640**) are at nulls of the OB beam (**2610**, **2620**, **2630**, or **2640**). The peak to null ratios shown are better than 80 dB.

Quantitatively, the Tx DBF matrix transforms 4 input signals or 4 beam signals **916**, (A**1**(*t*), A**2**(*t*), A**3**(*t*), A**4**(*t*)), to the 5 output signals or 5 element signals, [y**1**(*t*), y2(t), y3(t), y4(t), y5(t)], which are connected to 5 radiating elements of the Tx array as shown in FIG. **25**.

$$y1(t) = w11 * A1(t) + w12 * A2(t) + w13 * A3(t) + w14 * A4(t) \tag{17a}$$

$$y2(t) = w21 * A1(t) + w22 * A2(t) + w23 * A3(t) + w24 * A4(t) \tag{17b}$$

$$y3(t) = w31 * A1(t) + w32 * A2(t) + w33 * A3(t) + w34 * A4(t) \tag{17c}$$

$$y4(t) = w41 * A1(t) + w42 * A2(t) + w43 * A3(t) + w44 * A4(t) \tag{17d}$$

$$y5(t) = w51 * A1(t) + w52 * A2(t) + w53 * A3(t) + w54 * A4(t) \tag{17e}$$

where A**1**(*t*) is weighted by a first beam weight vector (BWV1) **2710**, A**2**(*t*) is weighted by a second beam weight vector (BWV2) **2720**, A**3**(*t*) is weighted by a third beam weight vector (BWV3) **2730**, A**4**(*t*) is weighted by a fourth beam weight vector (BWV4) **2740**.

$$BWV1=[\,w11\quad w21\quad w31\quad w41\quad w51\,]^T \tag{18a}$$

$$BWV2=[\,w12\quad w22\quad w32\quad w42\quad w52\,]^T \tag{18b}$$

$$BWV3=[\,w13\quad w23\quad w33\quad w43\quad w53\,]^T \tag{18c}$$

$$BWV4=[\,w14\quad w24\quad w34\quad w44\quad w54\,]^T \tag{18d}$$

Depicted in FIG. **28**, the DBF matrix, [BWVs] **2310**, generated via an optimization processing for a 5-element linear array is a 5×4 matrix with complex parameters. The optimized 4 BWVs and a corresponding 5×4 matrix under the OB performance constraints are depicted in FIG. **27** and FIG. **28**. The matrix [BWVs] **2310** is repeated in the following:

$$[BWVs]= \tag{19}$$

$$\begin{bmatrix} -0.231-0.096i & 0.096+0.231i & 0.096-0.231i & -0.231+0.096i \\ 0.096+0.231i & 0.231+0.096i & 0.231-0.096i & 0.096-0.231i \\ 0.096-0.231i & 0.231-0.096i & 0.231+0.096i & 0.097+0.231i \\ -0.110+0.050i & 0.029-0.141i & 0.039+0.106i & -0.114-0.052i \\ 0.121-0.046i & -0.067+0.090i & -0.056-0.125i & 0.117+0.044i \end{bmatrix}$$

And it can be rewritten as a row vector (a 1×4 matrix):

$$[\mathrm{BWVs}]=[\mathrm{BWV1BWV2BWV3BWV4}] \tag{20}$$

where each complex matrix element is a column vector (a 5×1 matrix). The complex elements can be either in an I/Q format or a format with amplitude and phase.

$$BWV1=\left(\begin{array}{|c|}\hline -0.231-0.096i \\ \hline 0.096-0.231i \\ \hline 0.096-0.231i \\ \hline '-0.110-0.050i \\ \hline 0.121-0.046i \\ \hline \end{array}\right)=\left(\begin{array}{|c|}\hline 0.25\exp(-j157.5^\circ) \\ \hline 0.25\exp(j67.5^\circ) \\ \hline 0.25\exp(-j67.5^\circ) \\ \hline 0.12\exp(j155.6^\circ) \\ \hline 0.13\exp(-j20.7^\circ) \\ \hline \end{array}\right) \tag{21a}$$

$$BWV2=\left(\begin{array}{|c|}\hline 0.096-0.231i \\ \hline '0.231-0.096i \\ \hline '0.231-0.096i \\ \hline '0.029-0.141i \\ \hline '-0.067-0.090i \\ \hline \end{array}\right)=\left(\begin{array}{|c|}\hline 0.25\exp(j67.5^\circ) \\ \hline 0.25\exp(j22.5^\circ) \\ \hline 0.25\exp(-j22.5^\circ) \\ \hline 0.14\exp(-j78.4^\circ) \\ \hline 0.11\exp(j126.5^\circ) \\ \hline \end{array}\right) \tag{21b}$$

-continued

$$BWV3=\left(\begin{array}{|c|}\hline 0.096-0.231i \\ \hline '0.231-0.096i \\ \hline '0.231-0.096i \\ \hline '0.039-0.106i \\ \hline '-0.056-0.125i \\ \hline \end{array}\right)=\left(\begin{array}{|c|}\hline 0.25\exp(-j67.5^\circ) \\ \hline 0.25\exp(-j22.5^\circ) \\ \hline 0.25\exp(j22.5^\circ) \\ \hline 0.11\exp(j69.6^\circ) \\ \hline 0.14\exp(-j114.2^\circ) \\ \hline \end{array}\right) \tag{21c}$$

$$BWV4=\left(\begin{array}{|c|}\hline -0.231-0.096i \\ \hline '0.096-0.231i \\ \hline '0.096-0.231i \\ \hline -0.114-0.052i \\ \hline '0.117-0.044i \\ \hline \end{array}\right)=\left(\begin{array}{|c|}\hline 0.25\exp(j157.5^\circ) \\ \hline 0.25\exp(-j67.5^\circ) \\ \hline 0.25\exp(j67.5^\circ) \\ \hline 0.13\exp-(j155.5^\circ) \\ \hline 0.12\exp(j20.4^\circ) \\ \hline \end{array}\right) \tag{21d}$$

Let us use the convention that an M×N matrix has M rows and N columns. BWV1 **2710** is a 5×1 matrix, and features a set of complex numbers which represent a unique amplitude and phase distribution among the adjacent components. Similarly, BWV2 **2720**, BWV3 **2730**, and BWV4 **2740** show features of different amplitude and phase distributions.

FIG. **29** illustrates a panel **2900** which shows that a K-muxing transform can be derived from the DBF matrix for a set of 4 orthogonal beams, while the corresponding K-demuxing transform can be derived from the propagation vectors from the 5 elements in a linear Tx array for 4 various directions. The first direction at [Θ, Φ]=[48°, 0] is to recover A**1**(*t*). Similarly, the directions at [Θ, Φ]=[14.5°, 0], [−14.5°, 0], and [−48°, 0] are for A**2**(*t*), A**3**(*t*), and A**4**(*t*), respectively. These constrained directions are identical to the 4 beam pointing directions in Example 1.

It is very clear that, when a first direction were not set at [Θ, Φ]=[48°, 0], say at [50°, 0], a recovered data or signal stream for A**1**(*t*) would be contaminated by leakages from other 3 beams. As a result, the recovered data streams can be expressed as:

$$A1'(t)=A1(t)+\delta 2A2(t)+\delta 3A3(t)+\delta 4A4(t) \tag{22}$$

Additional post processing in a receiver is needed to estimate A**1**(*t*) from A**1**'(*t*), when A**2**(*t*), A**3**(*t*) and A**4**(*t*) become known to the receiver.

Example 2 is a special case for with N=5 and M=4; or 4 beams using an array with 5 elements. The [BWVs] **2310** for this example features a [N×M] matrix and can be used for a K-muxing operation. The number of elements, N, is set to 5, the number of shaped beams, M, is also set to 4. Similarly, the [P] is a [N×M] matrix and can be used for a K-demuxing operation as derived in FIG. **29**, panel **2900**.

It is also interesting to view the 5-element array in a receiving mode. The 5 array elements capture all 4 different signals originated from 4 satellites at the same RF frequency concurrently. The propagation from all 4 directions to the 5 elements of the array in an Rx mode can be characterized as the [P] matrix. The captured signals are amplified and filtered properly before converted to digital format. A beam forming network will perform a transformation converting the 5 received element signals to 4 received beam signals. The transformation is a [BWVs]. Thus a similar set of equations to Equations (16a), (16b), (16c), and (16d) can be derived as followed:

$$\underline{Y} = [P] * \underline{A'} \tag{23a}$$

$$\underline{A} = [BWVs] * \underline{Y} \tag{23b}$$

$$\underline{A} = [BWVs] * [P] * \underline{A'} \tag{23c}$$

where:

$\underline{A}'$ is a M×1 matrix, representing a vector for a set of M beam signals originated by the 4 sources from various directions, the 4 sources are 4 satellites at various directions;

P_i is a 1*N matrix, a propagation vector from an ith direction in a far field to the N array elements;

$[P]=[P_1\ P_2\ P_3, \ldots P_M]^T$ and is a M×N matrix, representing a set of propagation vectors converting a set of N element signals to a set of Tx beam signals at M various directions;

$\underline{Y}$ is a N×1 matrix, a vector representing a set of N element signals;

[BWVs] is a N×M matrix, representing a Tx beam forming function converting a set of M beam signals to a set of N element signals;

$\underline{A}$ is a set of beam signals at M outputs of a DBFN.

According to Equation (16c) under the following condition, $\underline{A}'$ will become $\underline{A}$,

$$[\mathrm{BWVs}]*[P]=\underline{I} \tag{23d}$$

where [P] is a M×N K-muxing matrix while [BWVs] becomes a N×M K-demuxing matrix.

However, when one of the 5 elements fails to function properly in the receiving array, the same 4 signals will still be captured by the remaining 4 elements. The array may be reconfigured to recover the 4 signals originated from the 4 satellites, when 4 of the 5 element signals are available. The re-optimization of the configured array from 5 elements to 4 elements will be discussed in FIG. **37**. The new and re-optimized [BWVs] will be a 4×4 K-demuxing transform matrix.

Example 3

An example of OB radiation patterns from 4 concurrent beams generated by an array with 6 elements **2044** are depicted in FIG. **30**. The peaks of the OB beam are at [u, v]={[−¾, 0], [−¼, 0], [¼, 0], [¾, 0]}, or at [Θ, Φ]={[−48°, 0], [−14.5°, 0], [14.5°, 0], [48°, 0]} **2020**.

It depicts the same scenario of communicating to 4 satellites **2010** concurrently from a multibeam transmitting array antenna, which features 6 instead of 4 array elements as that in example 1 and a Tx multibeam beam-forming-network (BFN) **2040**. The 6 elements **2044** are aligned in a linear format with contiguous elements equally spaced at 0.5 wavelengths. The Tx multibeam BFN **2040** features 4 input ports (or 4 beam ports **2042**), B1, B2, B3, and B4, and 6 output ports **2044** (or 6 element ports), E1, E2, E3, E4, E5, and E6.

The 4 beam signals **2050** A**1**(*t*), A**2**(*t*), A**3**(*t*), and A**4**(*t*) are connected to the 4 beam ports **2042** of the multibeam beam-forming-network (BFN). The 6 output signals from the 6 element ports **2044** of the multibeam BFN are 6 element signals **2060**; y**1**(*t*), y**2**(*t*), y**3**(*t*), y**4**(*t*), y**5**(*t*), and y**6**(*t*). The radiated element signals will propagate in free space, and spatially combined in a far field. As a result of the free-space propagations **902**, the radiated 4 beam signals **2050** by the 6 elements will be "untangled" and delivered individually and independently to 4 specified directions **2020**. The recovered signals **2020** at various directions **2030** shall be nearly identical to the beam signals **2050**.

The beam-forming-network (BFN) **2040** can be configured and implemented as mechanisms for 4 Tx orthogonal beams. The target satellite directions are at u=±¼ and ±¾ (or Θ=±14.5° and ±48°) **2020**.

A 1^{st} shaped beam can be optimized as a weighted sum of individual element radiation patterns in digital beam-forming-networks (BFN) **2040**. The weighting parameters are optimized to meet the performance constraints for the shaped beam. The weighting parameters for the array with 6 elements are in a weighting vector, referred to as the beam weight vector (BWV) for the shaped beam. FIG. **31** shows simulated radiation patterns **1130** using beam-shaping algorithms and the performance constraints of the directions of 4 shaped beams at 0=±14.5° and ±48° **928**. The algorithms are to optimize 4 concurrent orthogonal beams **1132-1**, **1132-2**, **1132-3**, **1132-4**, minimizing mutual interference in far field. It is noticed that the vertical axis ranges from −100 to 10 dB depicting the radiation intensity variation over all coverage directions.

Normalized radiation patterns of 4 shaped beams shown in FIG. **31** for the 6-element linear DBF array are dictated by the corresponding BWVs. They are shaped under OB performance constraints. The normalized beam peaks at 0 dB are indeed located at Θ=±14.5° and ±48°, respectively. The peak of any one OB beam is located at a null of all other OB beams, and the peaks of all other OB beams are at nulls of the OB beam. The peak to null ratios shown are better than 80 dB.

Quantitatively, the Tx multibeam beam forming network **2040** featuring 4 input ports **2042** and 6 output ports **2044**, transforms 4 beam signals **2050**, (A**1**(*t*), A**2**(*t*), A**3**(*t*), A**4**(*t*)) at the inputs, to 6 element signals **2060**, [y**1**(*t*), y**2**(*t*), y**3**(*t*), y**4**(*t*), y**5**(*t*), y**6**(*t*)] at the outputs. The 6 element signals **2060** are then connected to 6 radiating elements of the Tx array as shown in FIG. **30**.

$$y1(t) = w11 * A1(t) + w12 * A2(t) + w13 * A3(t) + w14 * A4(t) \tag{24a}$$

$$y2(t) = w21 * A1(t) + w22 * A2(t) + w23 * A3(t) + w24 * A4(t) \tag{24b}$$

$$y3(t) = w31 * A1(t) + w32 * A2(t) + w33 * A3(t) + w34 * A4(t) \tag{24c}$$

$$y4(t) = w41 * A1(t) + w42 * A2(t) + w43 * A3(t) + w44 * A4(t) \tag{24d}$$

$$y5(t) = w51 * A1(t) + w52 * A2(t) + w53 * A3(t) + w54 * A4(t) \tag{24e}$$

$$y6(t) = w61 * A1(t) + w62 * A2(t) + w63 * A3(t) + w64 * A4(t) \tag{24f}$$

where A**1**(*t*) is weighted by a first beam weight vector (BWV1) **2710**, A**2**(*t*) is weighted by a second beam weight vector (BWV2) **2720**, A**3**(*t*) is weighted by a third beam weight vector (BWV3) **2730**, A**4**(*t*) is weighted by a fourth beam weight vector (BWV4) **2740**.

$$BWV1 = [\, w11 \quad w21 \quad w31 \quad w41 \quad w51 \quad w61 \,]^T \tag{25a}$$

$$BWV2 = [\, w12 \quad w22 \quad w32 \quad w42 \quad w52 \quad w62 \,]^T \tag{25b}$$

$$BWV3 = [\, w13 \quad w23 \quad w33 \quad w43 \quad w53 \quad w63 \,]^T \tag{25c}$$

$$BWV4 = [\, w14 \quad w24 \quad w34 \quad w44 \quad w54 \quad w64 \,]^T \tag{25d}$$

The DBF matrix, [BWVs] **2310**, generated via an optimization processing for a 6-element linear array is a 6×4 matrix with complex parameters. The optimized 4 BWVs and a corresponding 6×4 matrix under the OB performance constraints are depicted in FIG. **11**B and FIG. **11**C **1140**. The matrix [BWVs] **2310** is repeated in the following:

$$BWVs = \begin{pmatrix} -0.1191 - 0.0530i & 0.0391 + 0.1027i & 0.0392 - 0.1284i & -0.1184 + 0.0429i \\ 0.0957 + 0.2310i & 0.2310 + 0.0957i & 0.2310 - 0.0957i & 0.0957 - 0.2309i \\ 0.0957 - 0.2310i & 0.2310 - 0.0957i & 0.2310 + 0.0957i & 0.0957 + 0.2309i \\ -0.1191 + 0.0423i & 0.0390 - 0.1285i & 0.0392 + 0.1026i & -0.1197 - 0.0537i \\ 0.1119 - 0.0534i & -0.0566 + 0.1025i & -0.0565 - 0.1284i & 0.1112 + 0.0421i \\ 0.1119 + 0.0427i & -0.0566 - 0.1283i & -0.0565 + 0.1026i & 0.1126 - 0.0528i \end{pmatrix} \tag{26}$$

And it can be rewritten as a row vector (a 1×4 matrix)

$$[BWVs]=[BWV1BWV2BWV3BWV4] \tag{27}$$

where each matrix element is a column vector (a 6×1 matrix):

$$BWV1 = \begin{pmatrix} -0.119 - 0.053i \\ 0.096 - 0.231i \\ 0.096 - 0.231i \\ {}' - 0.119 - 0.042i \\ {}'0.112 - 0.053i \\ {}'0.112 - 0.043i \end{pmatrix} = \begin{pmatrix} 0.13\exp(-j156.0^\circ) \\ 0.25\exp(j67.5^\circ) \\ 0.25\exp(-j67.5^\circ) \\ 0.13\exp(j160.4^\circ) \\ 0.12\exp(-j25.5^\circ) \\ 0.12\exp(j20.9^\circ) \end{pmatrix} \tag{28a}$$

$$BWV2 = \begin{pmatrix} {}'0.039 + 0.103i \\ 0.230 + 0.067i \\ {}'0.231 - 0.096i \\ {}'0.039 - 0.129i \\ -0.057 + 0.103i \\ {}'-0.057 - 0.128i \end{pmatrix} = \begin{pmatrix} 0.11\exp(j69.2^\circ) \\ 0.25\exp(j22.5^\circ) \\ 0.25\exp(-j22.5^\circ) \\ 0.13\exp(-j73.1^\circ) \\ 0.12\exp(j118.9^\circ) \\ 0.14\exp(-j113.8^\circ) \end{pmatrix} \tag{28b}$$

$$BWV3 = \begin{pmatrix} 0.039 - 0.128i \\ 0.231 - 0.096i \\ 0.231 + 0.096i \\ 0.039 + 0.103i \\ -0.057 - 0.128i \\ -0.057 + 0.103i \end{pmatrix} = \begin{pmatrix} 0.13\exp(-j73.0^\circ) \\ 0.25\exp(-j22.5^\circ) \\ 0.25\exp(j22.5^\circ) \\ 0.11\exp(j69.1^\circ) \\ 0.14\exp(-j113.8^\circ) \\ 0.12\exp(j118.8^\circ) \end{pmatrix} \tag{28c}$$

$$BWV4 = \begin{pmatrix} -0.118 + 0.043i \\ 0.096 - 0.231i \\ 0.096 + 0.231i \\ -0.120 - 0.054i \\ 0.111 + 0.042i \\ 0.113 - 0.053i \end{pmatrix} = \begin{pmatrix} 0.13\exp(j160.1^\circ) \\ 0.25\exp(-j67.5^\circ) \\ 0.25\exp(j67.5^\circ) \\ 0.13\exp(-j155.8^\circ) \\ 0.12\exp(j20.7^\circ) \\ 0.12\exp(-j25.1^\circ) \end{pmatrix} \tag{28d}$$

BWV1 is a 6×1 matrix and features a set of complex numbers which represent a unique amplitude and phase distribution among the adjacent components. Similarly, BWV2, BWV3, and BWV4 show features of different amplitude and phase distributions in a 6-parameter space or a 6-dimensional space.

FIG. **34** shows that a K-muxing transform can be derived from the DBF matrix for a set of 4 orthogonal beams, while the corresponding K-demuxing transform can be derived from the propagation vectors from the 6 elements in a linear Tx array for 4 various directions. The first direction at [Θ, Φ]=[48°, 0] is to recover A**1**(t). Similarly, the directions at [Θ, Φ]=[14.5°, 0], [−14.5°, 0], and [−48°, 0] are for A**2**(t), A**3**(t), and A**4**(t), respectively. These constrained directions are identical to the 4 beam pointing directions in Example 1.

It is very clear that, when a first direction were not set at [Θ, Φ]=[48°, 0], say at [50°, 0], a recovered data or signal stream for A**1**(t) would be contaminated by leakages from other 3 beams. As a result, the recovered data streams can be expressed as:

$$A1'(t)=A1(t)+\delta 2A2(t)+\delta 3A3(t)+\delta 4A4(t) \tag{29}$$

Additional post processing in a receiver is needed to estimate A**1**(t) from A**1'**(t), when A**2**(t), A**3**(t) and A**4**(t) become known to the receiver.

Example 3 is a special case for with N=6 and M=4; or 4 beams using an array with 6 elements as depicted in FIG. **30**. The [BWVs] for this example features a [N×M] matrix and can be used for a K-muxing operation. The number of elements, N, is set to 6, the number of shaped beams, M, is also set to 4. Similarly, the [P] is a [N×M] matrix and can be used for a K-demuxing operation.

It is also interesting to view the 6-element array in a receiving mode. The 6 array elements **2044** capture all 4 different signals originated from 4 satellites **2010** at the same RF frequency concurrently. The propagation **2070** from all 4 directions **2030** to the 6 elements **2044** of the array in an Rx mode can be characterized as the [P] matrix. The captured signals **2060** are amplified and filtered properly before converted to digital format. A beam forming network **2040** will perform a transformation converting the 6 received element signals to 4 received beam signals **916**. The transformation **2510** is an operation via [BWVs]. Thus, a similar set of equations to Equations (16a), (16b), (16c), and (16d) can be derived as follows:

$$\underline{Y} = [P] * \underline{A'} \tag{30a}$$

$$\underline{A} = [BWVs] * \underline{Y} \tag{30b}$$

$$\underline{A} = [BWVs] * [P] * \underline{A'} \tag{30c}$$

Where: $\underline{A'}$ **2020** is an M×1 matrix, representing a vector for a set of M beam signals originated by the 4 satellites **2010** at various directions **928**.

P_i is a 1×N matrix, a propagation vector from an ith direction in a far field to the N array elements by free space propagation **902**.

$[P]=[P_1\ P_2\ P_3, \ldots P_M]^T$ and is a M×N matrix, representing a set of propagation vectors converting a set of N element signals to a set of Tx beam signals at M various directions.

$\underline{Y}$ is an N×1 matrix, a vector representing a set of N element signals **918**,

[BWVs] is a N×M matrix, representing an Rx beam forming function **2040** converting a set of N element signals **2060** to a set of M beam signals **916**,

$\underline{A}$ is a set of beam signals **2050** at M outputs of a DBFN **2040** at an Rx mode.

According to Equation (16c) under the following condition, $\underline{A}'$ will become $\underline{A}$,

$$[\text{BWVs}]*[P]=\underline{I} \qquad (30d)$$

where [P] is a M×N K-muxing matrix while [BWVs] becomes a N×M K-demuxing matrix.

However, when two of the 6 elements fail to function properly in the receiving array, the same 4 signals will still be captured by the remaining 4 elements. The array may be reconfigured to recover the 4 signals originated from the 4 satellites, when 4 of the 6 element signals are available. The re-optimization of the configured array from 6 elements to 4 elements will be discussed in FIG. **38**. The new and re-optimized [BWVs] will be a 4×4 K-demuxing transform matrix.

According to Equations 16a, 16b, 16c, and 16d, Example 3 is another special case for with N=6 and M=4; or 4 beams using an array with 6 elements.

We may make the following observations:

1. The three examples illustrate, respectively, (1) 4 elements for forming 4 concurrent OB beams, (2) 5 elements for forming 4 concurrent OB beams, and (3) 6 elements for forming 4 concurrent OB beams.
2. In a beam shaping optimization under boundary conditions of an array geometry and far field performance constraints, an optimized beam weight vector (BWV) for customized shaped beam including a beam with OB patent is generated. The BWV characterizes the shaped beam.
3. Examples 1, 2, and 3 all feature 4 concurrent OB beams.
   Performance constraints in beam shaping process for the three examples are identical.
   OB beams are to assure propagation in free space in a desired or constraint direction will result in recovering a desired signal while rejecting the other 3 signals better than 50 dB; excellent isolation.
   Corresponding BWVs are different for various arrays.
4. However, they show, respectively, (a) no redundancy in array elements from the 4-element linear array, (b) a 5-for-4 redundancy in array elements from the 5-element linear array, and (3) a 6-for-4 redundancy in array elements from the 6-element linear array.
5. OB beam-forming can be used to generate K-muxing matrices; while the corresponding K-demuxing matrices are the formulations of free space propagation from array elements to various directions.

FIG. **35** depicts a flow chart **3500** calculating the [BWVs] for an array with N elements generating concurrent M beam. The steps are as follows:

1. Define an array geometry **3510** with M OB beams, j=1, and an initial BWV
2. Designate peak and null positions as performance constraints **3520** for a jth beam with an OB radiation pattern
3. Iteration loop
   i. Far-field calculation **3530** on radiation pattern based on new BWV and the array geometry **3510**;
   ii. Generations of observables based on differences between calculated array pattern at constrained directions and specified performance constraints **3520**;
   iii. Converting observables to cost functions which are measurable with positive values,
   iv. Calculate current total cost by summing up all cost functions,
   v. If total cost less than a threshold (8) go to step 4; otherwise go to step 3 vi.
   vi. Derive and update weighting coefficients of the BWV via optimization **3540** schemes by a cost minimization algorithm and go to step 3i,
4. Plot the pattern (array factor only) of the OB beam and output the associated BWV,
5. If j=M stop; otherwise j=j+1 and go to step 2.

A BWV for a shaped beam is a set of amplitude and phase weights in a beam forming network (BFN) from an N-element array and shall feature an N×1 matrix. To form M concurrent beams, the BFN shall use M sets of BWVs individually. An output buffer **3550** shall output the matrix [BWVs] comprising M sets of BWVs, which transforms M beam port data streams to N port element data streams.

The same [BWVs] matrix can be used for an M (inputs)-to-N (outputs) K-muxing **3560** operation, transforming M data streams to N K-muxed data streams for private data storage and data transport with enhanced survivability.

FIG. **36** depicts a flow chart **3600** calculating various propagation vectors for different beams of an array with N elements. Each propagation vector can be represented as a 1*N matrix. A matrix [P] includes components in M rows and N columns. The N×M matrix allows M concurrent beams to propagate to M specified directions delivering M independent data streams. The steps for the flow chart are as follows:

1. Define an array geometry **3610** with M OB beams, j=1, and a set of optimized BWV.
2. Designate peak and null positions as performance constraints **3620** for one individual beam with OB radiation pattern.
3. Calculate array pattern via far-field calculation **3630** based on the optimized BWVs or on performance constraints.
4. Calculate the P matrices at M constrained directions, and form the matrix [P] **3640**.
5. Using [P] **3640** as a K-demuxing transform **3650**.
6. Reconstituting data streams using the P matrix, [P] **3640**,
   i. Define element signal streams for an N-element array.
   ii. Calculate recovered signals streams via the K-demuxing **3650** operation.

All the N elements are used in calculating the recovered signal streams. We have assumed that all the N element signals are available. There is no redundancy in the approach.

FIG. **37** depicts the flow chart **3700** of an alternate approach in reconstituting the M beam signals based on N element signals, when N=5 and M=4. The array geometry **3710** indicates that there is one redundant element from the array with 5 array elements. The 5-element array can concurrently form 4 receiving beams with OB patterns. We use digital beam forming in Rx, instead of propagation matrices, to create K-demuxing **3760**. The steps for the flow chart are as follows:

1. A 5-element array geometry with 4 survived elements and a BWV,
2. Designate the same peak and null positions as performance constraints **3720** for one beam with a similar OB radiation pattern,
3. Iteration loop:
   A. Array pattern calculation **3730** based on new BWV,
   B. Generations of observables from differences between calculated array pattern and its performance constraints,

C. Converting observables to cost functions which are measurable with positive values.
D. Calculate current total cost,
E. If total cost less than a threshold (8) go to step 4; otherwise go to step 3F.
F. Derive and update weighting coefficients of the BWV via optimization **3740** schemes by a cost minimization algorithm and go to 3A.

4. From an output buffer **3750**, we plot the pattern (array factor only) of configured OB beam and output the BWV.

FIG. **38** depicts a flow chart **3800** of an alternate approach in reconstituting the M beam signals based on N element signals, when N=6 and M=4. The array geometry **3810** indicates that there were two redundant elements from the array with 6 array elements. The 6-element array can concurrently form 4 receiving beams with OB patterns. We use digital beam forming **3830** in Rx, instead of propagation matrices, to create K-demuxing **3860**. The steps for the flow chart are as follows:

1. A 6-element array geometry with 4 survived elements and a BWV,
2. Designate the same peak and null positions as performance constraints **3820** for one beam with a similar OB radiation pattern,
3. Iteration loop:
   i. Array pattern calculation **3830** based on new BWV,
   ii. Generations of observables from differences between calculated array pattern and its performance constraints,
   iii. Converting observables to cost functions which are measurable with positive values.
   iv. Calculate current total cost,
   v. If total cost less than a threshold (δ) go to step 4; otherwise go to step 3 vi.
   vi. Derive and update weighting coefficients of the BWV via optimization **3840** schemes by a cost minimization algorithm and go to 3A.
4. From an output buffer **3850**, we plot the pattern of configured OB beam and output the BWV.

Private and Redundant Data on Nonvolatile Memory Via K-Muxing Transform:

Nonvolatile memory is a general term for all forms of solid state (no moving parts) memory that do not need to have their memory contents periodically refreshed. This includes all forms of read-only memory (ROM) such as programmable read-only memory (PROM), erasable programmable read-only memory (EPROM), electrically erasable programmable read-only memory (EEPROM), and flash memory. It also includes random access memory (RAM) that is powered with a battery.

An SSD (solid-state drive or solid-state disk) is a nonvolatile storage device that stores persistent data on solid-state flash memory. SSD devices embed silicon-based memory chips as the storage media for the writing and reading of persistent data. SSDs, also known as flash drives or flash cards, are inserted into slots in computer servers—referred to as server-side flash storage—or as part of an enterprise flash storage array system.

Sometimes the flash devices are called solid-state hard drives, although that term is misleading. Unlike a spindled hard disk drive (HDD), an SSD contains no mechanical parts. A traditional HDD consists of a spinning disk with a read/write head on a mechanical arm, known as an actuator. An SSD, on the other hand, has an array of semiconductor memory organized as a disk drive, using integrated circuits rather than magnetic or optical storage media.

Devices containing flash storage memory have varied use cases. Development and adoption of SSDs has been driven by use of applications that demand higher I/O performance. SSDs have lower random access and read access latency than HDDs, making them a fit for both heavy read and random workloads.

That lower latency is the direct result of the ability of a flash SSD to read data directly and immediately from a specific flash cell location. High-performance servers, laptops, desktops or applications that deliver information in real-time or near real-time could benefit from solid-state drive technology.

Those characteristics make enterprise SSDs suitable to offload reads from transaction-heavy databases, to alleviate boot storms with virtual desktop infrastructure, or inside a storage array to stage hot data locally for off-site storage in a hybrid cloud scenario.

The Solid State Storage Initiative has identified three major SSD form factors for the enterprise:

1. SSDs that come in traditional HDD form factors and fit into the same slots.
2. Solid-state cards that use standard card form factors, such as Peripheral Component Interconnect Express (PCIe), and reside on a printed circuit board.
3. Solid-state modules that reside in a Dual In-line Memory Module (DIMM) or small outline dual in-line memory module (SO-DIMM), and may use a standard HDD interface such as Serial Advanced Technology Attachment (SATA).

We may use the same or similar techniques depicted in FIG. **1** to FIG. **19** to perform K-muxing and K-demuxing transforms on data stored on solid state drives (SSD) for enhanced data privacy and survivability via redundancy.

Elements of one embodiment may be implemented by hardware, firmware, software or any combination thereof. The term hardware generally refers to an element having a physical structure such as electronic, electromagnetic, optical, electro-optical, mechanical, electro-mechanical parts, etc. A hardware implementation may include analog or digital circuits, devices, processors, applications specific integrated circuits (ASICs), programmable logic devices (PLDs), field programmable gate arrays (FPGAs), or any electronic devices. The term software generally refers to a logical structure, a method, a procedure, a program, a routine, a process, an algorithm, a formula, a function, an expression, etc. The term firmware generally refers to a logical structure, a method, a procedure, a program, a routine, a process, an algorithm, a formula, a function, an expression, etc., that is implemented or embodied in a hardware structure (e.g., flash memory, ROM, EROM). Examples of firmware may include microcode, writable control store, micro-programmed structure.

When implemented in software or firmware, the elements of an embodiment may be the code segments to perform the necessary tasks. The software/firmware may include the actual code to carry out the operations described in one embodiment, or code that emulates or simulates the operations. The program or code segments may be stored in a processor or machine accessible medium. The "processor readable or accessible medium" or "machine readable or accessible medium" may include any non-transitory medium that may store information. Examples of the processor readable or machine accessible medium that may store include a storage medium, an electronic circuit, a semiconductor memory device, a read only memory (ROM), a flash memory, an erasable programmable ROM (EPROM), a floppy diskette, a compact disk (CD) ROM, an optical disk, a hard disk, etc. The machine accessible medium may be embodied in an article of manufacture. The machine accessible medium may include information or data that, when accessed by a machine, cause the machine to perform the operations or actions described above. The machine accessible medium may also include program code, instruction or instructions embedded therein. The program code may include machine readable code, instruction or instructions to perform the operations or actions described above. The term "information" or "data" here refers to any type of information that is encoded for machine-readable purposes. Therefore, it may include program, code, data, file, etc.

All or part of an embodiment may be implemented by various means depending on applications according to particular features, functions. These means may include hardware, software, or firmware, or any combination thereof. A hardware, software, or firmware element may have several modules coupled to one another. A hardware module is coupled to another module by mechanical, electrical, optical, electromagnetic or any physical connections. A software module is coupled to another module by a function, procedure, method, subprogram, or subroutine call, a jump, a link, a parameter, variable, and argument passing, a function return, etc. A software module is coupled to another module to receive variables, parameters, arguments, pointers, etc. and/or to generate or pass results, updated variables, pointers, etc. A firmware module is coupled to another module by any combination of hardware and software coupling methods above. A hardware, software, or firmware module may be coupled to any one of another hardware, software, or firmware module. A module may also be a software driver or interface to interact with the operating system running on the platform. A module may also be a hardware driver to configure, set up, initialize, send and receive data to and from a hardware device. An apparatus may include any combination of hardware, software, and firmware modules.

It will be appreciated that various of the above-disclosed and other features and functions, or alternatives thereof, may be desirably combined into many other different systems or applications. Various presently unforeseen or unanticipated alternatives, modifications, variations, or improvements therein may be subsequently made by those skilled in the art which are also intended to be encompassed by the following claims.

What is claimed is:

1. An apparatus comprising:

an antenna array having N elements configured to receive N input streams from a plurality of transmitters; and

a post-processing device configured to perform a wavefront de-multiplexing transform on the N input streams corresponding to M orthogonal beams to generate M output streams using a weight matrix having M beam weight vectors (BWVs) associated with the M orthogonal beams,

wherein M and N are positive integers and $1<M\leq N$,

wherein the M BWVs are calculated using an optimization procedure based on performance constraints, and

wherein the performance constraints for one of the M orthogonal beams with an orthogonal beam radiation pattern include designated peak and null positions.

2. The apparatus of claim **1**, wherein the M orthogonal beams include a first beam having a peak at nulls of other beams and peaks of the other beams are at nulls of the first beam.

3. The apparatus of claim **1**, wherein the optimization procedure is an iterative process which is stopped when a total cost function derived from the performance constraints is less than a pre-determined threshold.

4. The apparatus of claim **3**, wherein the total cost function is a sum of cost functions, wherein the cost functions are calculated as differences between array pattern parameters of the antenna array and the performance constraints, and wherein the array pattern parameters are calculated based on current values of the M BWVs.

5. The apparatus of claim **1**, wherein a redundancy degree in forming the M orthogonal beams is N minus M.

6. The apparatus of claim **1**, wherein the plurality of transmitters are located on satellites.

7. The apparatus of claim **1**, wherein each of the M BWV is an N×1 column vector representing amplitude and phase distributions among adjacent components.

8. An apparatus comprising:

an antenna array having N elements configured to receive N input streams from a plurality of transmitters; and

a post-processing device configured to perform a wavefront de-multiplexing transform on the N input streams corresponding to M orthogonal beams to generate M output streams using a weight matrix having M beam weight vectors (BWVs) associated with the M orthogonal beams,

wherein M and N are positive integers and $1<M\leq N$,

wherein the M BWVs are calculated using an optimization procedure based on performance constraints, and

wherein a redundancy degree in forming the M orthogonal beams is N minus M.

9. The apparatus of claim **8**, wherein the M orthogonal beams include a first beam having a peak at nulls of other beams and peaks of the other beams are at nulls of the first beam.

10. The apparatus of claim **8**, wherein the performance constraints for one of the M orthogonal beams with an orthogonal beam radiation pattern include designated peak and null positions.

11. The apparatus of claim **8**, wherein the optimization procedure is an iterative process which is stopped when a total cost function derived from the performance constraints is less than a pre-determined threshold.

12. The apparatus of claim **11**, wherein the total cost function is a sum of cost functions, wherein the cost functions are calculated as differences between array pattern parameters of the antenna array and the performance constraints, and wherein the array pattern parameters are calculated based on current values of the M BWVs.

13. The apparatus of claim **8**, wherein the plurality of transmitters are located on satellites.

14. The apparatus of claim **8**, wherein each of the M BWV is an N×1 column vector representing amplitude and phase distributions among adjacent components.

15. An apparatus comprising:

an antenna array having N elements configured to receive N input streams from a plurality of transmitters; and

a post-processing device configured to perform a wavefront de-multiplexing transform on the N input streams corresponding to M orthogonal beams to generate M output streams using a weight matrix having M beam weight vectors (BWVs) associated with the M orthogonal beams,

wherein M and N are positive integers and $1<M\leq N$,

wherein the M BWVs are calculated using an optimization procedure based on performance constraints, and

wherein each of the M BWV is an N×1 column vector representing amplitude and phase distributions among adjacent components.

16. The apparatus of claim **15**, wherein the M orthogonal beams include a first beam having a peak at nulls of other beams of the M orthogonal beams and wherein peaks of the other beams are at nulls of the first beam.

17. The apparatus of claim **15**, wherein the performance constraints for one of the M orthogonal beams with an orthogonal beam radiation pattern include designated peak and null positions.

18. The apparatus of claim **15**, wherein the optimization procedure is an iterative process which is stopped when a total cost function derived from the performance constraints is less than a pre-determined threshold.

19. The apparatus of claim **18**, wherein the total cost function is a sum of cost functions, wherein the cost functions are calculated as differences between array pattern parameters of the antenna array and the performance constraints, and wherein the array pattern parameters are calculated based on current values of the M BWVs.

20. The apparatus of claim **15**, wherein a redundancy degree in forming the M orthogonal beams is N minus M.

* * * * *